Acyl-CoA Synthetase Isoform 1 Deficiency Impairs Beta-Oxidation In Mouse Heart And Adipose Tissue

Jessica Mary Ellis Wilcox

A dissertation submitted to the faculty of the University of North Carolina at Chapel Hill in partial fulfillment of the requirements for the degree of Doctor of Philosophy in the Department of Nutrition (Biochemistry), School of Public Health.

Chapel Hill
2010

Approved by:

Advisor: Rosalind A. Coleman

Reader: Terry P. Combs

Reader: Nobuyo Maeda

Reader: Deborah M. Muoio

Reader: Monte S. Willis

ABSTRACT

Jessica Ellis Wilcox: Acyl-CoA Synthetase Isoform 1 Deficiency Impairs Beta-Oxidation In Mouse Heart And Adipose Tissue

(Under direction of Dr. Rosalind A. Coleman)

The balance between fatty acid (FA) catabolism and anabolism plays a central role in obesity and obesity-related complications; and understanding derangements in metabolism that underlie disease will aid in setting strategies for treating disease. The activation of long chain FA for cellular metabolism requires the five mammalian long chain acyl-CoA synthetases (ACSL) that catalyze the conversion of long chain FA into their acyl-CoA derivatives. The reason mammals need five unique ACSL isoenzymes remains unknown. The purpose of this study was to determine the role of ACSL one (ACSL1) in FA metabolism in adipose tissue and heart. To study ACSL1 in adipose, we generated an adipose-specific ACSL1 knockout mouse, the *Acsl1*$^{A-/-}$ mouse. ACSL1 in adipose was believed to be essential for the synthesis of triacylglycerol. However, in *Acsl1*$^{A-/-}$ white and brown adipocytes, the rate of TAG synthesis was similar to controls, whereas FA oxidation in isolated adipocytes and mitochondria was reduced 50-90%. *Acsl1*$^{A-/-}$ mice had increased fat mass and were severely cold intolerant. Their reduced adipose FA oxidation and marked cold intolerance indicate that normal activation of FA for oxidation in adipose tissue *in vivo* requires ACSL1. To study ACSL1 in heart, we generated a multi-tissue temporally induced ACSL1 knockout mouse, *Acsl1*$^{T-/-}$. Although cardiac ACSL1 is the most abundant of the ACSL isoenzymes, its role in cardiac FA metabolism had remained unclear. In *Acsl1*$^{T-/-}$ mice, acyl-CoA synthetase activity was reduced ~90%, acyl-CoA content was reduced 65%,

and long-chain acyl-carnitine species and palmitate oxidation were 80-90% lower than in control hearts. *Acsl1*$^{T-/-}$ hearts developed hypertrophy, increased mitochondrial content, and had 5-fold greater phosphorylation of S6 kinase, a target of mTOR kinase. These data suggest that ACSL1 catalyzes the initial step in the pathway of heart FA oxidation and that without ACSL1, diminished FA oxidative capacity leads to mTOR activation and results in cardiac hypertrophy and increased mitochondria. Together, these data suggest that ACSL1 has a specific function in directing the metabolic partitioning of FA towards β-oxidation in both adipose tissue and heart. This dissertation has elucidated the novel role for ACSL1 as the first and required step for the oxidation of FA.

ACKNOWLEDGEMENTS

I am grateful to my family, friends, and husband for their support throughout my graduate studies. I am grateful to my mentor, Dr. Rosalind Coleman for her guidance, support, and dedication towards my successes as a doctoral student.

TABLE OF CONTENTS

LIST OF TABLES

Table

LIST OF FIGURES

s

ABRREVIATIONS

ACSL	Acyl-CoA synthetase
AMPK	Adenosine monophosphate-activated kinase
ASM	Acid soluble metabolites
BAT	Brown adipose tissue
BSA	Bovine serum albumin
C	Control
CL	Cardiolipin
CO2	Carbon dioxide
Con	Control
CPT	Carnitine palmitoyl transferase
CVD	Cardiovascular disease
DAG	Diacylglycerol
ER	Endoplasmic reticulum
FA	Fatty acid(s)
FATP	Fatty acid binding protein
GFP	Green florescent protein
PC	Phosphatidylcholine
PE	Phosphatidylethanolamine
PGC1	Peroxisomal proliferator gamma coactivator one
PKB/Akt	Protein kinase B
PKC	Protein kinase C
PL	Phospholipid
PLC	Phospholipase C
PPAR	Peroxisomal proliferator activated receptor
PS	Phosphatidylserine

mTOR	Mammalian target of rapamycin
RT-PCR	Real-time polymerase chain reaction
S6K	S6 protein kinase
T-/-	Acyl-CoA synthetase one multi-tissue knock out mouse, Acsl1T-/-
Tamox	Tamoxifen
TAG	Triacylglycerol
UCP1	Uncoupling protein one
WAT	White adipose tissue

CHAPTER I

INTRODUCTION

The current epidemic of obesity, diabetes, cardiovascular disease, and dyslipidemia is characterized by an imbalance of lipid metabolism. The ability of white adipose to both store fat as triacylglycerol and to oxidize fat for energy are critical factors of obesity and obesity-related complications such as diabetes and heart disease. In heart disease, such as diabetic cardiomyopathy, triacylglycerol (TAG) accumulates because fatty acid (FA) uptake is increased and FA oxidation is decreased. In cardiac hypertrophy, FA oxidation is reduced and the risk of cardiomyopathy and cardiovascular complications is increased. While the mechanisms that regulate the cellular uptake, activation, and metabolism of fatty acids are not fully understood, it is known that for nearly every biochemical pathway the conversion of FA to acyl-CoA is critical for metabolism. Acyl-CoAs have multiple fates including their incorporation into complex lipids, use in lipid remodeling, effects on signal mediation, regulation of transcription factors, and oxidation for energy. After cellular uptake of FA, long-chain acyl-CoA synthetase (ACSL) isoenzymes convert FA to acyl-CoA to both trap the fatty acid within the cell and simultaneously activate it. **The activation of long chain FA by ACSL is the first and essential step for the cellular metabolism of fatty acids.**

The five mammalian ACSL isoenzymes have unique coding region, tissue-dependent expression pattern, intracellular location, and are under different regulatory mechanisms. The reason mammals need five unique isoenzymes of ACSL remains unknown. Our group focuses on the role ACSL isoenzymes play in lipid metabolism. This

dissertation will focus on ACSL-isoenzyme-1 (ACSL1) which is the most abundantly expressed isoenzyme in human and rodent heart and adipose tissue. Data suggest that the ACSL isoenzymes channel FA towards specific metabolic pathways in a tissue-dependent manner. The literature suggests that ACSL1 plays a role in channeling fatty acids toward TAG in white adipose because PPARγ upregulates *Acsl1* in white adipose tissue, the overexpression of ACSL1 in adipocyte-precursor NIH-3T3 cells results in TAG accumulation, and A*csl1* mRNA expression increases 160-fold in differentiating 3T3L1 adipocytes concomitant with increased TAG formation [1-4]. However, in cardiac muscle ACSL1 is thought to channel FA toward oxidation because *Acsl1* mRNA is upregulated by PPARα in cardiomyocytes and in the developing mouse heart *Acsl1* mRNA increases X-fold concomitant with increases in FA oxidation rates [5, 6]. To determine if ACSL1 channels FA towards opposing metabolic pathways in heart and adipose tissue we have generated mice that lack ACSL1 specifically in adipose tissue or in heart, as well as a temporally-induced multi-tissue knockout. In the ACSL1 adipose-specific knockout mouse, $Acsl1^{A-/-}$, total ACSL activity for palmitate is reduced ~80% in white and brown adipose tissue. In the $Acsl1^{A-/-}$adipose tissue, mitochondrial FA oxidation is severely impaired, resulting in mice with increased adipose mass and marked cold intolerance. In both the temporally-induced heart-specific knockout, $Acsl1^{H-/-}$, and the multi-tissue knockout, $Acsl1^{T-/-}$, total ACS activity in the heart is reduced by 90-97%, as is the rate of mitochondrial FA oxidation. The lack of ACSL1 in the heart results in pathological hypertrophy and increased mitochondrial biogenesis that our data suggest is mediated through the activation of mTOR. Both the $Acsl1^{T-/-}$ and the $Acsl1^{H-/-}$ mice have enlarged hearts, confirming that the lack of ACSL1 specifically in cardiomyocytes impairs FA oxidation and elicits hypertrophy.

With the current obesity epidemic it is critical to understand the mechanisms that underlie the cellular uptake and processing of lipids. ACSL1 is a key enzyme of fatty acid

metabolism in both adipose tissue and heart, and characterizing its influence on cellular lipid metabolism is critical for the evaluation of the metabolic processes underlying obesity and heart disease. This work provides convincing data that ACSL1 activates FA for oxidation, not TAG synthesis, in adipose and cardiac tissue.

Specific Aims:

1. **Determine the role of ACSL1 in activating fatty acids for white adipose tissue using the adipose-specific ACSL1 knockout mice, *Acsl1*$^{A-/-}$, and primary adipocyte cultures from *Acsl1*$^{A-/-}$ mice.**

2. **Determine the role of ACSL1 in activating fatty acids in brown adipose tissue using the adipose-specific ACSL1 knockout mice, *Acsl1*$^{A-/-}$, and primary adipocyte cultures from *Acsl1*$^{A-/-}$ mice.**

3. **Determine the role of ACSL1 in activating fatty acids in the heart using the multi-tissue ACSL1 knockout mice, *Acsl1*$^{T-/-}$, and the heart-specific ACSL1 knockout mice *Acsl1*$^{H-/-}$.**

CHAPTER II

BACKGROUND

As the rates of obesity and heart disease rise around the globe, our knowledge of the physiological mechanisms underlying these disorders is expanding. While the data continues to mount, connecting obesity to disorders such as diabetes and heart disease, our 13understanding of lipid metabolism and its regulation in adipose tissue and heart remains unclear. ACSL1 has been manipulated and studied *in vitro* but little data exists on ACSL1 in adipose *in vivo*. I have used the *Acsl1*$^{A-/-}$ mice to study ACSL1 in adipose *in vivo*. In contrast, heart research has focused heavily on heart function and the associated disease outcomes; however, the cardiomyocyte metabolism that underlies heart function and heart disease remains relatively unexplored. I have used our *Acsl1*$^{T-/-}$ and *Acsl1*$^{H-/-}$ mice to study heart lipid metabolism in the absence of ACSL1 in a physiological system.

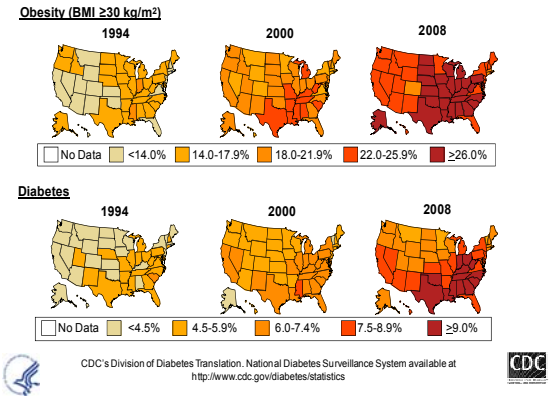

Figure 2.1. Age-adjusted Percentage of U.S. Adults Who Were Obese or Who Had Diagnosed Diabetes in 1994, 2000, and 2008 [7]. The epidemic of obesity and related complications is illustrated by the center for disease controls (CDC) records of the rising incidence of obesity and diabetes in the United States over the past two decades.

B.1. Acyl-CoA synthetase activates fatty acids and determines their metabolic fate.

Cellular fatty acids have many metabolic fates including storage as TAG, incorporation into phospholipids, and oxidization for ATP production. Nearly all FA metabolic pathways require the activation of FA to acyl-CoA. This reaction is catalyzed by acyl-CoA synthetase (ACS) in an ATP-dependent manner.

Fatty acid + ATP → acyl-AMP + PPi

Acyl-AMP + CoA → acyl-CoA + AMP

The ACS catalytic domain shares homology with the ANL superfamily, a family consisting of ACS, nonribosomal peptide synthetase, and luciferase (3). The homology between ACS and luciferase is so similar that mutation of a single residue (L345S) allows the *Drosophilia melangaster* ACS to gain luciferase activity (4).

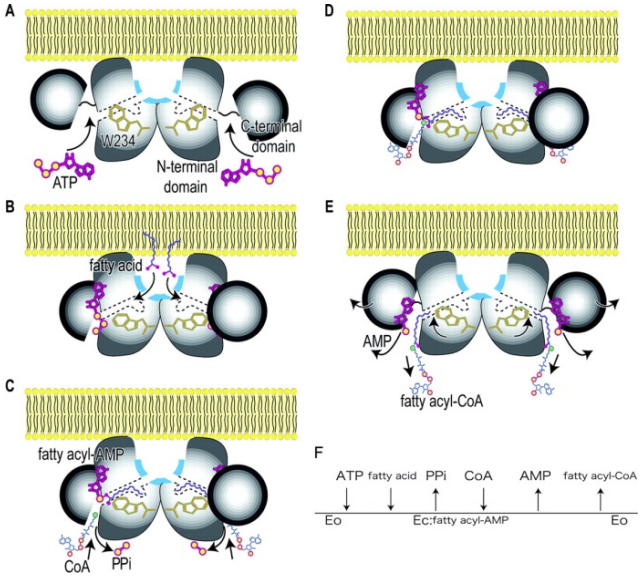

Figure 2.2: The schematic mechanism for the unidirectional ordered catalysis by ttLC-FACS, figure from Hisanaga, Y. et al. J. Biol. Chem. 2004; 279:31717-31726.

The structural conformation of ACS has been predicted from crystal structure analysis of a thermophilic bacterial long-chain acyl-CoA synthetase, schematic above [8]. After ATP

binds to ACS in the adenylate-forming conformation the C-terminus is rotated 140°, opening the gate to the fatty acid binding tunnel, and this rotation results in the thioester conformation. For long-chain ACS the C-terminal domain is predicted to remain closed throughout the entire ACS reaction so that the acyl-AMP intermediate is never released, which explains why the acyl-AMP intermediate has never been successfully isolated. Upon opening of the gate, a fatty acid enters the fatty acid-binding tunnel unidirectionally and travels toward the ATP binding site. A pyrophosphate is released when the fatty acyl-AMP complex is formed. The CoA then attacks the fatty acyl-AMP to form the acyl-CoA. Formation of the acyl-CoA opens the C-terminus domain and the acyl-CoA and AMP products are released from the enzyme. In 2009, Kochan et al. reported the crystal structure of human ACSM2A [9]. Analysis of this mammalian ACS crystal structure revealed the following: 1) in the adenylate-forming conformation a conserved lysine, Mg^{2+}, and the P-loop hold the pyrophosphate in the active site, 2) in the thioester conformation an Arg472-Glu365 salt bridge sterically blocks ATP binding, and 3) switching of the adenylate-forming conformation to the thioesterase conformation requires the presence of pyrophosphate. The isolation of additional mammalian ACSL crystal structures would increase our understanding of the protein structure, mechanism, and regulation.

Humans are predicted to have 26 genes that encode acyl-CoA synthetase enzymes. ACSs are grouped into 5 families according to their substrate preference for fatty acids of varying chain lengths [10]. The 26 predicted human ACSs include 5 families consisting of 3 short-chain, 6 medium-chain, 5 long-chain, 6 very-long chain, and 2 bubblegum isoenzymes, plus 4 additional likely acyl-CoA synthetase genes. The prediction for the 26 ACS genes is based on conserved amino acid sequences of 5 distinct motifs: Motif I-V. The predicted biochemical role for the five motifs are as follows: Motif I is the AMP-binding domain that helps to maintain AMP substrate in the proper orientation, Motif II is the linker motif that is thought to induce a conformational change to aid fatty acid and/or

CoA binding, Motif III is associated with substrate stabilization for the AMP-binding domain, Motif IV contains the gate-domain that allows fatty acid binding only after ATP binding-induced conformational change, and lastly, Motif V contains a conserved lysine that is thought to participate in a conformational change to create the CoA binding pocket [10]. The ACS amino acid sequences range from 438 to 739 amino acids including the five conserved motifs.

ACS post-translational regulation. Broad mass spectrometry surveys reveal a number of post-translational modifications to ACS enzymes, although the functional significance is generally unknown. An exception is the regulation on Lys-609 located on the C-terminus of the *Salmonella enterica* ACS, for which lysine acetylation inhibits activity by preventing formation of the thioester [11]. Similar regulation occurs by the SIRT acetylases on Lys-661 and Lys-635 of acetyl-CoA synthetase-1 and acetyl-CoA synthetase-2, respectively, and human acetyl-CoA synthetase 2 is regulated on Lys-642 [12]. In response to a calorie restricted diet, acetylation of Lys-534 of ACSM1 and Lys-510 of acyl-CoA synthetase family member-2 (Q8VCW8) increased 2.75-fold and 2.3-fold, respectively [13]. Dr. L.O. Li and Dr. J. Frahm of the Coleman lab have identified multiple ACSL1 acetylation sites (unpublished data). Additional research is required to connect the functional contribution of ACSL1 acetylation to its activity.

Mass spectrometry techniques used to identify post-translational modification in rat liver mitochondria showed acetylation at Lys-633 and phosphorylation at Tyr-85 of ACSL1 protein [14]. The phosphorylation site of ACSL1 is a predicted insulin receptor consensus site; however, insulin effects on this phosphorylation site and the ensuing effect on ACSL1 protein activity are unknown. Work by L.O. Li and J. Frahm of the Coleman lab have identified numerous phosphorylation sites by mass spectrometry for the ACSL1 protein, unpublished data. L.O. Li is currently mutating the predicted phosphorylated amino acids to evaluate the effects of phosphorylation on enzyme activity. These acetylated and

phosphorylated regulatory sites of ACSL1 support the idea of complex and acute regulation on ACSL activity.

Role of ACS in regulating transcription. ACSL can theoretically regulate transcription by modulating the intracellular content of FA and acyl-CoA, which are ligands for transcription factors. FA, for example, are ligands for PPARα and β/δ and may suppress SREBP1c target genes, and acyl-CoA is a possible ligand for HNF4α [15]. The role of ACS in regulating transcription was addressed by a study that used siRNA to knock down the long-chain ACS isoenzymes that are expressed in liver, ACSL1, 3, 4, and 5 and FATP2, 4, and 5 [16]. In primary rat hepatocytes the siRNA that targeted ACSL3, the only siRNA that affected transcription, elevated intracellular FA 82% and diminished PPARγ expression, as well as reporter gene activity for PPARγ, carbohydrate-responsive element-binding protein, SREBP1c, and the liver X receptor-α, together with the expression of the target genes for these transcription factors. Decreased use of [1-^{14}C]acetate for de novo lipogenesis and complex lipid synthesis confirmed the effect of diminishing the expression of genes involved in lipid synthesis. Although one might conclude that the knockdown of ACSL3 decreased transcriptional activities via an increase in a specific pool of FA ligand, Bu et al. argue that ACSL3 must control transcription in a ligand-independent manner because synthetic ligands did not normalize transcriptional activities of LXR and PPAR-γ [16].

ACS for long-chain fatty acids (ACSL) is a family consisting of 5 known independent mammalian isoenzymes: ACSL1, ACSL3, ACSL4, ACSL5, and ACSL6 [17]. Based on sequence homology, the ACSL isoenzymes consist of two subfamilies; ACSL1, -5, and -6 which share ~60% homology and ACSL3 and -4 which share ~70% homology and share ~30% with 1,5, and 6 [18]. The active sites of the ACSL proteins face the cytosol to produce an amphipathic acyl-CoA which could feasibly be partitioned either into the membrane compartment or the cytosolic compartment to provide a FA in a subcellular location optimal for a particular metabolic fate [19]. ACSL isoenzymes are

unique proteins that differ in their substrate preferences, enzyme kinetics, and tissue-specific expression [20-22], suggesting that each has a distinct function. ACSL proteins have been shown to interact with other ACS enzymes and binding proteins and it is predicted that these interactions may facilitate channeling of the acyl-CoA product [23].

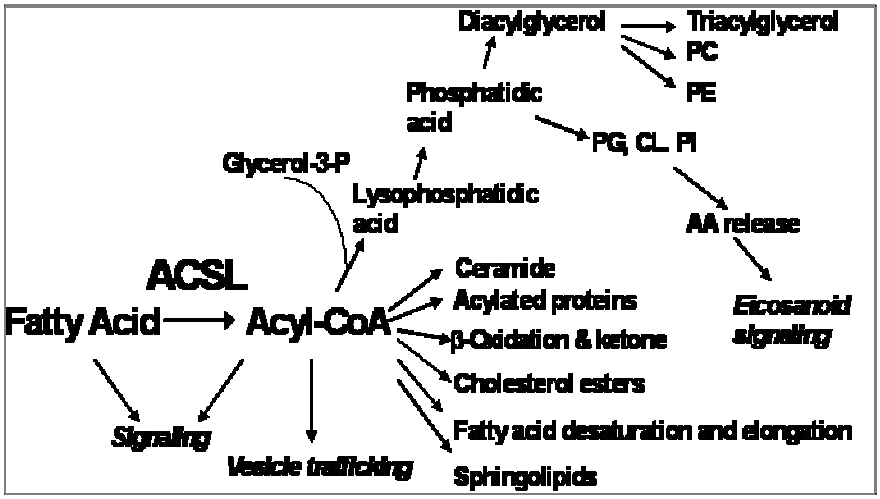

Figure 2.3. Pathways of acyl-CoA metabolism, adapted [24]
AA, arachidonic acid; ACSL,long-chain acyl-CoA synthetase; CL, cardiolipin; PC, phosphatidylcholine; PE, phosphatidylethanolamine; PG, phosphatidylglycerol; PI, phosphatidylinositol.

FA channeling. ACSL isoenzymes activate fatty acids with chain lengths of 12 to 24 carbons and ACSVL isoenzymes activate fatty acids with chain lengths of 16 to 24 carbons, yet the physiological roles of these enzymes remain unknown [25, 26]. We hypothesize that different ACS isoenzymes channel FA into specific downstream pathways and that the channeling could vary in a tissue-specific manner [27]. For example, ACSL1 liver-specific knockout primary hepatocytes, compared to controls, have 20% lower rates of FA incorporation into TAG and 4.5% reduced ASM production [28]. Whereas, ACSL1 adipose-specific knockout primary brown adipocytes, compared to controls, have normal rates of FA incorporation into TAG and 90% reduced ASM production (this dissertation). The ACSL1 adipose-specific knockout primary white adipocytes, compared to controls, have normal rates of FA incorporation into TAG and 50% reduced ASM production (this dissertation).

These data suggest that ACSL directs the metabolism of fatty acids similarly but to different degrees in adipose and liver. In Huh7 human hepatoma cells ACSL3 is found in lipid droplets and is important for vesicle secretion of ApoB-containing particles [29, 30]. A siRNA against ACSL3 expressed in Huh7 cells decreased oleate incorporation into PC, increased free cellular oleate, and inhibited vesicle secretion of ApoB-containing particles. However, siRNA against ACSL1 and ACSL4 in Huh7 did not change FA uptake or incorporation into complex lipids. The knockdown of ACSL3 in primary rat hepatocytes, compared to vector control cells, suppresses *de novo* fatty acid synthesis by 40% [16]. E.*coli* with absent FadD, a bacterial ACSL, has retarded cell growth, when grown on media containing FA as the sole energy substrate, that is rescued by ACSL5, but not by any other ACSL isoenzyme [31]. Together, these data suggest that ACSL isoenzymes impact cellular metabolism uniquely in different cell types, cell lines, and tissues, and that the isoenzymes are not able to compensate for one another.

The formation of specific complex lipids, TAG and PL, from [^{3}H]glycerol-3-phosphate is blocked by triacsin C, a fungal-derived competitive inhibitor of ACSL1,-4, and -3 activity, in fibroblasts, hepatocytes, and other cells [20, 32]. The incorporation of FA into TAG in hepatocytes is blocked by troglitazone, an inhibitor of ACSL4 [20]. The incorporation of [^{14}C]oleate into DAG and PL increases while its incorporation into cholesterol esters decreases when ACSL1 is overexpressed in primary hepatocytes [33]. In contrast, the overexpression of ACSL5 in rat hepatoma cells increases [^{14}C]oleate uptake and incorporation into TAG [34]. ACSL5 does not facilitate FA uptake when overexpressed in yeast, whereas the overexpression of ACSL1, 4, and 6 does [35]. Differential effects of individual ACSL isoenzymes support the notion that ACSL isoenzymes channel FA to distinct metabolic fates.

Several overexpression studies are inconsistent with knockdown studies and provide strikingly contradictory interpretations of the role of ACSL isoenzymes. For example, when

ACSL1 is overexpressed in rat primary hepatocytes, FA are incorporated into diacylglycerol and phospholipids, but not into cholesterol ester or secreted triacylglycerol [36], whereas ACSL1 knockout primary mouse hepatocytes have 20% reduced FA incorporation into TAG, but not DAG, CE, or PL. Overexpressed ACSL5 increased FA incorporation into diacylglycerol and triacylglycerol, but does not affect FA used for β-oxidation [34], whereas, overexpressing either human ACSL3 or rat ACSL5 in HepG2 cells increases palmitate oxidation [37]. Further, TAG content increased in NIH-3T3 fibroblasts when ACSL1/FATP1 was overexpressed [38] and TAG content increased in insulin-stimulated 3T3-L1 adipocytes when ACSL1 was knocked down [39].

We see two potential problems. The first is that overexpression of an enzyme may overwhelm downstream pathways that cannot readily accommodate excess substrate; the second problem is that studies in 3T3-L1 adipocytes are not always translatable to primary white or brown adipocytes. Proteomic analysis of mitochondria isolated from white adipose tissue, brown adipose tissues, and 3T3-L1 adipocytes reveals substantial differences [40]. Compared to mitochondria from adipose tissue, many proteins are down regulated in 3T3-L1 mitochondria. Further, ACSM (medium-chain ACS) isoenzymes are more abundant than ACSL isoenzymes in white adipose tissue mitochondria, suggesting greater medium-chain FA oxidative metabolism. ACSL1 and ACSL6 are particularly enriched in white adipose mitochondria, whereas ACSL5 is more abundant in mitochondria from brown adipose. Despite the high abundance of ACSL5 in brown adipose mitochondria, ACSL1 is required for adaptive thermogenesis and normal FA oxidation in brown adipose (shown in this dissertation). Thus, the function of ACSL5 in BAT remains unknown.

FA channeling could occur via protein-protein interactions. Immunoprecipitation of endogenous FATP1 from 3T3-L1 adipocytes followed by mass spectrometry identified mitochondrial 2-oxoglutarate dehydrogenase (OGDH), a key enzyme in the tricarboxylic acid cycle [41]. FATP1 enhances OGDH activity in proteoliposomes and

in 3T3-L1 cells that overexpress FATP1. FATP1 knockdown 3T3-L1 adipocytes showed decreased OGDH and TCA cycle activity. Over-expressed FATP1 and CPT1 also co-immunoprecipitate from L6E9 myotubes and rat skeletal muscle in vivo [42]. In 3T3-L1 adipocytes and L6E9 myotubes, FATP1 overexpression enhances FA oxidation, independent of ACS activity, suggesting that protein-protein interactions of FATP1 facilitate activities of FA oxidation proteins. Overexpressed ACSL1 and FATP1 co-immunoprecipitate in 3T3-L1 adipocytes [23], but it is not known whether endogenous ACSL1 and FATP1 proteins interact.

The data in this dissertation show that ACSL1 preferentially channels FA toward oxidation in several tissues. However, it remains unclear exactly how the ACSL1 enzyme could be shuttling its product towards a single metabolic pathway. The acyl-CoA produced by the ACS reaction has the chemical properties that would allow it to move freely within membranes and/or bind to proteins such as acyl-CoA binding proteins, thus all acyl-CoAs should theoretically be free to enter any downstream metabolic pathway on the cytosolic face of all subcellular membranes. These pathways include TAG synthesis, CE synthesis, PL synthesis, PL re-acylation, elongation, desaturation, protein acylation, and sphingolipid synthesis. We predict that the different ACSL isoenzymes have protein-protein interactions that put the acyl-CoA synthetase in direct contact with proteins specific to metabolic pathways. For example, we hypothesize that in muscle tissues, ACSL1 likely interacts with proteins such as M-CPT1 that would use the acyl-CoA as substrate to form acyl-carnitines for the oxidative pathway. The proteins that ACSL1 and other ACSLs interact with likely vary by tissue/cell type. Experiments are required to show the protein-protein interactions of ACSL1 in different tissues/cell types and under different hormonal/physiological conditions.

Figure 2.4. Protein-protein interactions may mediate ACSL channeling. We hypothesize that ACSL isoenzymes interact with proteins that facilitate the channeling of the acyl-CoA product to downstream pathways.

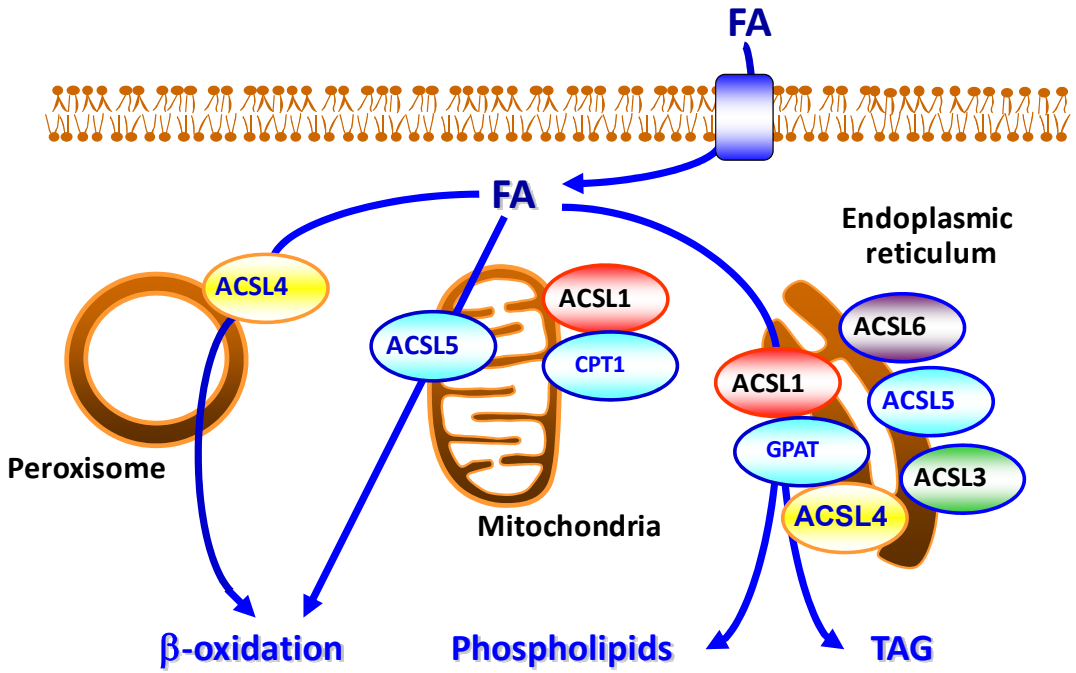

The Coleman Lab, specifically Dr. Jennifer Frahm and Dr. Lei Li, have recently generated data using mass spectrometry technologies that show ACSL1interacting with several mitochondria-specific oxidative proteins. More studies are required to explore how the protein-protein interactions of ACSL1 facilitate channeling, enzyme activity, and regulate metabolic flux. Such studies would include identifying the protein-interacting domains of ACSL1, mutating or truncating these domains, and assessing enzyme activity and rates of FA oxidation in the mutants.

The subcellular locations of ACS enzymes (reviewed in [26]), may influence the downstream metabolism of the acyl-CoA product. However, subcellular localization studies have yielded conflicting interpretations. Most have examined subcellular fractions that are limited in purity. Data from overexpression studies is also problematic because the location of overexpressed proteins may not mimic the endogenous condition. In one such example, the subcellular locations of overexpressed compared to endogenous FATP4/ACSVL5

differed [43]. Confocal microscopy with tested isoenzyme-specific antibodies will be required to determine precise locations of the acyl-CoA synthetases.

ACSL and cell growth. ACSL is required for complex lipid synthesis in rapidly growing cancerous cells, and the fungal metabolite triacsin C was initially reported to inhibit ACSL, diminish the synthesis of phospholipids, and decrease cell proliferation [44]. Triacsin C caused apoptosis of glioma cells, and, although it inhibits ACSL1, 3, and 4, but not ACSL5, overexpression of ACSL5 rescued the glioma cells [45, 46]. In this case, ACSL5 appeared to compensate for the inhibited isoenzymes. In a related publication, ACSVL3 (FATP3) was elevated in human gliomas [47]. When ACSVL3 RNA was knocked down, glioma cell growth was inhibited and the cells became less tumorigenic. Because these features were reversed when active myr-Akt was expressed, ACSVL3 was thought to maintain oncogenesis by regulating Akt function.

Effect of fatty acid activation on AMP-activated kinase. Because the synthesis of each acyl-CoA uses the equivalent of 2 ATP molecules and produces one AMP, it has been suggested that FA activation might increase cellular AMP/ATP ratios and activate AMP-activated kinase (AMPK). AMPK would then increase FA oxidation while blocking TAG synthesis. It would be surprising, however, if the conversion of FA to acyl-CoA triggered the activity of an energy deficit indicator in settings of energy surplus when TAG synthesis is prominent.

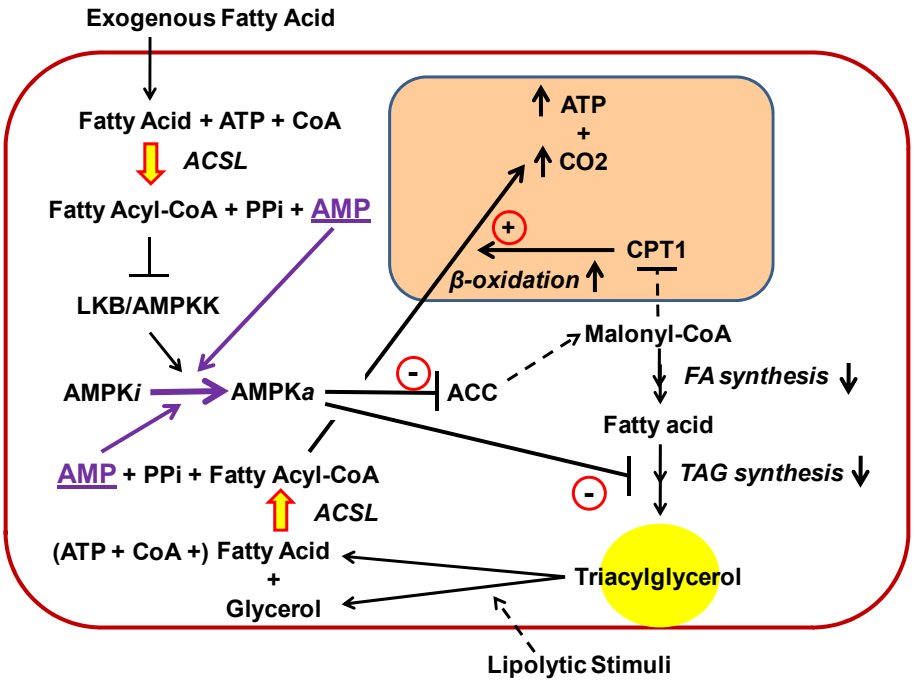

FIGURE 2.5. Potential interactions between ACSL and AMPK, [48]. When exogenous fatty acids enter the cell, are synthesized de novo, or are hydrolyzed from intracellular triacylglycerol stores, they must first be activated by a long chain acyl-CoA synthetase (ACSL) to form fatty acyl-CoAs. They can then enter downstream metabolic pathways. Because ATP is a substrate for ACSL and AMP is a product, the increased AMP/ATP ratio, a signal of low cellular energy stores, could theoretically activate AMP activated kinase (AMPK). Activated AMPK inhibits triacylglycerol synthesis and acetyl-CoA carboxylase (ACC). The resulting decrease in malonyl-CoA levels diminishes fatty acid synthesis and also relieves the inhibition of carnitine palmitoyltransferase-1 (CPT1) by malonyl-CoA, allowing the fatty acyl-CoA to be converted to acyl-carnitine and enter the mitochondria for b-oxidation. Thus, activated AMPK would generate an increase in ATP production. A prolonged lipogenic stimulus [which activates hormone-sensitive lipase (HSL)], may also inactivate AMPK to modulate these effects. It seems unlikely, however, that ACSL would activate AMPK under physiological conditions that stimulate triacylglycerol synthesis.

Studies in animals have not been performed to compare ACSL-mediated activation of AMPK under different physiological conditions, but metabolic adaptations to fasting and chronic caloric restriction in heart, muscle, and liver do not result in changes in AMPK activity [49], and when mice are placed in a cold environment, AMPK is not activated for several days despite a huge increase in ACSL-mediated FA activation [50]. Some experiments, however, support ACSL-mediated activation of AMPK. In 3T3-L1 adipocytes, stimulation of lipolysis results in activated AMPK [51]. The authors suggested that activation

of AMPK during lipolysis would “restrain the energy depletion and oxidative stress”. It might also permit use of released FA for β-oxidation within the adipocyte and conserve glucose during a “fast.” In a situation more akin to “feeding,” AMPK activation increased in 3T3-L1 adipocytes during insulin-stimulated palmitate uptake, although the AMP/ATP ratio changed minimally [52].

Studies in heart [53] and skeletal muscle [54-56] suggest that AMPK may be sensitive to the "lipid status" of the cell and that activation may be influenced by intracellular FA availability, independent of cellular AMP levels, with FAs, themselves, activating AMPK [57]. FA allosteric activation of AMPK increases the ability of LKB1 to phosphorylate the AMPK holoenzyme in vitro [58, 59]. It was postulated by Zhang et al, that elevated acyl-CoA levels in the liver and muscle of very long-chain acyl-CoA dehydrogenase, VLCAD, knockout mice lead to the activation of AMPK and increased FA oxidation [60]. FA added to L6 myotubes increases AMPK activity 40-50%, together with phosphorylation of AMPK Thr^{172} and acetyl-CoA carboxylase-β Ser^{218}, and the rate of palmitate oxidation almost doubles [59]. Surprisingly, no increase was detected in cell AMP content, and LKB1 was not activated. Because a dominant-negative AMPK adenovirus reduced basal FA oxidation and inhibited the stimulatory effects of FA pretreatment on FA oxidation, the authors suggested that FA might improve AMPK as a substrate for LKB1. However, in assays with purified components, 10-50 μM long-chain acyl-CoA directly inhibited AMPKK (LKB1), and it was suggested that the rise in long-chain acyl-CoA content that occurs when FA synthesis is enhanced would negate the effect of potential increases in AMP and prevent simultaneous FA synthesis and FA oxidation [61]. Although the cellular concentration of long-chain acyl-CoAs has been estimated at between 5-160 μM [62], acyl-CoAs are amphipathic and are probably bound either to cell membranes or to acyl-CoA binding protein; neither their free concentration nor their availability as substrates or inhibitors can be known with certainty.

ACS in Disease Mutations in ACS genes have been identified in large screening studies. An *Acsl5* single nucleotide polymorphism (SNP) (rs2419621; C>T) increased *Acsl5* mRNA abundance in skeletal muscle and was associated with improved weight loss. This SNP increases the transcriptional rate of *Acsl5* by enhancing activation of the gene by the myogenic-regulatory factor, MyoD [63]. This mutation also increases the differentiation of skeletal myoblast cells. The data suggest that persons with this SNP in ACSL5 may have an advantageous ability to increase muscle mass and caloric expenditure with diet and exercise.

High level of *Acsl3* methylation in umbilical cord white blood cells were strongly correlated with levels of maternal polycyclic aromatic hydrocarbons and with the mRNA abundance of *Acsl3* [64]. In a separate cohort, *Acsl3* methylation was associated with polycystic aromatic hydrocarbon exposure and childhood asthma [64]. These data suggest that maternal environmental exposures may affect childhood asthma through the methylation of *Acsl3*.

The knockdown of *Acsl4* in neurites reduces dendritic spine formation, suggesting a role for ACSL4 in the maturation and remodeling of neurons, and provides a link to the X-linked mental retardation associated with human mutations in ACSL4 [65]. In another study, a SNP (rs1324805) in the *Acsl4* gene was more prevalent in patients with the metabolic syndrome [66]. A third study found an *Acsl4* SNP (rs7887981) associated with increased liver fat or with increased circulating insulin and TAG in overweight subjects from two different cohorts [67]. It is not unknown how these SNPs affect the function of ACSL4, nor is it clear how the preference of ACSL4 for long-chain polyunsaturated FA may be involved.

A mutation within the *Fatp4* gene is associated with the ichthyosis prematurity syndrome (IPS), a disease characterized by severe skin abnormalities at birth [68]. Fibroblasts from an IPS patient had reduced ACSVL activity and reduced incorporation rates of very-long chain FA into complex lipids. These skin findings are like those of *Fatp4* null

mice which die in early life because of hyperproliferative hyperkeratosis [69], and suggest that FATP4 specifically plays a role in early epidermal development and that a deficit in this enzyme cannot be compensated for by other ACS enzymes. Data presented in this dissertation show that ACSL1 is critical for FA oxidation. The knockout of ACSL1 in mouse results in increased adipose mass and hypertrophy cardiomyopathy. Thus, SNPs in ACSL1 may be correlated with obesity and idiopathic hypertrophies.

B2. Acyl-CoA synthetase isoenzyme 1, ACSL1

ACSL1 was cloned in 1990 [70] and has since been found to be highly expressed in white and brown adipose tissue, heart and liver. It was speculated that ACSL1 channels fatty acids towards TAG synthesis in white adipose because the overexpression of ACSL1 in an adipocyte cell line increases fatty acid uptake and incorporation into complex lipids [71]. We have now examined how adipose is affected *in vivo* by the loss of ACSL1 and find that ACSL1 is critical for activating FA for oxidation, not TAG synthesis, in adipose tissue.

The role ACSL1 plays in the heart's ability to synthesize TAG and to oxidize FA has also been unclear. ACSL1 is upregulated during the development of the adult heart, which correlates with a metabolic switch from the use of glucose to use of FA as the hearts preferred ATP-generating substrate. Therefore, the heart may require ACSL1 for the activation of FA for subsequent oxidation. However, the 11-fold overexpression of ACSL1 in heart results in an 11-fold increase in heart TAG suggesting a role for ACSL1 in TAG synthesis [72]. The work highlighted in this dissertation through the use of two mouse models that lack ACSL1 in heart, shows that ACSL1 provides activated FA for cardiac oxidation.

ACSL1 cellular location may dictate its role in FA channeling. ACSL isoenzymes are intrinsic membrane proteins present in various subcellular compartments in a tissue-specific manner. The subcellular location of ACSL1 may dictate the fate of its acyl-CoA product according to the metabolic function of the organelle. For example, if ACSL1 is associated with the mitochondria or the endoplasmic reticulum in a given cell, then the acyl-CoA product may be channeled towards oxidation or TAG synthesis, respectively. In epithelial-like ptk2 cells and kidney HeLa and Cos-7 cells, the overexpression of an epitope-tagged ACSL1 shows co-localization with the mitochondrial marker OCT-GFP [73]. Mutation studies show that the N-terminus (66 amino acids) is sufficient to target ACSL1 to mitochondria [73]. In adipocytes, ACSL1 protein and mRNA are found in the subcellular fractions that contain endoplasmic reticulum and Golgi membranes that are associated with complex lipid synthesis [71, 74]. ACSL1 protein is also found in trace amounts in the plasma membrane and in nuclear fractions from adipocytes [71, 74]. ACSL1 protein was found in GLUT4-containing vesicles isolated from adipocytes, and its presence on the vesicles may be regulated by insulin [75]. Lipid droplets isolated by fractionation, and that may be contaminated with ER, from adipocytes contain ACSL1 and ACSL3 protein [74, 76]. All studies that have assessed ACSL1 subcellular location have used either tagged-ACSL1 overexpression models or fractionation methods. Both of these methods are flawed in that overexpression can result in artifactual localization that does not represent the native protein location, whereas fractionation methods are highly susceptible to incomplete isolation of membrane fractions and appropriate markers for complete fractionation are critical, but not always shown.

Therefore, the subcellular location of ACSL1 in adipocytes remains unresolved. It is not known how the subcellular location of ACSL1 in adipose affects the function of the enzyme nor is it understood how the protein is directed to and from a particular membrane. In the heart, the intracellular location of ACSL1 has not been reported. In this dissertation,

we show endogenous ACSL1 protein in mitochondrial fractions isolated from mouse heart and BAT.

Table 2.1. Subcellular location of ACSL1

Cell/tissue	Method	Mito	ER/Golgi	Nuclear	PM	GV	cytosol	LD	reference
Ptk2	OE-CM	X							Milger et al, 2006
Cos-7	OE-CM	X							Milger et al, 2006
Rat adipocytes	Frac-GV					X			Sleeman et al, 1998
3T3-L1	Frac	X	X	X	X				Gargiulo, et al 1999
HuH7	Frac-LD							X	
3T3-L1	Frac-LD							X	Brasaemle, et al, 2004
3T3-L1, WAT, BAT	Frac-mito	X							Forner et al, 2009
BAT, heart	Frac-mito	X							Ellis et al, 2010

Frac, fractionation; OE, overexpression; LD, lipid droplet; GV, Glut4-containing vesicles; CM, confocal microscopy; mito, mitochondria.

Manipulation of ACSL1 to understand function. To determine the function of ACSL1, numerous groups have manipulated its expression in various cell types. For example, both ACSL1 and 6, when overexpressed in PC12 neuronal cells, increase cellular uptake of fatty acids and their incorporation into complex lipids [3]. In contrast, the overexpression of ACSL1 in rat primary hepatocytes does not alter the rate of fatty acid uptake but increases FA incorporation into DAG and PL [33]. ACSL1 overexpression in human hepatoma HepG2 cells increases [^{14}C]-oleate incorporation into complex lipids by 40% [77]. Despite data obtained from hepatocytes *in vitro*, the ACSL1-liver specific knock out mouse, *Acsl1*$^{L-/-}$ does not exhibit changes in liver TAG or serum VLDL [78].

Table 2.2. ACSL1 manipulation in multiple tissues/cell types and outcome

Cell Type/Organ	ACSL1	FA Incorporation into lipids	FA uptake	Oxidation
NIH-3T3	OE	↑	↑	?
Rat 1° hepatocytes	OE	↑	-	-
HepG2	OE	↑	↑	-
PC 12	OE	↑	↑	?
Cos-7	OE	-	↑	?
Heart	OE	↑ TAG content	?	?
Huh7	KD	-	?	?
3T3-L1	KD	↑ TAG content with insulin		-

OE, overexpressed; KD, knock down; ?, not tested; -, no change observed

ACS and FA uptake. FA may enter cells via both concentration based flipping and protein-mediated transport [79]. It is likely that cellular retention depends on "vectorial acylation," the trapping of exogenous FA as an acyl-CoA within the cell and its subsequent use in downstream metabolic pathways [27]. Although FATP1 was discovered in a functional FA uptake screen [80], several FATP family members are not present on the plasma membrane [27], and so they are also called ACSVL to distinguish their ability to activate FA with chain lengths as long as 26 carbons [81]. The overexpression of ACSL1 and/or FATP1/ACSL4 (a very long-chain acyl-CoA synthetase that is highly expressed in white adipose) in NIH 3T3-L1 adipocyte-precursor cells increased the rate of lipid incorporation into TAG [23], [38]. The overexpression of ACSL1 **or** FATP1 in NIH 3T3 cells increased fatty acid uptake 50% while the overexpression of both ACSL1 **and** FATP1 increased fatty acid uptake 150% suggesting a synergistic relationship [71]. Overexpressed ACSL1 and FATP1 co-immunoprecipitated in 3T3-L1 adipocytes suggesting direct interaction [23], but it is not known whether endogenous ACSL1 and FATP1 proteins interact. While overexpressed ACSL1 increases FA uptake in NIH fibroblasts [71] and COS cells [73], FA uptake was unaffected by overexpressing [36] or knocking out ACSL1 in

primary hepatocytes [78] or 3T3-L1 adipocytes [39]. It is likely that conflicting data concerning results of FA uptake by the same ACSL isoenzyme reflect differences in the techniques for measuring uptake [27], the artificial effect of overexpression, tissue-specific subcellular location, and tissue-specific interacting proteins. ACSL1 overexpression in kidney-derived Cos-7 cells also increased oleate uptake but did not increase oleate incorporation into specific lipids [73]. FATP4 overexpression increased FA uptake, however, an FATP4 mutant that ablates its ACS activity no longer increased FA uptake suggesting that ACS activity is the factor driving FA uptake [73]. FATP1 overexpression enhances adipocyte fatty acid uptake and TAG accumulation *in vitro*, however, the knockout of FATP1 in mice did not alter adipose weight or size nor did microchip analysis show compensation by other FATP or ACSL isoenzymes [82]. Therefore, it has been unclear if ACSL1 affects the rate of FA uptake in adipose *in vivo* or whether the absence of ACSL1 would decrease fatty acid uptake.

Because all five ACSL isoenzymes have unique subcellular locations and tissue specific expression, we hypothesize that ACSL is regulated by multiple mechanisms including transcriptional activation and repression, post-transcriptional modification, post-translational modification, allosteric modification, and phosphorylation. If all of these mechanisms are in play to regulate the activity of ACSL isoenzymes in a precise manner, we predict that overexpression of ACSL in cell culture or *in vivo* may lead to artificial results due to loss of these regulatory mechanisms. Therefore, the interpretations derived from the overexpression or knock down of ACSL1 in cell culture may not reflect the enzyme's true physiological role. Furthermore, cell lines are often tumor-derived or made immortal. Thus, cell lines *in vitro* often have metabolism different from the tissue from which they were derived and different cell lines have differing metabolic activities. We predict that studying the loss of ACSL1 in mice will provide a better model to study the physiological role of ACSL1.

B3. White adipose tissue Background

The main function of white adipose tissue (WAT) is to store excess body fuel in the form of TAG and to regulate satiety, food intake, insulin sensitivity, pregnancy, and menses through its endocrine activity. Humans and rodent models with lipodystrophy and lipoatrophy usually have severe insulin resistant diabetes. Conversely, humans and rodent models with obesity or excessive WAT mass often suffer from severe insulin resistant diabetes together with multiple metabolic complications. Therefore, it is clear that an optimum range of WAT mass is required to maintain normal metabolism and prevent the onset of diabetes.

How is ACSL1 regulated in adipose? *Acsl1* mRNA is the most abundantly expressed ACSL isoenzyme in rodent white adipose tissue in which the expression *acsl3*, -*4*, and -*5* is relatively minor [83]. Because adipose is the major storage site for TAG, and ACSL1 is the major ACSL isoenzyme, we thought that ACSL1 may be critical in activating FA destined for TAG synthesis. ACSL1 in adipose is regulated by a variety of physiological conditions, nutritional components, and hormones. For instance, *acsl1* transcription is upregulated in adipose/adipocytes by exposure to insulin, PPARγ agonists, and retinoic acids, all of which regulate lipid anabolism physiologically [2, 84-86]. Conversely, *acsl1* mRNA in adipose or adipocytes is down-regulated by corticosteroids, exercise training, adrenaline, and other activators of cyclic-AMP that are linked to lipid catabolism [84, 87, 88]. However, the data conflict because not all PPARγ agonists or cAMP activators increase or decrease *acsl1* mRNA.

In vitro, ACSL activity increases 100-fold and *acsl1* mRNA expression increases 160-fold in differentiating 3T3L1 adipocytes [1, 3, 89]. Meanwhile, as 3T3L1 cells differentiate into adipocytes and accumulate TAG, the expression of the other ACSL isoenzymes remains unchanged [90]. Therefore, as adipocytes accumulate lipid *in vitro*, the

expression of ACSL1 is induced, suggesting the enzyme's involvement in lipid anabolism. The typical adipocyte differentiation cocktail includes dexamethasone, 1-methyl-3-isobutylxanthine (MIX), and insulin. Dexamethasone and MIX reduce *acsl1* mRNA in 3T3L1 adipocytes, whereas, insulin increases *acsl1* mRNA. Insulin is required for insulin-like growth factor receptor (IGF-R) stimulation for mitotic clonal expansion that is essential for adipocyte differentiation in 3T3L1 cells. in contrast, mouse embryonic fibroblasts, MEFs or mesenchymal tissue containing preadipocytes, do not require mitotic clonal expansion or insulin for differentiation and lipogenesis [91]. It is unknown whether *acsl1* mRNA is induced in the presence of lipogenesis but in the absence of insulin. Perhaps insulin increases *acsl1* mRNA as a secondary effect of IGF-R stimulation, and ACSL1 may not serve a critical role in lipogenesis of differentiating 3T3-L1 cells. Differentiating primary pre-adipocytes express *l-cpt1* mRNA whereas mature adipose tissue expresses both L-CPT1 and M-CPT1 [92]. The role that FA oxidation plays in WAT has not been extensively investigated [93]. Apart from the normal demands of cellular metabolism, adipocytes require energy both to synthesize FA *de novo* and for ACS-mediated activation of FA to acyl-CoAs for TAG synthesis. The potential importance of FA β-oxidation in WAT is supported by the observation that mitochondrial proteins increase 20- to 30-fold in WAT after treatment with a PPARγ agonist or during 3T3-L1 adipocyte differentiation [94, 95]. The physiological stimuli that increase the rate of FA oxidation in WAT are unknown, but treating 3T3-L1 cells with an adipocyte-differentiation cocktail plus rosiglitazone increases the content of both mitochondrial ACSL1 protein and proteins required for FA oxidation, suggesting coordinated regulation [96]. Whether the increase in ACSL1 during adipocyte differentiation is part of the mitochondrial biogenesis or the lipogenic program is unknown.

Some research suggests that ACSL1 is not involved in lipid anabolism. For example, in humans, researchers were surprised to find that *Acsl1* mRNA in subcutaneous fat is inversely correlated with central obesity and insulin resistance in a small Swedish

cohort of healthy males [97]. In liver, heart and adipose tissue, *Acsl1* mRNA is upregulated by PPARα, a transcription factor that increases the expression of genes involved in the oxidation of FA [6]. Therefore, the role of ACSL1 in TAG formation in adipose has remained unclear. Data presented in this dissertation shows that ACSL1 is not the critical activator of FA for TAG synthesis, but that ACSL1 is critical for FA oxidation in adipose.

It is important to note that many studies do not specify the specific ACSL isoenzyme and therefore, interpretation of the specific role of the ACSL isoenzymes is difficult. It is also important to consider that most adipose-related ACSL1 research has been conducted using 3T3-L1 cells, an immortalized cell line that has undergone multiple passages and for which an artificial hormonal cocktail is used to induce the accumulation of lipid and therefore may not accurately represent the metabolism of an adipocyte *in vivo*. By creating an adipose specific knockout mouse we have studied ACSL1 physiologically.

Table 2.3. ACSL1 discrepancy in adipose

ACSL1	Fast	Refed
mRNA	-	↓
Protein	↓	↑
Activity	↓	-

The vast majority of research illustrates changes in ACSL1 in adipose tissue and adipocytes, supporting a role for ACSL1 in lipid anabolism. However, following a 48-hr fast, rat visceral white adipose has reduced total ACSL activity and reduced ACSL1 protein, but no change in *acsl1* mRNA.

Furthermore, fasting followed by refeeding for 24 hours normalizes ACSL total activity and increases ACSL1 protein, but reduces *acsl1* mRNA levels [83]. The discrepancies between ACSL1 activity, protein, and mRNA levels, highlighted by Mashek et al, indicate that the ACSL isoenzymes are under complex regulatory mechanisms that are not well understood. Moreover, most research on ACSL1 is based on changes in protein or mRNA levels that may not necessarily correlate with the activity of the enzyme, suggesting that previous research may have misleading interpretations. The antibody used to quantify ACSL1 protein

reported by Mashek et al and others does not recognize ACSL1 specifically (Li and Ellis, unpublished data). In order to ascertain the function of ACSL1 in adipose, we have specifically ablated the ACSL1 gene exclusively in adipose tissue in order to study the effects in a living system.

B4. Brown Adipose Tissue

Brown adipose tissue (BAT) functions to provide heat for mammals in response to cold exposure. The role of brown adipose tissue and its metabolism have been extensively reviewed [98-100]. Brown adipose tissue is found in small mammals including rodents and in human newborns. However, recent evidence indicates that adult humans contain BAT depots [101]. Brown adipocytes contain multi-locular lipid droplets and a high abundance of mitochondria. The mitochondria of BAT contain large amount of uncoupling protein-1, UCP1. UCP1 is located on the inner mitochondrial membrane where it uncouples the electron transport chain from ATP synthesis and is almost exclusively expressed in BAT [102]. The hydrogen ions pumped into the inner mitochondrial membrane space by the electron transport chain are pumped through the UCP1 protein, and not pumped through the ATP synthase complex, resulting in the production of heat instead of ATP. The heat-generating ability of UCP1 is thought to be an exclusive property of UCP1 and not of the related proteins UCP2, -3, -4, or -5.

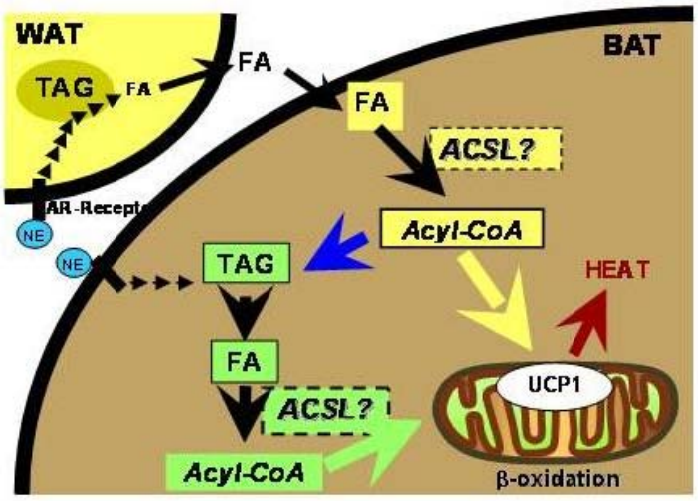

Figure 2.6 (Above). BAT produces heat through adrenergic stimuli, FA oxidation, and UCP1. UCP1 is stimulated by cold exposure via the adrenergic receptors of brown adipocytes that are activated by norepinephrine. Adrenergic signaling activates lipolysis, stimulates UCP1, and activates the transcription of multiple genes of mitochondrial biogenesis, FA oxidation, lipogenesis and *ucp1*. Under these lipolytic conditions UCP1 is activated by fatty acids, and potentially by acyl-CoA [103-105]. Both cold exposure and adrenergic stimulation cause large increases in FA oxidation by BAT, increases whole body oxygen consumption and heat production.

Cold Thermoneutral

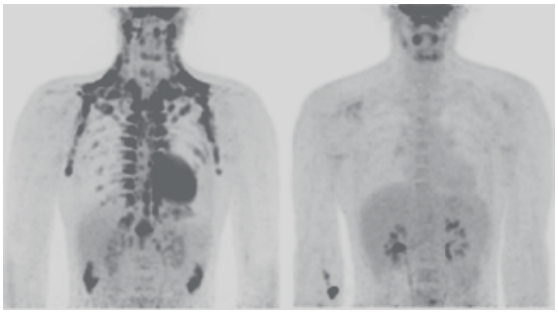

Figure 2.7 (Above). BAT Activity as Assessed by PET–CT with 18F-FDG. "Comparative PET–CT scans reveal the patterns of 18F-FDG uptake in the same subject from the lean group after exposure to cold and under thermoneutral conditions." [106]

In April of 2009 three publications in the New England Journal of Medicine were reported that identified the existence of brown adipose depots in adult humans by the uptake of 18F-fluorodeoxyglucose (18F-FDG) positron-emission tomographic and computed tomographic (PET–CT) [106-108]. These studies further characterized the adult BAT by

histology and by the mRNA expression of the BAT-specific UCP1 protein.

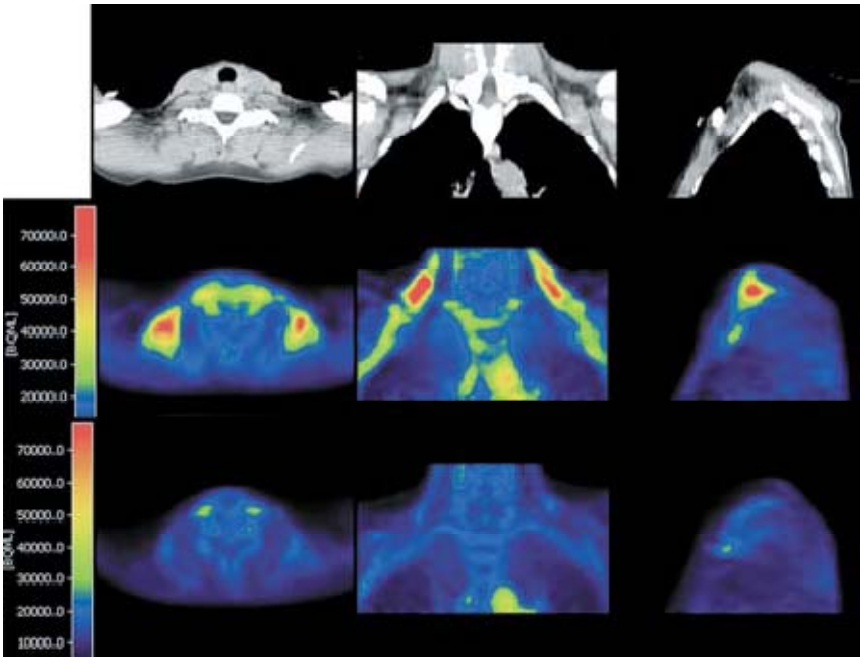

Figure 2.8. BAT in adult humans by CT-PET. "Computed Tomographic (CT) and Positron-Emission Tomographic (PET) Images from the Neck and Upper Thoracic Region, Obtained during Cold and Warm Conditions. Panel shows images of the neck and upper thoracic region from subjects. The top row shows individual CT images, the middle row shows PET images, with the glucose analogue 18F-fluorodeoxyglucose (18F-FDG) as a tracer, during cold conditions, and the bottom row shows PET images with 18F-FDG during warm conditions. The image on the left side of each row represents a transaxial slice, the image in the middle a coronal slice, and the image on the right side a sagittal slice from the region of activated brown adipose tissue. The color index to the left of the PET images shows the level of 18F-FDG uptake, with red indicating the highest level." [107]

ACSL1 and Brown Adipose Tissue. According to mRNA abundance, *acsl1* and *acsl5* are the highest expressed ACSL isoenzymes in rodent brown adipose tissue [83]. Proteomic analysis of mitochondria isolated from white adipose tissue, brown adipose tissue, and 3T3-L1 adipocytes reveals ACSL1 protein in adipose mitochondria [40]. ACSL1 and ACSL6 are particularly enriched in white adipose mitochondria, whereas ACSL5 is more abundant in mitochondria from brown adipose. Very little research has been done to elucidate the roles of ACSL1 and ACSL5 in brown adipose. ACSL protein was found to be located on the mitochondrial outer membrane through fractionation experiments on pig BAT,

however, no specification of the ACSL isoenzyme could be made at the time because ACSL had not been cloned [109]. Total ACSL activity in BAT is unchanged when rats are exposed to cold (4°C) for 0.5, 1, 7, 12 or 15 days [110]. However, the same group found a 2-fold increase in total ACSL activity in BAT from rats exposed to cold for 3 days or stimulated with a β-adrenergic agonist [111]. The reason for the discrepancy between these studies was not discussed. *Acsl5,* but not *acsl1,* mRNA is increased in the BAT of cold exposed FVB-N mice [112]. These data implicated ACSL5 in oxidation in BAT, however, LACS5, the human homolog of ACSL5, is expressed in erythrocytes which do not contain intracellular membranes (i.e. mitochondria) and do not oxidize FA, shedding doubt on ACSL5 and its role in oxidation [113]. Moreover, it is well established that mouse strains such as FVB-N and C57Bl/6 differ in their response to cold exposure and in their regulation of genes involved in adaptive thermogenesis [114, 115].

Other models of cold intolerance. Norepinephrine signaling though the β-adrenergic receptor is the most potent signal that activates cold-induced adaptive thermogenesis in BAT. This is evident from the β-adrenergic receptor knockout mice that are cold intolerant with core body temperature dropping below 30°C in a 4°C environment within 2-3 hours [116]. UCP1 knockout mice body temperature also drops below 30°C in a 4°C environment within 4-6 hours [117]. UCP1 is the only protein known to create heat by proton pumping in the mitochondria of BAT, so, it is not surprising that UCP1 knockout mice are cold intolerant. Because of the potential role that UCP1 plays in energy homeostasis, the UCP1 knockout mice were expected to be obese, however, they are lean and become no more obese on a high-fat diet than controls [118]. Alternatively, mice that almost completely lack BAT (UCP-DTA) are obese but only moderately cold intolerant with their body temperature dropping to 35°C in a 4°C environment within 30 hours [119]. The discrepancy in these phenotypes has led to exploration of alternative means of

thermogenesis and compensatory mechanisms in UCP-DTA mice which have complex non-UCP1-dependent phenotypes.

Table 2.4: Mouse models of cold sensitivity

Mouse	Time to 30°C (hours)	Function
ACSL1-KO	2-5	Oxidation
SCAD-KO	1-4	
MCAD-KO	1	
LCAD-KO	2-4	
VLCAD-KO	2-4	
ATGL-KO	3	Lipolysis
Caveolin-1-KO	24	
UCP1-KO	2-6	Uncoupling
BAT-ablated	30	
βAR-KO	2-3	NE signaling
FATP1-KO	10	FA uptake

Aside from the UCP1 protein itself, fatty acid oxidation is required for generation of protons that act as substrate for UCP1. The requirement of oxidation during cold thermogenesis is exemplified by the knock out mouse models of the acyl-CoA dehydrogenase enzymes of FA oxidation, namely, the knockout of short-chain-, medium-chain-, long-chain-, and very long-chain acyl-CoA dehydrogenase. In all these knockout mice body temperature drops below 30°C in a 4°C environment within 1-4 hours with fasting [120-122]. These data represent the critical role that FA oxidation plays in adaptive thermogenesis.

The supply of fatty acids for oxidation during adaptive thermogenesis is from intracellular and extracellular sources through the activation of lipolysis in both white and brown adipose tissue. As such, mice that lack proteins required for lipolysis, namely, adipose triacylglycerol lipase (ATGL) and caveolin-1, a protein that aids lipolytic activity, are

cold intolerant with core body temperature dropping below 30°C in a 4°C environment within and 24 hours, respectively [123, 124]. It is unknown whether intracellular-derived FA stores are metabolized by different enzymes than extracellular-derived FA. It is possible that ACSL1 activates fatty acids derived from specific pools, i.e. intra-cellular versus extra-cellular FA pools.

CHAPTER III

THE ROLE OF ACSL1 IN ADIPOSE TISSUE

The majority of studies in 3T3-L1 adipocytes and that examined *acsl1* mRNA *in vivo* conclude that the enzymatic action of ACSL1 is likely involved in the synthesis of TAG in white adipose. We and others have shown that ACSL1 mRNA abundance, protein amount, and enzyme activity are not directly correlated and that ACSL1 does not increase TAG synthesis in all cell lines and tissues. Furthermore, *acsl1* mRNA is upregulated by transcription factors that regulate both genes of FA oxidation and genes of lipogenesis. These data raise doubt that ACSL1 is involved in TAG synthesis. Therefore, we have assessed the true role of ACSL1 in adipose by knocking it out specifically in adipose of mice, *Acsl1*$^{A-/-}$ mice. Data presented in this dissertation suggest that ACSL1 is critical for activating FA for oxidation, not TAG synthesis. Impaired adipose FA oxidation in the *Acsl1*$^{A-/-}$ mice renders the mice with increased fat mass and cold intolerance.

Adipose acyl-CoA synthetase-1 directs fatty acids towards β-oxidation and is required for cold thermogenesis

Jessica M. Ellis,[1] Lei O. Li,[1] Pei-Chi Wu,[1] Timothy R. Koves,[2] Olga Ilkayeva,[3] Robert D. Stevens,[3] Steven M. Watkins,[4] Deborah M. Muoio,[2] and Rosalind A. Coleman[1]

[1]Department of Nutrition, University of North Carolina, Chapel Hill, NC 27955 US

[2]Department of Medicine, Duke University, Durham, NC 27714 US

[3]Sarah W. Stedman Nutrition and Metabolism Center, Duke University, Durham, NC 27710

[4]Lipomics Technologies, West Sacramento, CA 95691 US

Corresponding author: Rosalind A. Coleman, Department of Nutrition, CB# 7461, University of North Carolina at Chapel Hill, Chapel Hill, NC 27599, USA.

Tel: 919-966-7213

Fax: 919-843-8555

email: rcoleman@unc.edu

Running title: Adipose-specific acyl-CoA synthetase-1 knockout

Keywords: fatty acid oxidation; cold thermogenesis; brown adipose; triacylglycerol

Abbreviations: ACSL, long-chain acyl-CoA synthetase; ASM, acid soluble metabolites; BAT, brown adipose tissue; CO_2, carbon dioxide; DAG, diacylglycerol; FA, fatty acids; PL, phospholipids; TAG, triacylglycerol; UCP1, uncoupling protein one; WAT, white adipose tissue.

Summary:

Acyl-CoA synthetase-1 (ACSL) contributes 80% of total ACSL activity in adipose tissue and was believed to be essential for the synthesis of triacylglycerol. We predicted that an adipose-specific knockout of ACSL1 (*Acsl1*$^{A-/-}$) would be lipodystrophic, but, compared to controls, *Acsl1*$^{A-/-}$ mice had 30% greater fat mass when fed a low fat diet, and gained weight normally when fed a high fat diet. *Acsl1*$^{A-/-}$ adipocytes incorporated [^{14}C]oleate into glycerolipids normally, but fatty acid oxidation rates were 50-90% lower than in control adipocytes and mitochondria. *Acsl1*$^{A-/-}$ mice were markedly cold intolerant, and β_3-adrenergic agonists did not increase oxygen consumption, despite normal adrenergic signaling in brown adipose tissue. The reduced adipose FA oxidation and marked cold intolerance of *Acsl1*$^{A-/-}$ mice indicate that normal activation of FA for oxidation in adipose tissue *in vivo* requires ACSL1. Thus, ACSL1 has a specific function in directing the metabolic partitioning of fatty acids towards β-oxidation.

Highlights

- Adipose knockout of long-chain acyl-CoA synthetase 1 decreases ACS activity 80%
- Mice lacking ACSL1 are cold intolerant
- ACSL1 activates fatty acids that are directed towards β-oxidation

•

Introduction

Dysfunctional lipid metabolism underlies the development of obesity and obesity-related complications such as hepatic steatosis, diabetes, and heart disease. Although the mechanisms that regulate the cellular uptake, activation, and metabolism of fatty acid (FA) are not fully understood, nearly all pathways of FA metabolism require the acyl-CoA synthetase–mediated conversion of FAs to acyl-CoAs (FA + CoA + ATP → acyl-CoA + AMP + PPi). Acyl-CoAs have multiple fates, including use in complex lipid formation and lipid remodeling, effects on signal transduction, activation of transcription factors, and oxidation to provide cellular energy. Long-chain acyl-CoAs are formed by a family of five acyl-CoA synthetases (ACSL), ACSL1, ACSL3, ACSL4, ACSL5, and ACSL6, and by several fatty acid transport proteins (FATP). ACSL isoenzymes are intrinsic membrane proteins whose active sites face the cytosol to produce acyl-CoAs which are either partitioned into the facing membrane monolayer where they can encounter downstream metabolic enzymes [19, 125], or transported to different organelles by the cytosolic acyl-CoA binding protein [126]. The ability of amphipathic acyl-CoAs to move freely within a single membrane monolayer or to be transported to distant membranes should render all acyl-CoAs metabolically equivalent, no matter which ACSL isoenzyme catalyzes their formation. Yet, gain-of-function studies suggest that each of the ACSL isoform has a distinct function in directing acyl-CoAs to one or more specific downstream pathways [34, 36].

The functions of the ACSLs are of particular interest in adipose tissue because of the central role that white adipose tissue (WAT) plays in energy storage and that brown adipose tissue (BAT) plays in energy dissipation. In WAT, *Acsl1* mRNA is the most abundantly expressed isoform, with relatively lower expression of *Acsl3*, *-4*, and *-5* [27]. *Acsl1* mRNA in liver is upregulated by PPARα ligands [85], whereas its mRNA in WAT is increased by PPARγ agonists (Gerhold, 2002; Shimomura et al., 1993). In differentiating 3T3-L1 adipocytes, ACSL

specific activity and mRNA expression increase 100- and 160-fold, respectively [3, 4], whereas the expression of the other *Acsl* isoenzymes remains unchanged [90]. This induction of *Acsl1* expression suggested that ACSL1 is upregulated as part of the program of adipocyte differentiation culminating in triacylglycerol (TAG) synthesis and storage. Consistent with this interpretation, an expression cloning strategy designed to find cDNAs that augment FA uptake and incorporation into TAG cloned ACSL1 [80]. Further, overexpressed ACSL1 in 3T3-L1 adipocytes increases FA uptake and incorporation into TAG [23, 38, 71]. In order to examine the putative role of ACSL1 in TAG synthesis, we created a mouse deficient in adipose ACSL1, and predicted that these mice would be unable to synthesize and store TAG in adipocytes. Surprisingly, however, the $Acsl1^{A-/-}$ mice had normal fat stores, but severely impaired adipose FA oxidation, suggesting not only that ACSL1 catalyzes the initial required step in FA oxidation, but also that it specifically directs FA towards mitochondrial β-oxidation.

Results

Generation of mice that lack ACSL1 specifically in adipose tissue

Mice with *Loxp* sequences inserted on either side of exon 2 in the *Acsl1* gene [127] and backcrossed to the C57Bl/6 strain six times were crossed with mice in which Cre expression is driven by the aP2 promoter [B6.Cg-Tg (Fabp4-cre) 1Rev/J; Jackson Laboratories, Bar Harbor ME] to generate adipose-specific *Acsl1* knockout mice (*Acsl1*$^{A-/-}$). Littermates lacking the C*re* gene (*Acsl1*$^{flox/flox}$) were used as controls.

ACSL1 protein was virtually absent in brown, gonadal, and inguinal adipose tissue from *Acsl1*$^{A-/-}$ mice (**Fig. 1A**). ACSL specific activity was 80% lower than in controls, confirming that ACSL1 is, functionally, the major ACSL in adipose tissue (**Fig. 1B**), with the remaining 20% of ACSL activity catalyzed by other ACSL isoenzymes in adipocytes and all ACS enzymes in stromovascular tissue [83]. Confirming the tissue-specificity of the knockdown, ACSL1 protein and total ACSL specific activity were unaffected in *Acsl1*$^{A-/-}$ liver (**Fig. 1A, B**). Real-time PCR showed nearly absent expression of *Acsl1* mRNA in *Acsl1*$^{A-/-}$ gonadal and brown adipose tissue, but unchanged expression of the other four *Acsl* isoenzymes and a 50% reduction in *Fatp1* mRNA, a related ACS (**Fig. 1C, D**). Thus, other acyl-CoA synthetases did not compensate for the loss of ACSL1.

Acsl1$^{A-/-}$ mice have increased fat mass and synthesize TAG normally

Despite the 80% loss of adipose ACSL activity, *Acsl1*$^{A-/-}$ mice had increased adiposity. When fed a 10%-fat diet, *Acsl1*$^{A-/-}$ body weights were similar to controls (**Fig. 2A**), but MRI analysis showed that the mice had 30% more body fat (**Fig. 2B**). Consistent with the MRI data, gonadal fat depot weights were ~40% greater in mice fed chow or 10%-fat diets (**Fig. 2C**). Gonadal

adipose tissue histology, adipocyte size, GPAT specific activity, and AMPK phosphorylation were similar between genotypes (**Fig. 2D-G).** No genotype differences in liver or BAT weights were observed.

No diet-related differences were observed between genotypes in plasma glucose, FA, cholesterol, or insulin concentrations (**Table S1**). However, plasma TAG concentrations were 17% lower in *Acsl1*$^{A-/-}$ mice. A 45%-fat diet resulted in weight gain, adiposity, and insulin resistance that was similar in both genotypes (**Fig. 2A, Table S1**). Loss of ACSL1 could theoretically change the cellular content and ratio of its FA substrate and acyl-CoA product, thereby altering the availability of ligands for PPARγ and PPARα [128, 129], however target genes of these transcription factors did not change significantly in *Acsl1*$^{A-/-}$ gonadal WAT (**Table S2**).

When fed a low-fat diet, the amount of phospholipid extracted from epididymal WAT was similar in both genotypes, but *Acsl1*$^{A-/-}$ WAT contained more TAG, DAG, and FA per fat pad (**Fig. 2H**). With the high-fat diet, no differences were present between control and *Acsl1*$^{A-/-}$ lipid classes in epididymal WAT. BAT from *Acsl1*$^{A-/-}$ and control mice fed either diet also contained similar amounts of all lipid classes (**Fig. S1A, B**). Thus, lack of ACSL1 did not impair adipose TAG accumulation.

Confirming normal TAG synthesis in both isolated white gonadal adipocytes and cultured primary white adipocytes from control and *Acsl1*$^{A-/-}$ mice, the rates of [1-^{14}C]oleate incorporation into TAG and phospholipid were similar, indicating that the lack of ACSL1 did not impair FA incorporation into complex lipids (**Fig. 2I,J**). Thus, despite greater than 100-fold increases in *Acsl1* mRNA and ACSL specific activity during fat cell differentiation [3, 4], TAG synthesis does not require FA activation by ACSL1. We conclude that the increased fat mass did not result from impaired lipolysis because in 24h fasted mice and in media from white adipose tissue

explants with or without exposure to lipolytic stimuli (**Fig. 2K-M, Table S3**) FA and glycerol release were similar between genotypes.

Differences in FA species content in adipose tissue.

We did not expect to find major changes in FA species because each of the purified ACSL isoenzymes *in vitro* can activate a wide range of long-chain, saturated and unsaturated FA [90]. However, compared to controls, *Acsl1*$^{A-/-}$ mice fed both the low-fat and high-fat diets contained 20-30% less 18:2n6 in TAG from brown and gonadal white adipose (**Fig. S1C, D**). The TAG fraction of BAT from *Acsl1*$^{A-/-}$ mice was composed of 15% more 16:0 than controls fed the low-fat diet (**Fig. S1E**). In *Acsl1*$^{A-/-}$ BAT, the PL fraction from mice fed the high-fat diet contained 30% more 16:0 and 15%, 22%, and 14% less 18:0, 18:2n6, and 20:4n6, respectively, than controls (**Fig. S1F**). No other differences in the major fatty acid species were observed. These small, but statistically significant, alterations in lipid composition of adipose tissues suggest that ACSL1 does contribute to the relative content of esterified FA species in neutral lipids and phospholipids, despite the minimal differences in FA preference observed *in vitro*.

Fatty acid oxidation was impaired in white adipocytes from *Acsl1*$^{A-/-}$ mice

Compared to mature adipocytes isolated from control mice, the rate of [1-^{14}C]oleate incorporation into CO_2 and acid soluble metabolites (ASM) was 50% lower in *Acsl1*$^{A-/-}$ adipocytes (**Fig. 2N**). CO_2 and ASM represent complete and incomplete products of fatty acid oxidation; thus, the 50% reduction of FA incorporation into these oxidative products reflects reduced β-oxidation and suggests that impaired FA catabolism could have caused the larger WAT depots in the *Acsl1*$^{A-/-}$ mice.

Decreased FA oxidation rendered *Acsl1*$^{A-/-}$ mice cold intolerant

FA oxidation increases markedly in BAT during cold exposure. To generate heat and maintain normal body temperature, ATP production is reduced when activated uncoupling protein (UCP1) increases the flux of protons through the electron transport chain and dissipates the mitochondrial proton gradient [130]. Fasted wildtype mice can maintain their body temperature above 35°C for as long as 24 h at 4°C [131]. In striking contrast, however, the body temperature of the *Acsl1*$^{A-/-}$ mice fell below 30°C within 3 h (**Fig. 3A**). During cold exposure, both genotypes shivered similarly, and gastrocnemius total ACSL activity (**Fig. S4A**) and *Acsl1* mRNA abundance (data not shown) did not change in *Acsl1*$^{A-/-}$ mice. In shivering muscle, fuel preference and the contribution of muscle heat to total body heat remain unclear [132]; however, plasma FFA and VLDL were not limiting for either *Acsl1*$^{A-/-}$ skeletal muscle or BAT (**Fig. 6C, D)**.

Direct measurements of FA oxidation rates in BAT homogenates from *Acsl1*$^{A-/-}$ mice showed that the rate of [1-^{14}C]palmitate incorporation into CO_2 and ASM was 36% lower than controls (**Fig. S5C**). Because label dilution occurs when fatty acid oxidation is measured in cells with a high lipid content, we confirmed this oxidation defect by monitoring O_2 consumption in conscious *Acsl1*$^{A-/-}$ and control mice in Oxymax chambers. Whole body O_2 consumption normally increases in response to adrenergic stimuli and reflects an increase in electron transport chain activity. Isoproterenol, a non-specific β-adrenergic receptor agonist, increased O_2 consumption 51% in control mice, but only 18% in *Acsl1*$^{A-/-}$ mice (**Fig. 3B**). This blunted response indicates that whole body oxidation is diminished. When CL-316243, an adipose-specific, β_3-adrenergic receptor agonist [133] was injected, O_2 consumption increased 30% in control mice, but only 2% in *Acsl1*$^{A-/-}$ mice, showing that the block in adrenergic-mediated oxidation was adipose-specific (**Fig. 3B,S5B**).

In mitochondria from *Acsl1*$^{A-/-}$ BAT, the production of CO_2 from [1-^{14}C]palmitate oxidation was reduced 62% (**Fig. 3E,G**), and this reduction in mitochondrial FA oxidation correlated

directly with the amount of mitochondrial ACS activity and ACSL1 protein present in each of three mitochondrial preparations (**Fig. 3F,S4F,E**). In contrast, CO_2 production from [1-^{14}C]pyruvate oxidation was similar to that of control mitochondria, showing that *Acsl1*$^{A-/-}$ BAT mitochondria are functional for substrates other than FA. The 31% reduction in [1-^{14}C]palmitoyl-CoA oxidation (**Fig. 3G**) suggests that FA oxidation may require the generation of acyl-CoA at the mitochondrial membrane, and/or that the mechanism by which ACSL1 directs its acyl-CoA product towards mitochondrial oxidation may be partially disrupted by homogenization. The rate of oxygen consumption in control and *Acsl1*$^{A-/-}$ BAT mitochondria was similarly increased by UCP1-dependent pyruvate stimulation and, in both genotypes, GDP effectively reduced oxygen consumption by inhibiting UCP1 (**Fig. S4**). These data show that ACSL1 deficient BAT mitochondria have full UCP1 activity and that *Acsl1*$^{A-/-}$ cold intolerance is not due to impaired UCP1 function. Taken together, these data from live mice, BAT homogenates, and isolated mitochondria indicate that cold intolerance of the *Acsl1*$^{A-/-}$ mice resulted from impaired FA oxidation and show that ACSL1 is absolutely required for cold-adaptive thermogenesis in BAT.

After 4 h at 4°C, BAT from control mice depleted its lipid droplets, but lipid droplets were retained in *Acsl1*$^{A-/-}$ BAT (**Fig. 3C**). Control mice lost ~50% of BAT lipid stores after 4 h of cold exposure, whereas the TAG content in *Acsl1*$^{A-/-}$ BAT did not change (**Fig. 3D)**. Liver and WAT histology was similar at 21^{o}C and 4^{o}C in both genotypes (data not shown). Although TAG retention in *Acsl1*$^{A-/-}$ BAT after cold exposure could be due to impaired lipolysis, the increase in plasma FA and glycerol in cold-exposed *Acsl1*$^{A-/-}$ mice is consistent with active TAG lipolysis in WAT (**Fig. 6B,C**), and in differentiated primary brown adipocytes from *Acsl1*$^{A-/-}$ mice, the release of FA into the media was greater than controls under basal conditions and similar after adrenergic stimuli, demonstrating that *Acsl1*$^{A-/-}$ brown adipocytes lipolyzed intracellular triacylglycerol normally (**Fig. 3I**). Surprisingly, compared to control cells, glycerol release in *Acsl1*$^{A-/-}$ brown adipocytes was blunted by ~50% after adrenergic stimulation (**Fig. 3H**). Reduced

release of glycerol by *Acsl1*$^{A-/-}$ brown adipocytes could result from increased conversion to glycerol-3-P for lipid synthesis or because the glycerol was oxidized as an alternative substrate. After 3 h of isoproterenol exposure, both *Acsl1*$^{A-/-}$ and control differentiated brown adipocytes had similar ~33% reductions in [^{14}C]oleate-labeled TAG (**Fig. 3J**), indicating that both lipolysis and FA re-esterification after lipolysis were unaffected by ACSL1 deficiency. [1-^{14}C]Oleate incorporation into ASM was 90% lower in *Acsl1*$^{A-/-}$ brown adipocytes than in controls, consistent with the marked decrease in FA oxidation (**Fig. 3K**). Thus, in cold-exposed *Acsl1*$^{A-/-}$ BAT, the retention of lipid droplets probably reflects an influx of FA that cannot be oxidized without ACSL1 and are, therefore, incorporated into neutral lipid.

Thermogenic regulation of adrenergic and oxidative genes was normal in *Acsl1*$^{A-/-}$ mice

β-adrenergic signaling during cold exposure induces the expression of genes that activate mitochondrial biogenesis, heat production, and oxidative capacity. At 4^{o}C both control and *Acsl1*$^{A-/-}$ mice upregulated mRNA levels of *Ucp1* and PPAR-γ coactivator-1α (*Pgc1α*) 2- and 30-fold, respectively (**Fig. 4A,B**). These increases indicate that adrenergic-stimulated signaling was unimpaired in *Acsl1*$^{A-/-}$ BAT [134].

Compared to controls, the mRNA expression of muscle-type carnitine palmitoyltransferase-1 (*mCpt1*) was significantly higher in the *Acsl1*$^{A-/-}$ BAT at 21^{o}C, and cytosolic thioesterase-1 (*Cte1*) was significantly higher after cold exposure, suggesting that the lack of ACSL1 might increase cellular FA to activate PPARα-mediated transcription (**Fig. 4C**). However, the expression of other PPARα-regulated genes, medium-chain acyl-CoA dehydrogenase (*Mcad*), acyl-CoA oxidase (*Aox*), and *Pparα,* did not differ between the genotypes, suggesting that the lack of ACSL1 does not affect all PPARα target genes with or without 4 h of cold exposure.

Because *Acsl1*$^{A-/-}$ BAT retained lipid droplets after cold exposure, we measured genes that encode lipogenic and substrate-producing proteins that would normally increase during cold

exposure. *Acsl1*$^{A-/-}$ BAT should have been able to lipolyze and/or endocytose circulating TAG-rich lipoproteins and to make use of these exogenous FA sources, because the lipogenic genes lipoprotein lipase (*Lpl*) and VLDL-receptor (*Vldl-r*) had similar expression patterns with or without cold exposure in both genotypes (**Fig. 4D**). Similarly, 1-acylglycerol-3-phosphate O-acyltransferase-1 (*Agpat1*) increased in both genotypes, as did *Gpat4*, a major GPAT in BAT [135]. These data suggest that the retained lipid droplets in *Acsl1*$^{A-/-}$ BAT were not caused by abnormal regulation of genes required for TAG synthesis.

BAT expression of *Acsl3* and *Acsl4* (but not *Acsl1, Acsl5, or Acsl6*) was upregulated in both genotypes in response to cold (**Fig. 4E**), and long-chain acyl-CoA content in cold exposed *Acsl1*$^{A-/-}$ BAT did not differ from controls (**Fig. 6E**). These data indicate that acyl-CoAs synthesized by other ACSL isoenzymes were unavailable for β-oxidation and that maintenance of normal body temperature requires acyl-CoAs synthesized by ACSL1.

Acyl-carnitines were reduced in *Acsl1*$^{A-/-}$ BAT

To gain further insight into the consequences of ACSL1 deficiency, we used mass spectrometry to profile a targeted array of intermediary metabolites. Long-chain acyl-carnitines accumulate when their production by mitochondrial CPT1 exceeds their flux through β-oxidation [136]. In wild type mice, cold exposure lowered major long-chain acyl-carnitine species and increased β-hydroxybutyryl-carnitine (4-OH), a strong marker of increased β-oxidation and ketone metabolism (**Figs. 5A-C, S2B**). This profile is consistent with activation of mitochondrial uncoupling and a shift in flux limitation from long-chain acyl-CoA dehydrogenase to short-chain β-hydroxy-acyl-CoA dehydrogenase. In contrast, under thermoneutral conditions, BAT concentrations of most long-chain acyl-carnitine species were markedly lower in *Acsl1*$^{A-/-}$ mice compared to controls. Taken together with our measures of FA oxidation, this finding suggests impaired delivery of long-chain acyl-CoAs to CPT1. During cold exposure, although *Acsl1*$^{A-/-}$ BAT had increases in several long- and short-chain acyl-carnitines, these remained

substantially lower than in controls (**Figs. 5A-C, S2B,C**). BAT levels of acetyl-carnitine (C2), which is derived from acetyl-CoA, were similar between genotypes, suggesting that increased catabolism of glucose and/or amino acids in the *Acsl1*$^{A-/-}$ mice partially compensated for impaired FA oxidation.

In control mice the BAT content of most organic acids was maintained during cold exposure, with the exceptions of lactate and succinate which declined (**Fig. 5D-F**). Compared to controls, lactate was lower in *Acsl1*$^{A-/-}$ mice, regardless of temperature, consistent with enhanced pyruvate oxidation and a shift in cellular redox state. The lower levels of succinate in *Acsl1*$^{A-/-}$ BAT may reflect disinhibition of succinate dehydrogenase (complex II). Notably, BAT levels of several amino acid-derived CoA species (propionyl-CoA, succinyl-CoA, 3-methylcrotonyl-CoA, isovaleryl-CoA) were elevated in *Acsl1*$^{A-/-}$ compared to control mice, principally during cold exposure (**Fig. 5G,H**). These elevations are consistent with a compensatory increase in protein catabolism and amino acid oxidation. Supporting this interpretation, the concentrations of branched chain and anaplerotic amino acids (valine, leucine/isoleucine, tyrosine) were elevated in the *Acsl1*$^{A-/-}$ mice, whereas alanine, the major gluconeogenic amino acid, was decreased (**Fig. 5I,J**).

Hypoglycemia and hyperlipidemia in *Acsl1*$^{A-/-}$ mice after adrenergic stimuli

Plasma glucose decreased in both genotypes during cold exposure, however, the plasma glucose concentration in *Acsl1*$^{A-/-}$ mice fell 58% more than in the controls (**Fig. 6A**). Similarly, after β-adrenergic stimulation with isoproterenol or CL-316243, *Acsl1*$^{A-/-}$ plasma glucose was 36% or 19% lower, respectively, than controls. The larger decrements in glucose in *Acsl1*$^{A-/-}$ mice after cold exposure and β-adrenergic agonists, but not after 24 h of fasting (**Table S3**), suggest enhanced glucose use by *Acsl1*$^{A-/-}$ BAT. Plasma glycerol increased similarly in both genotypes, both during cold exposure and after isoproterenol injection; however, in response to

CL-316243, circulating glycerol increased 14% in controls, but decreased 15% in *Acsl1*$^{A-/-}$ mice, consistent with the reduced glycerol release by *Acsl1*$^{A-/-}$ primary brown adipocytes (**Fig. 3H**). Again, the glycerol decrease in BAT may reflect its increased use as an alternate oxidative substrate (**Fig. 6B**). FA concentrations after cold exposure or CL-316243 were 30% higher in *Acsl1*$^{A-/-}$ mice compared to controls (**Fig. 6C**); this increase in plasma FA induced by β-adrenergic stimuli, but not after 24 h of fasting, provides additional evidence for intact *Acsl1*$^{A-/-}$ lipolytic activity and is consistent with diminished use of FA for oxidation in BAT. In response to cold exposure, plasma TAG, another potential source of FA for BAT metabolism, decreased 41% in control mice, but was unchanged in *Acsl1*$^{A-/-}$ mice despite elevated *Lpl* mRNA (**Figs. 6D, 4E**), probably as a result of hepatic recycling of the elevated plasma FA into VLDL.

Discussion

After a long-chain FA enters a cell, its metabolic fate is determined by the metabolic demands of the cell, the availability of other energy substrates, PPARα- and PPARγ-mediated changes in enzymes of complex lipid synthesis and β-oxidation [137], and the relative content of intracellular AMP which controls AMP-activated kinase and, thus, CPT1 [138]. Here we show that ACSL1 contributes critically to adipose FA metabolism by catalyzing the formation of acyl-CoAs that are used for β-oxidation. If all acyl-CoAs were metabolically equivalent, one would expect that the rates of acyl-CoA incorporation into all metabolic end products would be diminished equally and that adipose from *Acsl1*$^{A-/-}$ mice would have impairments in both FA oxidation and complex lipid synthesis. However, the role of adipose ACSL1 in catalyzing the key initial step in FA oxidation is supported by the normal rate of FA incorporation into complex lipids and the 50-90% reduction in the rate of FA oxidation in white and brown adipocytes and in BAT mitochondria from *Acsl1*$^{A-/-}$ mice, together with the inability of *Acsl1*$^{A-/-}$ BAT to oxidize FA for thermogenesis. Although the content of acyl-CoA in BAT was similar in control and *Acsl1*$^{A-/-}$ mice, these acyl-CoAs were unavailable for β-oxidation in the absence of ACSL1. The inability of the other ACSL isoenzymes to direct acyl-CoAs towards β-oxidation, especially during the physiological stress of acute cold exposure in BAT, indicates that ACSL1 has a distinct function in partitioning FA, and that the other ACSL isoenzymes in adipose tissue cannot compensate for its absence. Our data also suggest that the importance of FA oxidation in WAT has been underestimated.

Acute cold exposure stimulates norepinephrine release, which induces adipocyte TAG lipolysis via β-adrenergic receptors (**Fig. 7**). In BAT, lipolyzed FA activates UCP1 to dissipate the mitochondrial proton gradient; activation of UCP1 results in energy expended in the form of heat rather than ATP generation. Thermogenesis is maintained primarily through FA oxidation; glucose cannot maintain euthermia at 4^{o}C in knockout mice deficient in short-chain-, medium-

chain-, long-chain-, or very-long-chain acyl-CoA dehydrogenases [139-141]. When *Acsl1*$^{A-/-}$ mice were exposed to a 4°C environment, their body temperature dropped below 30°C within 2 to 5 h, despite the normal increase in BAT catecholamine-regulated genes. Because no method exists to distinguish between FA and acyl-CoAs as activators of UCP1 [142, 143], the actual activator of UCP1 could be acyl-CoA generated by ACSL1. If this were true, *Acsl1*$^{A-/-}$ mice would be cold intolerant because UCP1 is not activated. However, impaired acyl-CoA oxidation was observed directly in BAT mitochondria, brown primary adipocytes, and BAT homogenates, and in isolated gonadal adipocytes which do not require UCP1 activation. In addition, compared to control mice, the *in vivo* rate of oxygen consumption of *Acsl1*$^{A-/-}$ mice at 21°C was 60% lower, and when stimulated by isoproterenol or by an adipose-specific β_3 adrenergic receptor agonist, was more than 90% lower, indicating reduced flux through the electron transport chain and reduced adipose mitochondrial oxidation. Finally, *Acsl1*$^{A-/-}$ UCP1 uncoupling was activated by pyruvate and inhibited by GDP, indicating normally activated UCP1 (**Fig. S4**) [144].

The role that FA oxidation plays in WAT has not been extensively investigated [93]. Apart from the normal demands of cellular metabolism, adipocytes require energy both to synthesize FA *de novo* and to activate FA to acyl-CoAs for TAG synthesis. Our data show that the loss of ACSL1 in WAT reduced FA oxidation 50% and resulted in a 30% increase in adipose mass. Although it is possible that ACSL1 is not the sole isoform in WAT that can activate the FA that is targeted towards β-oxidation, we attribute the increased WAT mass in *Acsl1*$^{A-/-}$ mice to diminished use of FA for energy generation within WAT itself, because mice that cannot use BAT for thermogenesis are not obese unless they are kept at a thermoneutral temperature [145]. The potential importance of FA β-oxidation in WAT is supported by the observation that mitochondrial proteins increase 20- to 30-fold in WAT after treatment with a PPARγ agonist or during 3T3-L1 adipocyte differentiation [94, 95]. The physiological stimuli that increase the rate of FA oxidation in WAT are unknown, but treating 3T3-L1 cells with an adipocyte-differentiation

cocktail plus rosiglitazone increases the content of both mitochondrial ACSL1 protein and proteins required for FA oxidation, suggesting coordinated regulation [96].

The AMP generated by the ACSL1 reaction may activate AMP kinase in 3T3-L1 adipocytes stimulated with isoproterenol or forskolin [51, 146]. However, AMPK phosphorylation was not altered in *Acsl1*$^{A-/-}$ WAT (**Fig. 2F**), and acute cold exposure does not activate AMPK in BAT [50]. Thus AMPK activity does not mediate the cold intolerance of *Acsl1*$^{A-/-}$ mice. When RNAi was used to knockdown ACSL1 in 3T3-L1 adipocytes [146], the cells increased FA efflux during lipolysis, suggesting that ACSL1 activates and re-esterifies FA that has been lipolyzed from intracellular TAG. Our results suggest a different function. If reesterification were impaired in *Acsl1*$^{A-/-}$ adipose, one would expect that an acute cold challenge would deplete TAG stores in BAT and that WAT would contain less TAG. However, *Acsl1*$^{A-/-}$ mice retained their BAT lipid stores at 4^{o}C, suggesting that reesterification was not diminished. Further, in *Acsl1*$^{A-/-}$ primary brown adipocytes, loss of [^{14}C]-labeled FA in TAG after lipolytic stimuli was similar to controls, and in white adipose explants, the release of FA and glycerol was similar between genotypes with or without lipolytic stimuli. Although the increased release of FA from brown adipocytes (Fig. 3I) could suggest diminished reesterification under basal conditions, both genotypes had similar losses of [^{14}C]oleate that had been incorporated into TAG and in the release of FA under lipolytic conditions. These data confirm normal rates of lipolysis and, together with the cold intolerance and increased adipose mass of the *Acsl1*$^{A-/-}$ mice, are consistent with normal FA reesterification. In fact, a proteomics study demonstrates marked differences in the protein expression of mitochondria from 3T3-L1 adipocytes and those from primary mouse adipocytes, so it is not surprising to find functional differences in these two cell types [40, 146].

Based on the dramatic increase in *Acsl1* mRNA and total ACSL activity in differentiating 3T3-L1 adipocytes [3, 4], we had predicted that adipocyte ACSL1 would catalyze the synthesis of acyl-CoAs destined for TAG synthesis. However, both mature and primary differentiated

white adipocytes from *Acsl1*$^{A-/-}$ mice incorporated [^{14}C]oleate into TAG normally, and *Acsl1*$^{A-/-}$ fat depots were larger than those of controls. Further, *Acsl1*$^{A-/-}$ mice became obese and insulin resistant when fed a high-fat diet. Although the lack of ACSL1 in white and brown adipose tissue reduced ACSL specific activity by 80%, the remaining ACSL activity, derived from other ACSL and FATP isoenzymes, was able to synthesize acyl-CoAs directed towards normal TAG biosynthesis. Thus, ACSL1 is not required for TAG synthesis in adipose tissue.

How does ACSL1 channel acyl-CoAs towards β-oxidation? In adipocytes, subcellular fractionation studies identified ACSL1 on the plasma membrane, microsomes and mitochondria [71], on GLUT4 vesicles [75], and on lipid droplets [76]. In BAT and WAT ACSL1 protein has also been found in mitochondria fractions (this ms; [40]). However, even if ACSL1 were located solely on the mitochondrial outer membrane, its ability to channel its acyl-CoA product towards β-oxidation remains difficult to conceptualize. Long-chain acyl-CoAs are water-soluble, amphipathic molecules that can partition into membranes or bind to cytosolic carriers like acyl-CoA binding protein. Thus, acyl-CoAs should be able to move freely within the membrane monolayer at their site of synthesis, and to travel between different organelles. Direct physical interaction of ACSL1 with other proteins, such as CPT-1, is the most likely explanation for acyl-CoA channeling, but evidence for such interaction is lacking.

In summary, the loss of ACSL1 in adipose tissue produced mice with increased adiposity and severe cold intolerance. Adipocytes derived from *Acsl1*$^{A-/-}$ mice had normal rates of FA incorporation into TAG and normal loss of TAG stores after lipolysis, but had reduced rates of FA oxidation. Although deficient ACSL1 in liver, which expresses relatively more of the ACSL4 and ACSL5 isoenzymes, results in only a minor defect in FA oxidation [127], we conclude that the function of ACSL1 in adipose tissue is to activate FA destined for β-oxidation.

Experimental Procedures

Animal Treatment: *Acsl1*$^{A-/-}$ and littermate *Acsl1*$^{flox/flox}$ control mice were housed in a pathogen-free barrier facility (12 h light/dark cycle) in accordance with the UNC IACUC, with free access to water and food (Prolab RMH 3000 SP76 chow). For the diet study, mice were fed a low-fat (10%) diet (D12450B, Research Diets) or a high-fat (45%, primarily from lard) diet (D12451) *ad libitum* from age 8 to 25 wk. Weights were measured weekly. Body fat mass was assessed by magnetic resonance imaging analysis (EchoMRI-100, Echo Medical Systems, LLC) in 5 mo old mice. For thermogenesis experiments, mice were fasted for 4 h and placed in a 4°C environment without food. Temperature was measured hourly with a rectal probe thermometer (Thermalert TH-5, physitemp). Mice were removed from the cold when core temperature dropped below 28°C or at 4 h. Rates of O_2 consumption were determined in Oxymax chambers (Columbus Instruments) after mice were acclimated overnight. Data were collected from mice for 3 h after saline injection. After isoproterenol or CL-316243 was injected (10 mg/kg), O_2 consumption was measured for an additional 3 h, and then plasma was collected in 5% 0.5 M EDTA. Plasma TAG, beta-hydroxybutyrate (Stanbio), cholesterol, FFA, glucose (Wako), and free and total glycerol (Sigma) were measured colorimetrically. Adiponectin was measured by ELISA (Linco). Oral glucose tolerance tests were performed by gavaging with glucose (2.5 mg/kg body weight) and measuring tail blood glucose at baseline, 15, 30, 60, and 120 minutes (One Touch Ultra glucometer, Lifescan, Inc).

Enzyme Assays: ACSL initial rates were measured with 50 μM [1-^{14}C]palmitic acid, 10 mM ATP, and 0.25 mM CoA with total membrane fractions (0.5-4.0 μg) [147]. GPAT was measured with 800 μM [^{3}H]glycerol-3-phosphate and 82.5 μM palmitoyl-CoA [148].

Adipocyte studies: Adipose explants were isolated and release of FFA and glycerol was measured [149]. Epididymal adipocytes were isolated [150]. Rates of CO_2 and ASM production

from [1-^{14}C]oleate (Perkin Elmer) were measured in aliquots of the reaction mixture after incubating with 0.5 mL buffer containing 10 μM [1-^{14}C]oleate for 1.5 h in a 10% adipocyte solution. The incubation chamber contained a center well filled with filter paper and was sealed with a rubber stopper. Carbon dioxide was trapped by adding 200 μl 70% perchloric acid to the reaction mixture and 300 μl of 1 M NaOH to the center well, and incubating the samples at RT for 45 min. The center well was then placed into scintillation fluid and counted. The acidified reaction mixture was incubated overnight at 4°C and centrifuged at 4,000 rpm for 30 min before aliquots of the supernatant were counted for [^{14}C]-labeled ASM. For FA incorporation, a 10% adipocyte solution was incubated with 0.5 mL buffer containing 10 μM [1-^{14}C]oleate and 90 μM unlabeled oleate for 2 h. Brown and white pre-adipocytes from control and *Acsl1*$^{A-/-}$ adipose tissue [151] were differentiated into adipocytes for 7-14 days and exposed to 500 μM oleate with 0.6 μCi [1-^{14}C]oleate per 60 mm dish for 3 hours. Cells were then harvested or labeled media was removed, replaced with growth media for 21 hours and cells were harvested or 10 μM isoproterenol was added to media for an additional 3 hours followed by harvest. FA released into the media were measured colorimetrically (Wako) in unlabeled control plates. Total lipid was extracted from the cells into $CHCl_3$ [152]. The lipid extract was dried under N_2, resuspended in $CHCl_3$ and chromatographed with authentic lipid standards run in parallel on 0.25-mm silica gel G plates in hexane:ethyl ether:acetic acid (80:20:1; v/v). The ^{14}C-labeled lipids were detected and quantified with a Bioscan 200 Image System.

Fatty acid oxidation in BAT: Freshly isolated BAT was minced and homogenized with a motor-driven Teflon pestle and glass mortar in ice-cold buffer A (100 mM KCl, 40 mM Tris·HCl, 10 mM Tris base, 5 mM $MgCl_2 \cdot 6H_2O$, 1 mM EDTA, and 1 mM ATP, pH 7.4) at a 20-fold dilution (wt/vol) or mitochondria was isolated [153], resuspended in buffer A and the rate of [1-^{14}C]palmitate, [1-^{14}C]palmitoyl-CoA, or [1-^{14}C]pyruvate, was measured [154]. Isolated BAT mitochondria (20 μg protein) in buffer (70 mM sucrose, 220 mM mannitol, 10 mM KH_2PO_4, 2 mM $MgCl_2$, 2 mM

HEPES, 1 mM EDTA, 0.1% BSA, 3 mM malate, and 1.3 µg/mL oligomycin) were loaded onto XF24 plates and rates of O_2 consumption were measured according to the manufacturer's instructions with a Seahorse X24F Analyzer (Seahorse Bioscience) during the consecutive addition at 4 min intervals of 5 mM pyruvate, 2 mM GDP, and 1 µM FCCP.

Acknowledgements: We thank Dr. S.K. Fried for her advice about fat cell isolations and Drs. A.S. Greenberg and J.W. Perfeld for their advice about adipocyte histology. This work was supported by NIH grants DK59935 (RAC), a grant from the American Diabetes Association (DMM), a postdoctoral fellowship (LOL) and a predoctoral fellowship (JME) from the American Heart Association-Mid-Atlantic Region, a pre-doctoral training grant HL069768 (JME), P30 DK034987, and P30 DK056350.

Supplemental Information

Supplement includes 4 figures, 4 tables, and additional experimental procedures. **Figures:**

Figure 3.1. Generation of mice that lack ACSL1 specifically in adipose tissue
A) Representative immunoblot against ACSL1 protein and **B**) ACSL activity in control and *Acsl1*$^{A-/-}$ liver, brown, gonadal, and inguinal adipose of 20 wk old mice, n=5-7. ACSL isoenzyme mRNA expression in **C**) gonadal adipose and **D**) brown adipose from 20 wk old control and *Acsl1*$^{A-/-}$ mice, n=6. Data represent mean ± SEM; *, P≤0.05 versus control.

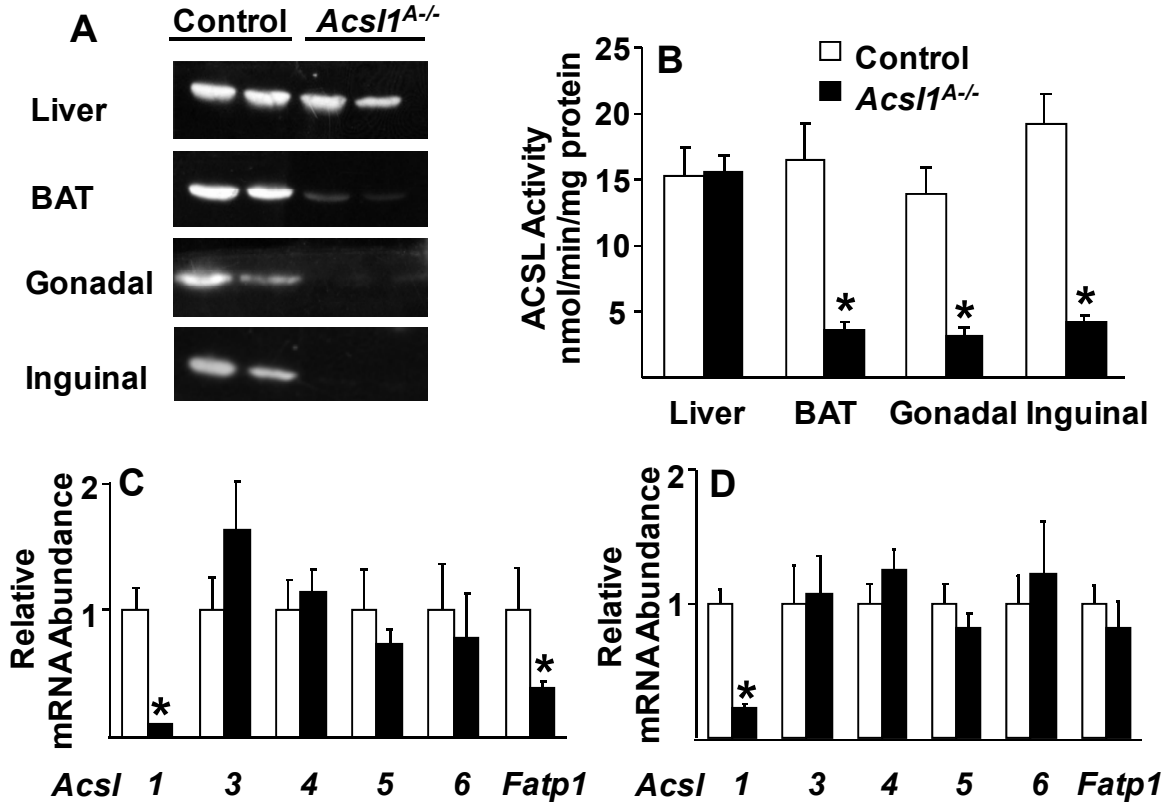

Figure 3.2. *Acsl1*$^{A-/-}$ mice have increased fat mass

A) Body weight from 6 to 24 weeks of age in mice fed LFD or HFD, n=10-15. **B**) Total body fat measured by MRI in 26 wk old control and *Acsl1*$^{A-/-}$ male mice, n=5-7. **C**) Fat depot weight as a percent of body weight (BW) in 20-26 wk old control and *Acsl1*$^{A-/-}$ male mice, n=10-15. **D**) Representative sections from control and *Acsl1*$^{A-/-}$ epididymal WAT and **E**) mean cells size from sections stained for hematoxylin and eosin, scale bars = 50 μM. **F**) AMPK phosphorylation, relative to total AMPK, from control and *Acsl1*$^{A-/-}$ inguinal adipose, n=4-5. **G**) Total GPAT activity in control and *Acsl1*$^{A-/-}$ gonadal adipose, n=6. **H**) Lipid content of control and *Acsl1*$^{A-/-}$ epididymal WAT in 6 mo old male mice fed LFD or HFD diet for 4.5 mo, n=5. [1-^{14}C]Oleate incorporation into (**I**) glycerolipids or (**N**) acid soluble metabolites (ASM) and carbon dioxide (CO_2), n=3-4, by control (C) and *Acsl1*$^{A-/-}$ (*A*$^{-/-}$) mature epididymal adipocytes, n=6. **J**) [1-^{14}C]Oleate incorporation into (**I**) glycerolipids by control and *Acsl1*$^{A-/-}$ cultured primary adipocytes. **K**) Plasma FA in control and *Acsl1*$^{A-/-}$ mice fasted for 4 or 24 hours, n=6-8. Release of (**L**) FA or (**M**) glycerol from control and *Acsl1*$^{A-/-}$ gonadal adipocyte explants basally or with 10μM isoproterenol (Iso), n=8. HFD, high-fat diet; LFD, low-fat diet; TAG, triacylglycerol; DAG, diacylglycerol; PL, phospholipids; FA, fatty acids. Data represent mean ± SEM *, P≤0.05 versus control; # P≤0.05 chow or LFD versus HFD within genotype.

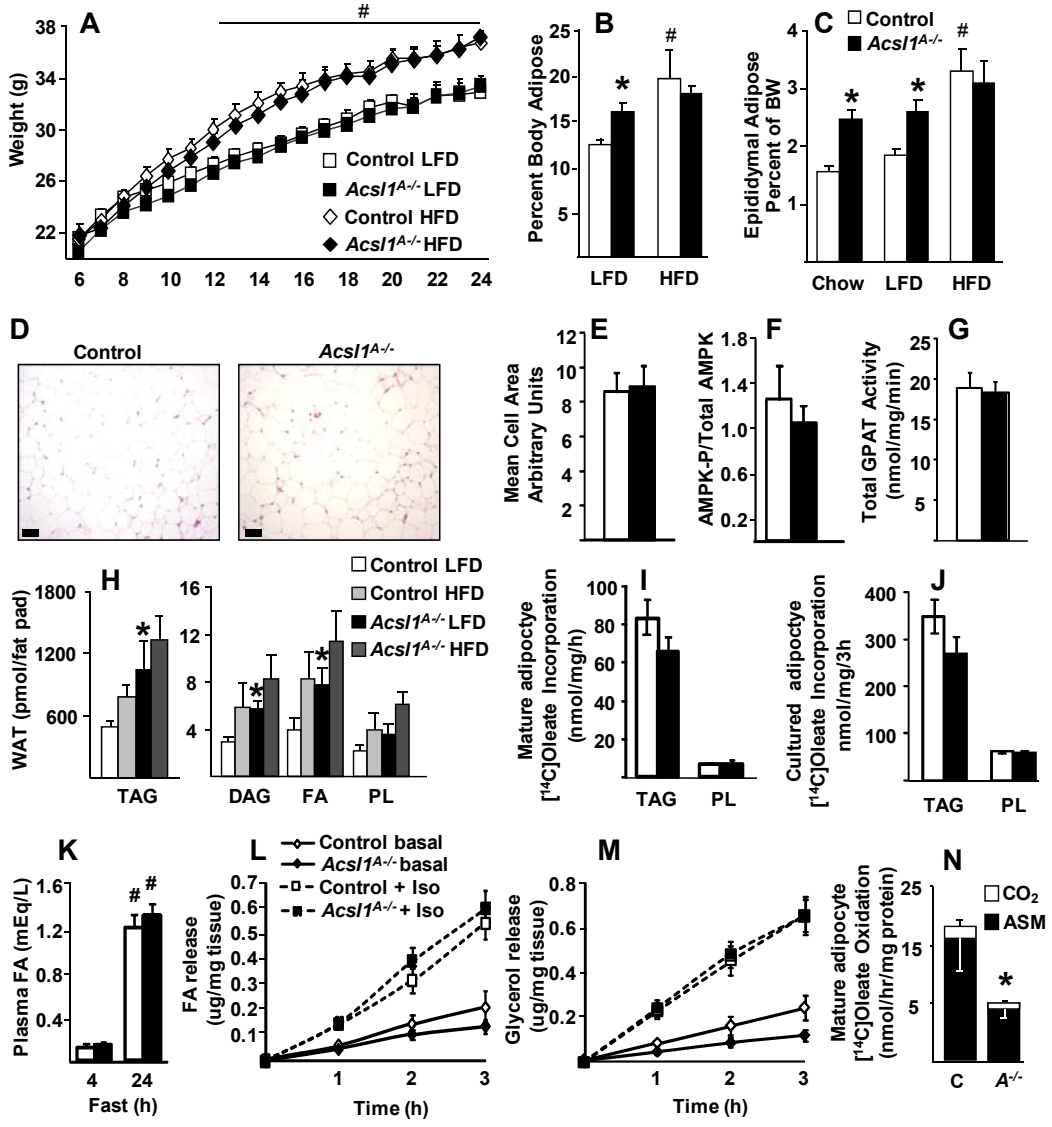

Figure 3.3. *Acsl1*$^{A-/-}$ mice are cold intolerant due to impaired FA oxidation

A) Body temperature of fasted control and *Acsl1*$^{A-/-}$ male mice exposed to a 4°C environment for 4 h, n=14-16. **B**) Control and *Acsl1*$^{A-/-}$ male mouse O_2 consumption was monitored in a metabolic chamber for 3 h before and after injection of isoproterenol (Iso) or CL-316243 (CL) (10 mg/kg), n=6-8. **C**) Representative BAT histology stained for hematoxylin and eosin in control and *Acsl1*$^{A-/-}$ mice before and after cold exposure for 2-4 h when *Acsl1*$^{A-/-}$ body temperature reached 30°C; scale bars = 50 μm. **D**) TAG content of BAT from control and *Acsl1*$^{A-/-}$ mice fasted at 21°C or at 4°C for 4 h, n=5-6. BAT mitochondrial (**E,F**) [1-^{14}C]palmitate and (**G**) [1-^{14}C]palmitoyl-CoA and [1-^{14}C]pyruvate oxidation into carbon dioxide (CO_2) from control and *Acsl1*$^{A-/-}$ mice, n=3. **F**) Control (C) and *Acsl1*$^{A-/-}$ (*A*$^{-/-}$) ACSL1 immunoblot and protein, and CO_2 production from [1-^{14}C]palmitate by 3 mitochondrial preparations (A-C), relative to control. Control and *Acsl1*$^{A-/-}$ cultured primary brown adipocyte release of (**H**) glycerol and (**I**) FA with or without 10μM isoproterenol, and incorporation of [1-^{14}C]oleate into (**J**) TAG and (**K**) ASM, n = 3. Data represent mean ± SEM *, P≤0.05 versus control; # P≤0.05 21°C versus 4°C within genotype.

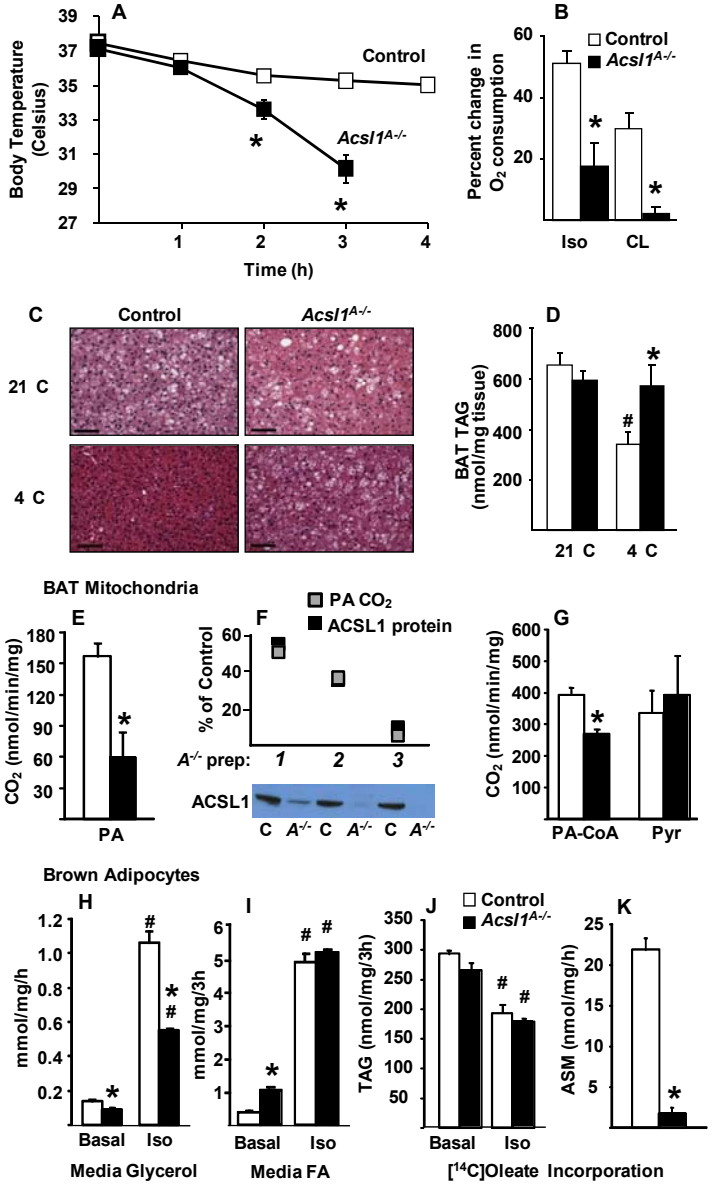

Figure 3.4. Thermogenic regulation of genes was normal in *Acsl1*$^{A-/-}$ mice
BAT mRNA levels were quantified by real-time PCR for genes of **A,B**) adrenergic regulation **C**) FA oxidation **D**) lipogenesis and **E**) acyl-CoA synthetases in BAT from male control and *Acsl1*$^{A-/-}$ mice without or with 4°C exposure, relative to *cyclophilin A* expression, n=6. Data represent mean ± SEM; *, P≤0.05 *Acsl1*$^{A-/-}$ versus control; # P≤0.05 21°C versus 4°C within genotype. A, *Agpat*; G, *Gpat*

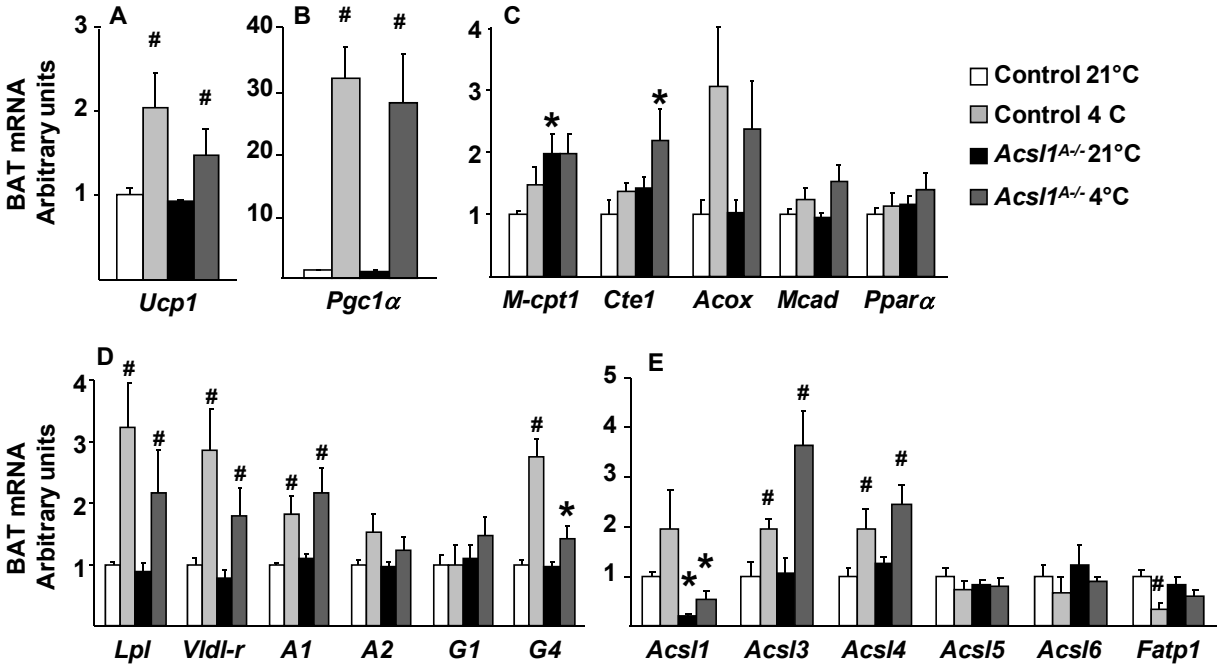

Figure 3.5. Long-chain acyl-carnitines were reduced in *Acsl1*$^{A-/-}$ brown adipose tissue **A,B,C**) Free, acetyl-, and acyl-carnitine content in BAT with and without cold exposure at 4°C. **D**) Lactate and, **E,F**) Citric acid cycle intermediates, **G,H**) short-chain acyl-CoA, **I**) amino acids, and J) total amino acid content in BAT with and without 4°C exposure, n=7. DC, dicarboxylated acyl-carnitines; OH, hydroxylated acyl-carnitines; Asx, aspartate/asparagine; Gsx, glutamate/glutamine. Data represent mean ± SEM *, P≤0.05 versus control; # P≤0.05 21°C versus 4°C within genotype (n=6-10).

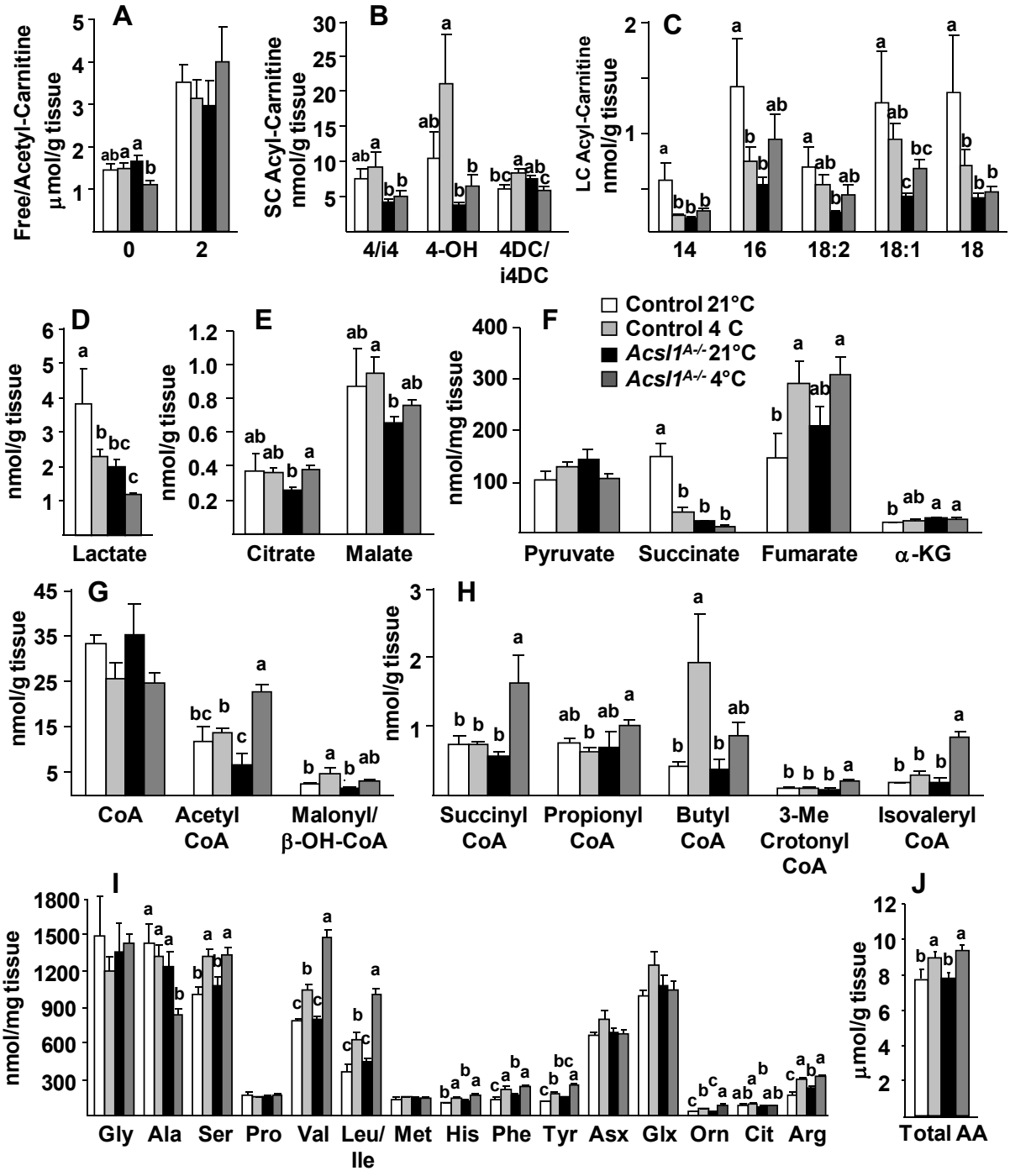

Figure 3.6. Plasma metabolites and BAT acyl-CoAs in *Acsl1*$^{A-/-}$ mice after adrenergic stimuli. Plasma glucose (**A**), glycerol (**B**), FA (**C**), and TAG (**D**) from control and *Acsl1*$^{A-/-}$ mice fasted for 4 h at 21°C or 4°C, or before (T_0) and 3 h after isoproterenol (Iso) or CL-316243 (CL) injection (10 mg/kg), n=6-8. **E**) Sum of long-chain acyl-carnitines (C14-C20) in control (C) and *Acsl1*$^{A-/-}$ ($A^{-/-}$) with or without cold exposure for 2-4 h. Data represent mean ± SEM; *, P≤0.05 versus control; # P≤0.05 21°C or T_0 versus treated within genotype.

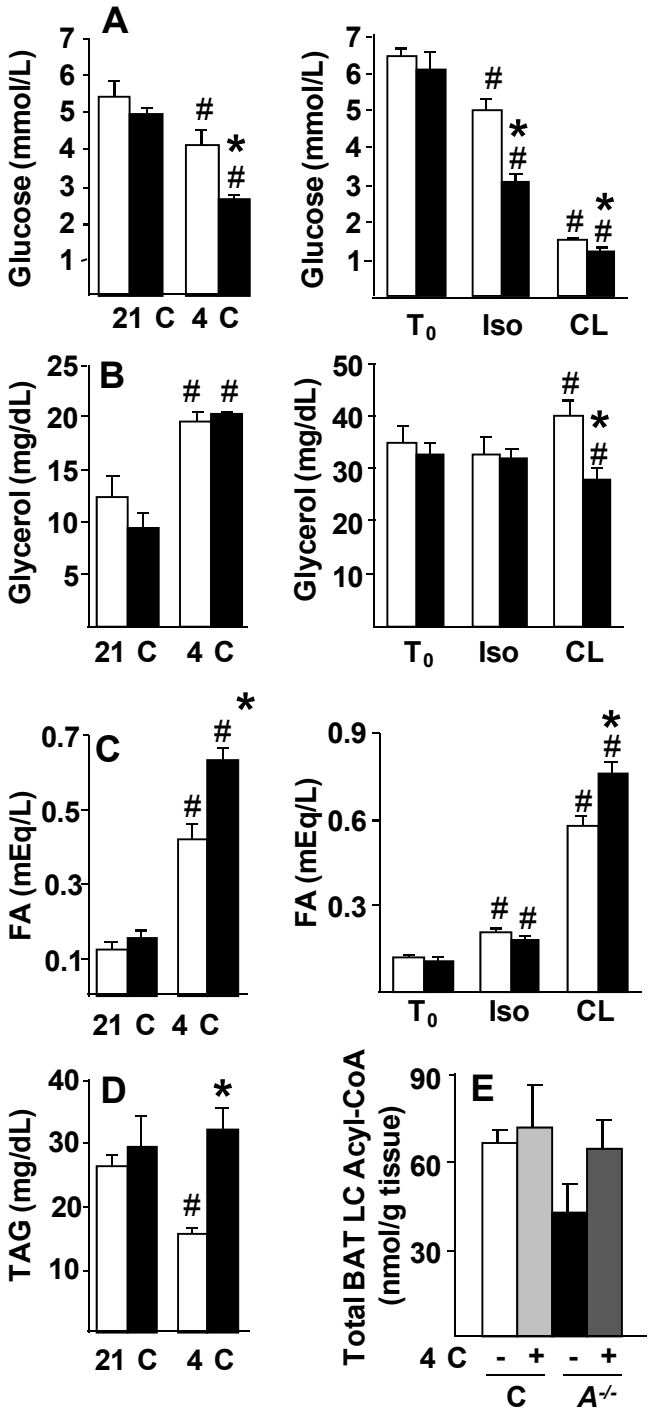

Figure 3.7. BAT fatty acid metabolism in cold-exposed mice. When norepinephrine activates β-adrenergic receptors, activated protein kinase A (PKA) induces PGC1α in brown adipocytes which, together with FA, activate transcription factors that upregulate genes required for mitochondrial oxidative and thermogenic functions. PKA also activates hormone sensitive lipase (HSL) which lipolyze triacylglycerol (TAG) in white and brown adipose cells. FA released from WAT and from VLDL (via lipoprotein lipase [LPL]) enters brown adipocytes and are activated by ACSLs to form acyl-CoAs that can be esterified to form TAG or are oxidized. FA lipolyzed from TAG stores in brown adipocytes are activated by ACSL1, enter mitochondria, and are oxidized. FA also activates UCP1 which uncouples the mitochondrial proton gradient, producing heat.

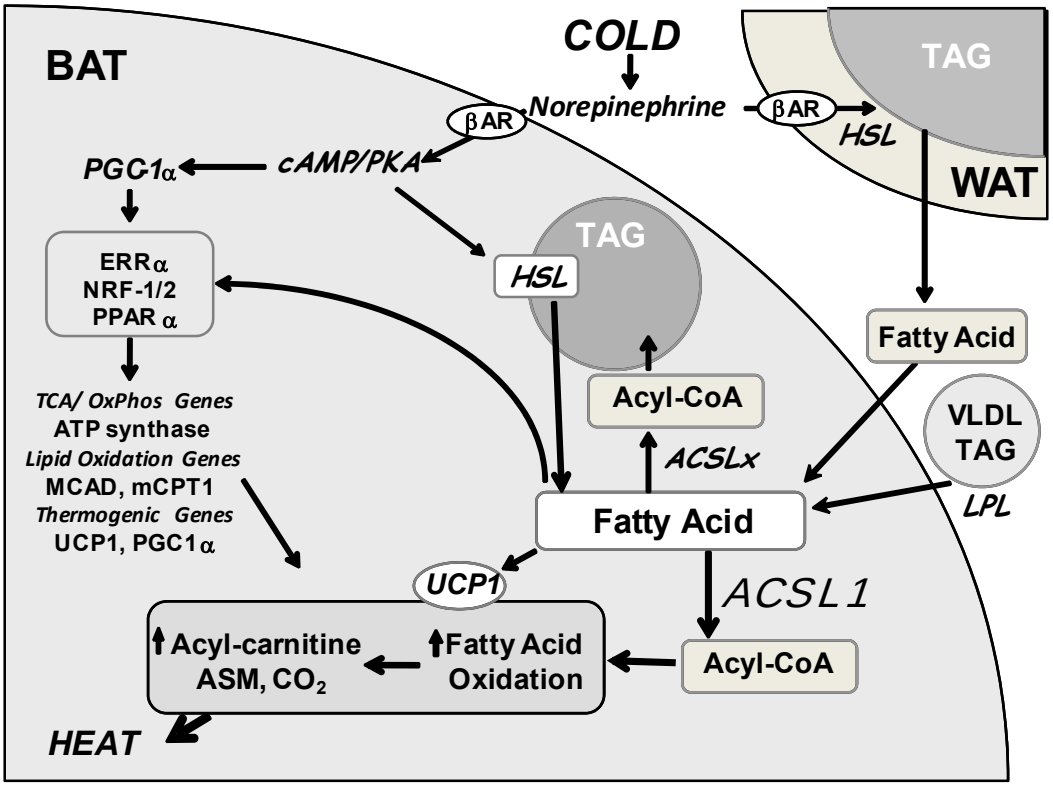

Supplementary Figure 3.8. Lipid composition of adipose tissue from *Acsl1*$^{A-/-}$ mice

A,B) Lipid content of control and *Acsl1*$^{A-/-}$ BAT in 6 mo old male mice fed a 10%-fat (LFD) or 45%-fat (HFD) diet for 4.5 mo, n=5. **C, D**) epididymal WAT and **E,F**) BAT lipid species content in TAG and PL, n=5. Data represent mean ± SEM; groups not sharing letters are significantly different by 2-way ANOVA, P≤0.05. TAG, triacylglycerol; DAG, diacylglycerol; PL, phospholipids; FC, cholesterol; FA, non-esterified fatty acids.

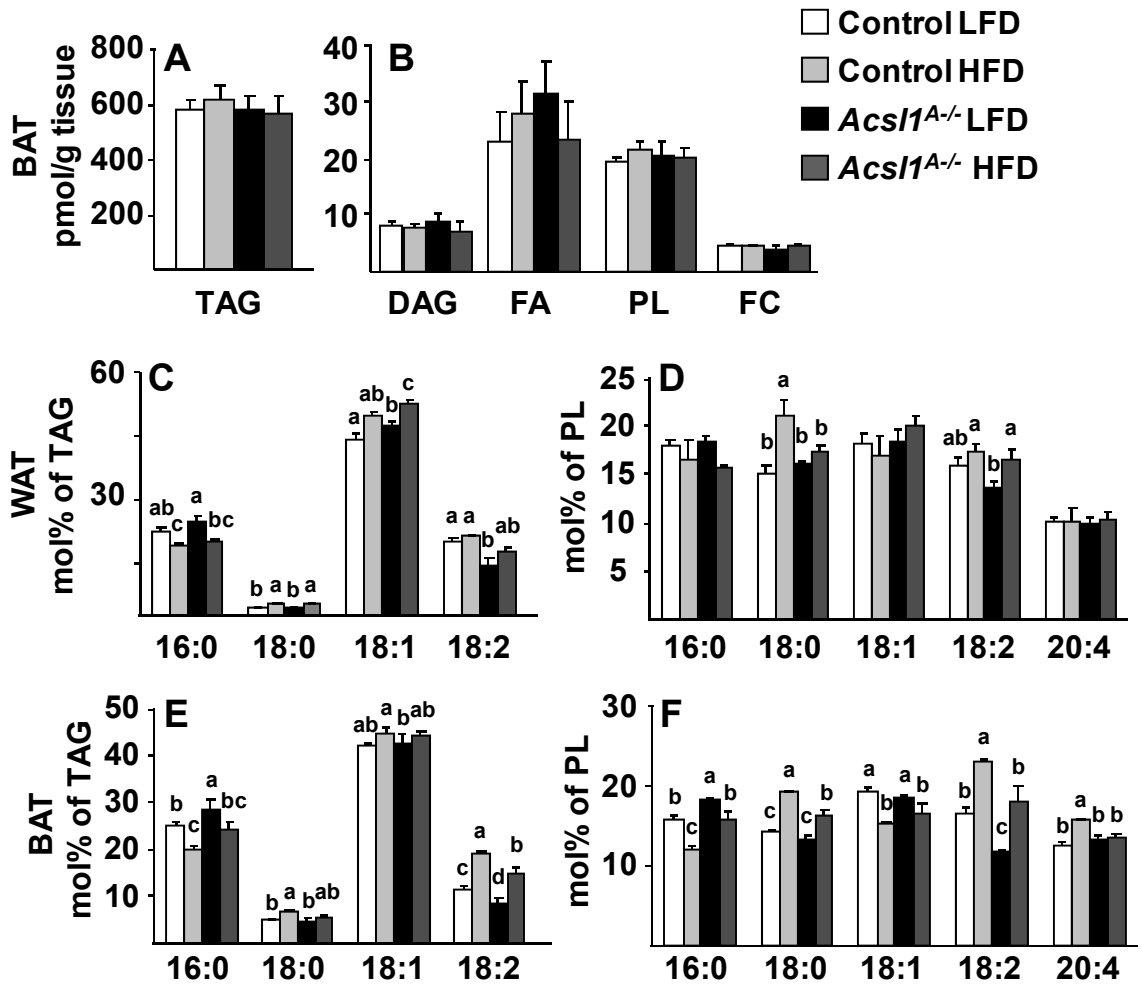

Supplementary Figure 3.9. Acyl-carnitines in *Acsl1*$^{A-/-}$ brown adipose tissue

Acyl-carnitine content in BAT with and without cold exposure for 4 h at 4°C, number corresponds to carbon-chain length, n=6-10. DC, dicarboxylated acyl-carnitines; OH, hydroxylated acyl-carnitines. Data represent the mean ± SEM; groups not sharing letters are significantly different by 2-way ANOVA, P≤0.05.

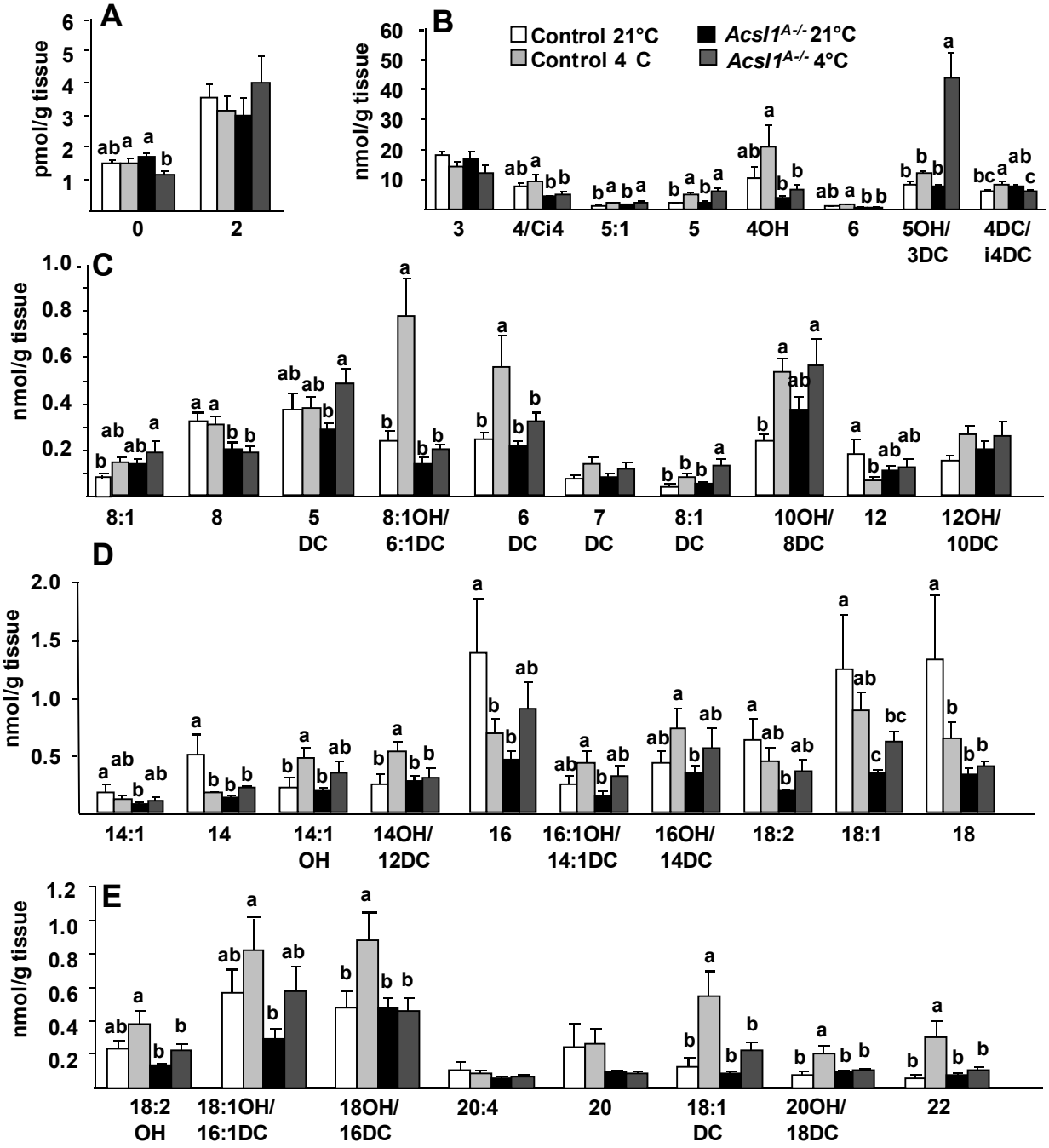

Supplementary Figure 3.10. Acyl-CoA in *Acsl1*$^{A-/-}$ brown adipose tissue

Acyl-carnitine content in BAT with and without cold exposure for 4 h at 4°C, number corresponds to carbon-chain length, n=4-6. OH, hydroxylated acyl-CoA. Data represent the mean ± SEM; groups not sharing letters are significantly different by 2-way ANOVA, P≤0.05.

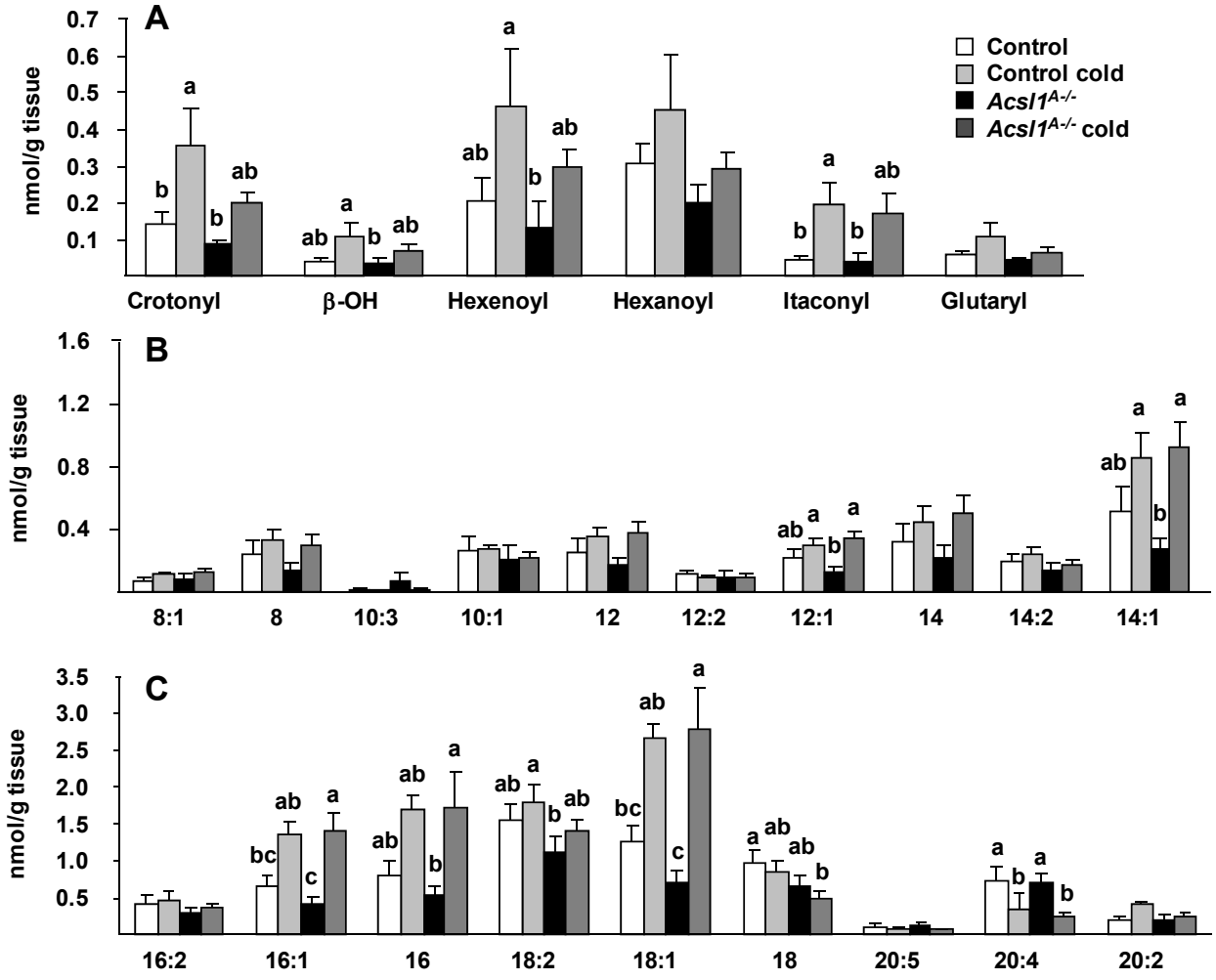

Supplementary Figure 3.11. Oxygen consumption and ACSL activity in BAT mitochondria and muscle

A) Total ACSL activity in control and *Acsl1*$^{A-/-}$ gastrocnemius muscle with or without cold exposure, n =6. **B**) Absolute oxygen consumption in mice with or without CL-1316243 (10mg/kg) stimulation, n = 6. C) [1-^{14}C-palmitate] oxidation into carbon dioxide (CO_2) from control and *Acsl1*$^{A-/-}$ BAT homogenates, n=5-6. Total ACSL activity (**D**) and ACSL1 protein (**E**) in control and *Acsl1*$^{A-/-}$ BAT mitochondria, n=3. **F**) Rate of oxygen consumption in control and *Acsl1*$^{A-/-}$ isolated brown adipose mitochondria (20 µg protein) exposed to 5 mM pyruvate (Pyr), 2 mM GDP, and 1 µM FCCP (carbonyl cyanide *P*-trifluoro-methoxyphenyl-hydrazone) as indicated. Data represent mean ± SEM *, P≤0.05 versus control; # P≤0.05 21°C versus 4°C within genotype. OCR, oxygen consumption rate.

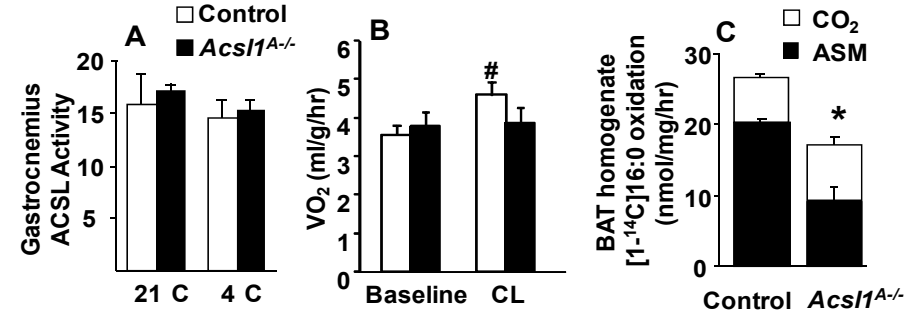

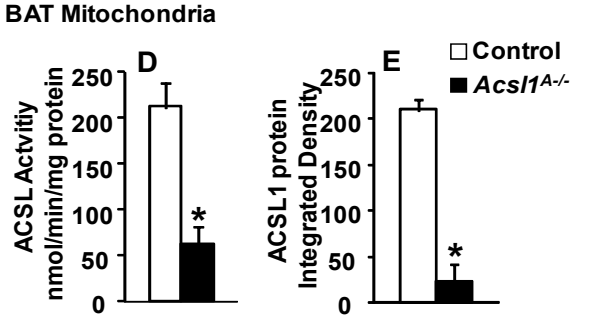

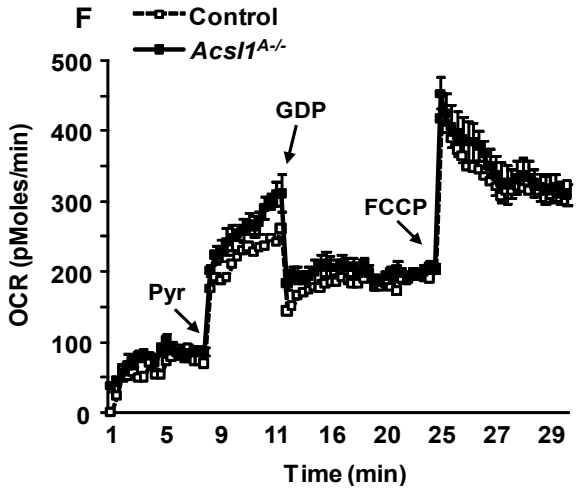

Supplementary Table 1 (3.1)

TAG synthesis was similar in control and *Acsl1*$^{A-/-}$ mice

Plasma metabolites in 20 week old control and *Acsl1*$^{A-/-}$ male mice fasted for 4 h, n=10-12. TAG, triacylglycerol; FA, fatty acids; OGTT-AUC, oral glucose tolerance test-area under the curve; ND, not determined. Data represent mean ± SEM; Students T-test's: *, P≤0.05 *Acsl1*$^{A-/-}$ versus control within diet; # P≤0.05 low-fat vs. high-fat diet within genotype.

	Low-Fat Diet		High-Fat Diet	
	Control	***Acsl1*$^{A-/-}$**	**Control**	***Acsl1*$^{A-/-}$**
Body Weight (g)	33.1 ± 0.7	33.3 ± 0.8	37.3 ± 1.8#	36.6 ± 1.4#
% Body Fat	12.2 ± 0.8	16.0 ± 1*	19.7 ± 3#	17.9 ± 8
Epididymal fat (% of BW)	1.83 ± 0.1	2.6 ± 0.2 *	3.3 ± 0.4#	3.1 ± 0.4#
Plasma TAG (mg/dL)	30 ± 2	25 ± 2 *	33 ± 4	28 ± 1
Plasma Cholesterol (mg/dL)	111 ± 6	118 ± 7	135 ± 12#	144 ± 6#
Plasma FA (mEq/L)	0.24 ± 0.02	0.24 ± 0.02	0.17 ± 0.02	0.21 ± 0.05
Plasma Glucose (mg/dL)	162 ± 5	160 ± 7	164 ± 7	170 ± 4
OGTT-AUC (mg/dL)	3710 ± 374	2576 ± 513	4950 ± 250#	6828 ± 842#
Plasma Insulin (μg/mL)	0.32 ± 0.03	0.57 ± 0.23	0.38 ± 0.05	0.61 ± 0.16
Plasma Adiponectin (μg/mL)	12.8 ± 0.6	14.0 ± 0.8	ND	ND

Supplementary Table 2 (3.2)

Lipogenic gene expression was similar in control and *Acsl1*$^{A-/-}$ WAT

Gonadal adipose mRNA levels were quantified by real-time PCR in male mice fed the low-fat diet for 20 wk, n=6. Data represent $2^{\wedge-\Delta CT}$ of *Acsl1*$^{A-/-}$ fold-change over control and normalized to *cyclophilin A*. Data represents mean ± SEM. No significant differences were found between *Acsl1*$^{A-/-}$ and control values by 2-way Student's T-test.

Gene	Fold change relative to control	Function
Vldl-r	1.63 ±0.4	FA uptake
Ldl-r	1.46 ±0.4	
Caveolin-1	1.02 ±0.2	Lipolysis
Cte1	1.13 ±0.2	FA oxidation/ PPARα
l-Cpt1	1.08 ±0.2	
Mcad	1.22 ±0.3	
Atp syn	1.58 ±0.6	
Pparg	1.10 ±0.3	FA synthesis/ PPARγ
Ap2	0.98 ±0.2	
Fas	1.64 ±0.4	
Cd36	1.95 ±0.9	

Supplementary Table 3 (3.3)

***Acsl1*$^{A-/-}$ mice respond normally to fasting**

Body weight and plasma glucose, fatty acids (FA), and β-hydroxybutyrate (β-OH) in 4 h and 24 h fasted control and *Acsl1*$^{A-/-}$ mice, n=5-8. Data represent mean ± SEM; Students T-test's: *, P≤0.05 *Acsl1*$^{A-/-}$ versus control at same fasting time; $^{\#}$ P≤0.05 30 h versus 4 h within genotype.

	Controls		***Acsl1*$^{A-/-}$**	
Hours Fasting	**4**	**24**	**4**	**24**
Weight (g)	23 ± 1	21 ± .5$^{\#}$	24 ± .6	22 ± .6$^{\#}$
Glucose (mg/dL)	150 ± 4	102 ± 7$^{\#}$	157 ± 11	91 ± 6$^{\#}$
FA (mEq/L)	0.12 ± 0.1	1.2 ± 0.1$^{\#}$	0.1 ± 0.1	1.3 ± 0.1$^{\#}$
β-OH (mEq/L)	0.4 ± 0.1	1.7 ± 0.1$^{\#}$	0.4 ± 0.1	2.3 ± 0.2$^{\#*}$

Supplementary Table 4 (3.4), Primer sequences used for RT-PCR

Gene	Forward	Reverse
Acsl1	TGGGGTGGAAATCATCAGCC	CACAGCATTACACACTGTACAACGG
Acsl3	CAATTACAGAAGTGTGGGACT	CACCTTCCTCCCAGTTCTTT
Acsl4	TGCCAAAAGTGACCAGTCCTATG	TGTTACCAAACCAGTCTCGGGG
Acsl5	TCCCAGCCCACCTCTGATGATGTG	ACAAACTGTCCCGCCGAATG
Acsl6	TGAATGCACAGCTGGGTGTA	ATGTGGTTGCAGGGCAGAG
Fatp1	CGCTTTCTGCGTATCGTCTGCAAG	AAGATGCACGGGATCGTGTCT
Ucp1	GTGAAGGTCAGAATGCAAGC	AGGGCCCCCTTCATGAGGTC
Pgc1a	CAACATGCTCAAGCCAAACCAACA	CGCTCAATAGTCTTGTTCTCAAATGGG
m-cpt1	CAACTATTATGCCATGGATTTTGTGCTT	CGATACATGATCATGGCGTGAACG
Cte1	GCAGCCACCCCGAGGTAAA	GCCACGGAGCCATTGATG
Acox	GGTGGACCTCTGTCTTGTTCA	AAACCTTCAGGCCCAAGTGAG
Mcad	ACTTCGTGGCTTCGTCTAGA	GAGCAGGTTTCAAGATCGCA
Ppara	ATGCCTTAGAACTGGATGACA	GCAACTTCTCAATGTAGCCTA
Lpl	GCTGGAAAGTGCCTCCATTG	CTGCTGGCGTAGCAGGAAGT
Vldl-r	TGACGCAGACTGTTCAGACC	GCCGTGGATACAGCTACCAT
Agpat1	CACCCAGGATGTGAGAGTCTG	CTGACAACGTCCAGGCGAGG
Agpat2	GCAACGACAATGGGGACCTG	ACAGCATCCAGCACTTGTACC
Gpat1	CTCGTGTGGGTGATTGTGAC	AGCAAGTCCTGCGCTATCAT
Gpat4	TGTCTGGTTTGAGCGTTCTG	TTCTGGGAAGATGAGGATGG
Cav1	CGGGAACAGGGCAACATCTA	TGTGTCCCTTCTTTCTGC
Atp Syn	GTCCCGGGCTATTGCTGAGTTG	TCCCCATGTGACCCGTGAAGA
Pparg	CCAGAGCATGGTGCCTTCGCT	CAGCAACCATTGGGTCAGCTC
Ap2	CAGAAGTGGGATGGAAAGTCG	CGACTGACTATTGTAGTGTTTGA
Fas	TTCGGCTGCTGTTGGAAGTCAG	ACCCACCCAGACGCCAGTGTTC
Cd36	CAACCACTGTTTCTGCACTG	CAGGCTTTCCTTCTTTGCAC
CyloA	AGCACTGGGGAGAAAGGATT	CATGCCTTCTTTCACCTTCC
Gapdh	GGCATGGACTGTGGTCATGA	ATGGGTGTGAACCACGAGAA

Supplementary Experimental Procedures

RT-PCR: Tissue RNA was isolated (Qiagen RNeasy Lipid Tissues Kit), cDNA was synthesized (Applied Biosystems High Capacity cDNA RT Kit), and the reaction was performed using SYBR Green (Applied Biosystems) detection with specific primers (**Table S4**) with equal amounts of cDNA (10 ηg/reaction), and detected by a Taq-man thermocycler (BioRad). Results were normalized to *cyclophilin A* or *gapdh* and expressed as arbitrary units of $2^{-\Delta CT}$.

Immunoblots: Total membrane fractions were equally loaded (70 μg) and electrophoresed on 10% SDS polyacrylamide gels, then transferred to PVDF membrane, blocked with 5% milk-TBST for 1h, incubated with primary antibody (1:1,000) anti-ACSL1, phospho-AMPKα Thr172, or AMPKα primary antibody (Cell Signaling Technologies #4047, 2535, 2532 , washed, and incubated with secondary antibody 1:10,000 (Cell Signaling Technologies, goat anti-rabbit). Protein was visualized with the Western Blot R-Probe Kit (Pierce).

Histology: Tissue was fixed in 4% paraformaldehyde-PBS for 24 h, transferred to 70% ethanol, embedded in paraffin, serial sectioned, and stained with hematoxylin and eosin. Adipocyte size was quantified [149].

B.5 Heart and ACSL1 Background

The heart is an organ responsible for supplying the body with nutrients, oxygen, hormones, and other circulating factors. The human heart beats an average of 72 times per minute and is required to sustain life. The constant activity of the heart demands high levels of energy production. If the energy demands of the heart are not adequately supplied, due to a lack of oxygen or defects in cardiomyocyte metabolism, the heart may cease to perform and life cannot be sustained. Research has been focused on maintenance of heart function under challenged conditions, such as arrhythmia, cardiac hypertrophy, and cardiomyopathy, however, the metabolic underpinnings that are responsible for these conditions remain incompletely understood.

How is ACSL1 regulated in Heart? While *acsl1* mRNA is the most abundantly expressed of all ACSL isoenzymes, all ACSL isoenzymes are expressed in adult rodent heart [83]. FATP1/ACSVL4 is expressed at low levels, whereas, FATP4/ACSVL5 and the heart-specific FATP6/ACSVL2 are the major ACSVL isoenzymes expressed in heart [25]. The regulation of ACSL1 has been investigated in adipose, muscle, and liver, but data are limited on the role and regulation of ACSL1 in the heart. In primary cardiomyocytes, fatty acid exposure leads to increased intracellular lipid droplets and increased FA oxidation with simultaneous increases in mRNA expression of *acsl1* [155]. In cardiomyocytes *acsl1* is regulated by PPARα, a transcription factor that upregulates genes of fatty acid oxidation. The promoter region of the *acsl1* gene contains a PPAR response element (PPRE) that is similar to the PPRE of acyl-CoA oxidase, a key

enzyme in lipid peroxisomal oxidation [156, 157]. *Acsl1* mRNA is upregulated when isolated cardiomyocytes are incubated with PPARα, but not PPARγ, agonists [6, 155, 158]. *Acsl1* mRNA in the heart of PPARα null mice is reduced 60%, showing that ACSL1 is mainly regulated by PPARα [159]. Because PPARα is a major regulator of FA oxidation genes such as carnitine palmitoyltransferase I and acyl-CoA oxidase, we postulate that ACSL1 is simultaneously upregulated by PPARα in order to provide the acyl-CoA substrate that these enzymes require for lipid oxidation and subsequent energy production. PPARα and PPARγ agonists supplemented to rat diet for 2 weeks increased *acsl1* mRNA expression in adipose, liver, and skeletal muscle; however, the agonists did not elicit changes in *acsl1* mRNA expression in heart [6]. In conclusion, ACSL1 mRNA expression is regulated *in vitro* by fatty acid exposure, PPARα agonists and insulin; however, its expression *in vivo* remains unchanged by fasting, high-fat feeding, and PPARα agonists [6].

Table 2.5: ACSL1 regulation in Heart

	ACSL1 mRNA in Heart	
Manipulation	***In vitro***	***In vivo***
PPARα -/-	-	down
PPARα agonist	up	NC
PPARγ agonist	NC	NC
Fatty Acids	up	NC
Insulin	up	NC
Development	-	up
Fasting	-	NC
High-Fat Diet	-	NC

Acsl1 mRNA is also regulated by the estrogen-related family of transcription factors, (ERR) that coactivates with PGC1α and control the substrate shift from neonatal cardiomyocytes to adult cardiomyocytes. Knockout mouse models of two ERR isoenzymes (ERRα and ERRγ) result in reduced *acsl1* mRNA expression coupled to reduced oxidative ability and ATP synthesis in the heart [160-162]. These data imply

that ERR is necessary for the expression of ACSL1 in heart and that without ERR the cardiomyocytes fail to mature into adult cardiomyocytes that use fatty acids as the primary substrate for ATP production.

FA oxidation provides 60-70% of total energy for the heart. Intracellular TAG-derived FA provide ~10% of energy requirements under normal conditions and the other 50-60% is from extracellular circulating free FA and FA derived from lipase activity on circulating lipoproteins. However when the circulating fatty acid supply is limited, TAG-derived FA can provide up to 50% of total energy requirements for the working heart [163]. The energy source preferred by the heart is controlled by substrate availability and transcriptional and hormonal regulation. Rat neonatal cardiomyocyte exposure to glucose or FA leads to glycogen or TAG accumulation, respectively, indicating that substrate availability is the major regulator of uptake. *In vivo* and *in vitro*, exposure to fatty acids, independent of glucose, leads to an increase in FA oxidation with a concomitant upregulation of *acsl1* mRNA [155]. While the prenatal heart relies primarily on glucose for ATP, the adult heart relies on FA for ATP with the rates of FA oxidation increasing from day 0 to 60 in the rat heart [164]. Total ACSL activity is very low in the embryonic (E16.5) and neonatal heart but increases 90-fold and 6-fold in the adult heart, respectively. This transition matches the shift in substrate preference for glucose (prenatal heart) to fatty acids (adult heart) [5]. Furthermore, the developmental rise in ACSL activity from the embryonic heart to the adult heart correlates with the concomitant 6-fold rise in the *acsl1* without increases in *acsl*-3,-4, -5 or -6 mRNA expression [5]. These increases in ACSL activity and *acsl1* mRNA expression in heart correlate with increases in the heart workload, rates of ATP generation, oxidative preference for FA, and expression of the FA oxidative genes acyl-CoA oxidase and malonyl-CoA acyl dehydrogenase [5]. Together these studies imply that ACSL1 in heart is regulated by PPAR and ERR and that ACSL1 directs fatty acids towards oxidation in the heart.

The 11-fold overexpression of ACSL1 in the mouse heart is characterized by a lipotoxic cardiomyopathy and myocyte cell death associated with TAG and PL accumulation [165]. The 11-fold overexpression of ACSL1 increases fatty acid accumulation characterized by a 11-fold increase in myocardial TAG and 2-fold increase in myocardial phosphatidylcholine, implying that ACSL1 provides FA for complex lipid synthesis in heart. However, because the authors did not measure rates of FA oxidation, FA uptake, or acyl-CoA accumulation, it is unknown if oxidation was altered by ACSL1 overexpression. We hypothesize that ACSL1 provides FA for oxidative metabolism but does not regulate the rate of oxidation; therefore, the overexpression of ACSL1 in heart may increase the acyl-CoA substrate for oxidation without an increase in the demand for oxidation resulting in the accumulation of acyl-CoA, some of which may be stored as TAG and PL. Excessive accumulation of acyl-CoA, along with other lipid intermediates, may activate signaling pathways and/or increase oxidative stress causing cell death (lipotoxicity) and excessive cell death can lead to cardiomyopathies characterized by cell death, fibrotic activity, and cardiac dysfunction. It is also possible that the oxidative rate was increased in the ACSL1-heart specific overexpressing mice and that the accumulation of toxic lipid oxidation byproducts led to a state of oxidative stress that resulted in the death of cardiomyocytes. Without knowing the changes in oxidation of the ACSL1-heart overexpressing mouse it is difficult to determine the true role of ACSL1 in heart and the cause of the cardiomyopathy. A similar model of cardiomyocyte lipotoxicity with the accumulation of TAG and PL occurs in the heart-specific 8-fold overexpression of FATP1/ACSVL4, an ACSVL that is not highly expressed in heart. Cardiac FATP1 overexpression increased rates of FA uptake 4-fold and rates of fatty oxidation 2-fold [166]. On the other hand, the FATP1 null mouse has normal heart function, thus the lack of a cardiac phenotype in the FATP1 null mice invalidates interpretations made about its function from the overexpression of FATP1 in

heart [82]. FATP6/ACSVL2 is a heart specific FATP/ACSVL, yet little is known about its role in the heart [167]. The overexpression of ACSL1 by 11-fold and FATP1 by 8-fold in the heart likely led to non-endogenous subcellular location of these membrane-associated enzymes, to the accumulation of "lipotoxic" acyl-CoA, and limited the cellular regulatory mechanisms (i.e. phosphorylation, acetylation, and protein-protein interaction) on the excessive abundance of these proteins.

B.6 Fatty Acid Oxidation in the Heart

Because of the new-found role for ACSL1 in providing acyl-CoAs for FA oxidation in adipose (Aim 1 and Aim 2), the following sections will describe the oxidative pathway in context to the heart and how defects in oxidation affect cardiac outcomes. Our understanding of oxidative pathways has expanded over the past century since beta-oxidation was first theorized in 1904. However, many questions remain regarding regulation of the oxidative pathway and the consequences of dysregulation. For the oxidation of fatty acids, three different pathways are known; alpha-, beta-, and omega-oxidation. β-oxidation for long-chain fatty acids occurs in the mitochondria and for very-long chain fatty acids occurs in peroxisomes. β-oxidation is the most predominant oxidative pathway in the heart, whereas the less predominate pathways of α-oxidation of phytanic acids and ω-oxidation of medium to very-long chain fatty acids occur at the endoplasmic reticulum. For β-oxidation, cellular FA must first enter the mitochondria. Entry requires the FA to be converted to an acyl-CoA by an acyl-CoA synthetase, after which the CoA is exchanged for a carnitine molecule by the enzyme carnitine-palmitoyl transferase-one (CPT I) located on the outer mitochondrial membrane. CPT1 is allosterically inhibited by malonyl-CoA and is currently considered the major regulator of the rate of FA oxidation. Acyl-carnitines cross mitochondrial

membranes via the carnitine-acyl-carnitine translocase (CACT). Once inside the mitochondria, CPT II exchanges the carnitine for a CoA to re-create an acyl-CoA within the mitochondria. The acyl-CoA is then subject to beta-oxidation, a process that consists of 4 reactions constituting one cycle that removes 2 carbons from the acyl chain per cycle. The first reaction of the cycle is performed by an acyl-dehydrogenase which exists in 4 isoforms that together allow the complete metabolism of nearly all chain-length fatty acids. These 4 isoforms are named: short-chain, medium-chain, long-chain, and very long-chain acyl-CoA dehydrogenases (SCAD, MCAD, LCAD, and VLCAD, respectively). The 2 carbon acetyl-CoA that is removed by each cycle of beta-oxidation enters the citric acid cycle for complete oxidation.

Fatty acid oxidation in hypertrophy. Fatty acids are the major source of energy production for the heart [168, 169]. Fatty acid oxidation is reduced while glucose oxidation is increased in hypertrophic hearts. Hypertrophy of the heart occurs due to increased cell size of cardiomyocytes. On one hand cardiac hypertrophy is considered compensatory and protective in athletes and pregnant women. Hypertrophy that occurs in athletes does not negatively alter heart function, structure, or metabolism. On the other hand cardiac hypertrophy was found to be a Framingham risk factor for heart failure and arrhythmia. Hypertrophy that occurs due to causes such as; hypertension, obesity, valuvar heart disease, and mutations in genes of contractile function; results in altered contractility, systolic/diastolic dysfunction, and a shift towards glycolytic metabolism. In the latter case hypertrophy is accompanied by the re-induction of the fetal gene program. The fetal heart uses glucose as the primary oxidative substrate. It is unknown if the shift in oxidation, from lipolytic to glycolytic, is causal or consequence of ensuing cardiac hypertrophy. In the Framingham heart study, left ventricular hypertrophy (LVH) was identified in ~18% of the population and in ~42% of the population over the

age of 70 [170]. The LVH was independently associated with increasing age, blood pressure, obesity, valve disease, and myocardial infarction [170]. LVH in the Framingham population was also associated with increasing BMI, skinfold thickness, and blood pressure [171].

Impaired fatty acid oxidation: Cause or consequence of hypertrophy? It has remained unclear whether the shift in oxidation from lipolytic to glycolytic, is a cause or a consequence of hypertrophy. The conclusion that cardiac hypertrophy can result from reduced FA oxidation is supported by several mouse models with genetically or chemically impaired FA oxidation.

Figure 2.9. Does cardiac pathological hypertrophy occur independent of metabolic shift or does the metabolic shift cause hypertrophy?

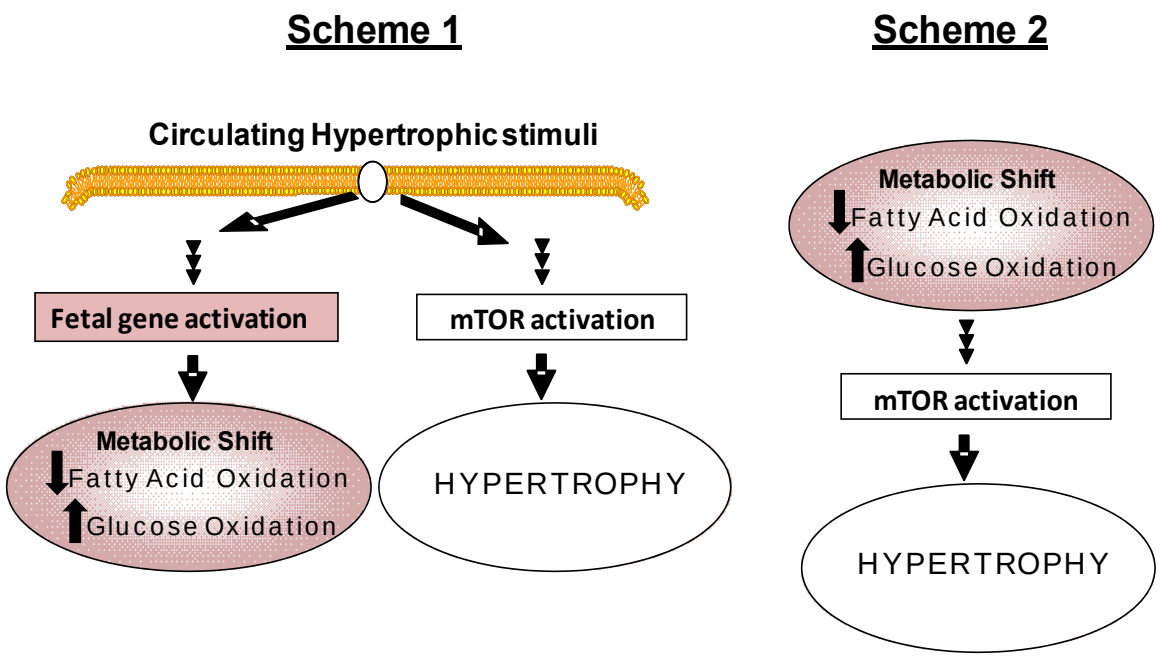

Models of energy imbalance and cardiac hypertrophy. A number of studies have focused on mouse models of energy imbalance in the heart. Most have induced hypertrophy by stress/ischemia or pressure overload and shown that the heart reverts to a fetal program with increased uptake and oxidation of glucose. Under these conditions,

FA oxidation is down-regulated, as are the mRNA levels of PPARα and other genes required for FA oxidation like MCAD, MCD, mCPT1 and the peroxisomal gene AOX [172]. On the other hand, most animal models with deficiencies in the genes required for FA oxidation develop cardiac hypertrophy with a reversion of gene expression to a "fetal" state [173]. These genes encode for proteins involved in the conversion of acyl-CoAs to acyl-carnitines, transport of the acyl-carnitines into the mitochondrial matrix, and enzymes required for β-oxidation.

Impaired carnitine transporters and cardiac outcomes. The oxidation of FA depends on the transport of carnitine into cells by several carnitine transporters, OCTN1 (SLC22A4), OCTN2 (SLC22A5) and OCT6 (SLC22A16) [174]. In humans, defects in the Na^+-carnitine co-transporter (OCTN2) cause a cardiomyopathy characterized by cardiac lipid accumulation and hypertrophy. The cardiomyopathy improves with carnitine supplementation in older patients [175] . The juvenile visceral steatosis mouse mimics this human defect of systemic carnitine deficiency because of a spontaneous KO of OCTN2, resulting in cardiac lipid accumulation and hypertrophy and a 2-fold increase in cardiac mitochondria [176] with preserved respiratory chain enzyme activities [177, 178]. However, despite increased mitochondrial content, adenine nucleotides were only 60% of that in control hearts suggesting an energy deficit. Treatment with L-carnitine improved and treatment with L-carnitine plus a PPARα agonist further improved LV function and the survival rate of the JVS mice, suggesting that at least part of their problem was a deficiency in PPARα function in addition to impaired FA oxidation [179].

The heart expresses two CPT isoforms: L-CPT1 and M-CPT1. Human deficiencies have been identified; however, patient clinical features are variable. In rats, chemical inhibition of both CPT1 isoforms causes cardiomyocyte hypertrophy with a 25% increase in heart weight [180]. A mouse KO of the L-CPT1 is not viable, and

although the heterozygotes had a 50% decrease in CPT1 activity in liver, they showed no hepatic steatosis or heart abnormality, likely due to the relatively low expression of L-CPT1 in heart [181]. Similarly, the homozygous KO of the M-CPT1 was an embryonic lethal before E9.5-11.5 and the heterozygote had a 50% decrease in activity in heart, however the authors did not examine heart-specific changes in energy metabolism or histology [182]. The transport of acyl-carnitine into the mitochondrial matrix (and transport of carnitine out) requires CACT, and humans with CACT deficiency have early-infant death and develop cardiorespiratory problems [183]. It was thought that an accumulation of "toxic" long-chain acyl-carnitines might be the major problem [183]. In one report of an infant who succumbed to a cardiac tachyarrhythmia had a marked accumulation of lipid droplets in the myocardium, liver, and kidney, and a "virtually complete elimination of mitochondria from cardiomyocytes" [184]. Thus a deficiency in CACT is lethal at least in part due to cardiac dysfunction. CPT-II converts acyl-carnitines in the mitochondrial matrix back to acyl-CoAs to undergo β-oxidation. Human deficiency of CPT-II is autosomal recessive and results in a severe deficit of energy metabolism [185]. No animal models of CPT-II deficiency have been reported. In conclusion, carnitine deficiency at the cellular or mitochondrial level results in, often lethal, cardiomyopathies characterized by cardiac lipid accumulation, mitochondrial biogenesis, and hypertrophy.

Impaired fatty acid oxidation at the mitochondria and cardiac outcomes. It is interesting that L-CPT1, M-CPT1, and CACT all result in lethality or early life-threatening disease whereas a defect in one of the dehydrogenase enzymes of β-oxidation does not. Humans with deficiencies in medium-chain acyl-CoA dehydrogenase (MCAD) and long-chain acyl CoA dehydrogenase (LCAD) have reported dilated and hypertrophic cardiomyopathies [186]. In mouse models that lack MCAD and

LCAD, the heart phenotypes have not been extensively studied. VLCAD knockout mice are resistant to high-fat diet induced obesity [60]. The authors suggest that resistance to obesity in VLCAD-KO mice is due to the excess of acyl-CoAs that activate AMPK and increase rates of FA oxidation. In patients with VLCAD deficiencies, two clinical syndromes were reported, a milder form with hypoketotic hypoglycemia and a severe syndrome with early death and a hypertrophic cardiomyopathy [187]. VLCAD knockout mouse hearts have an accumulation of microvesicular lipid, marked mitochondrial proliferation, and cardiac hypertrophy [188]. VLCAD-KO mice had ventricular tachycardias and their cardiomyocytes had increased levels of cardiac ryanodine receptor 2, phospholamban, and calsequestrin with increased [^{3}H]ryanodine binding in heart microsomes plus altered Ca^{2+} dynamics [189]. A mouse defective in the beta-subunit of the mitochondria trifunctional protein (MTP or Hadhb), the enzyme that catalyzes the last three steps of the 4-step beta-oxidation cycle after the acyl-dehydrogenases, had reduced MTP activity presenting with cardiac arrhythmia and sudden death between 9 and 16 months of age. Histology showed multifocal cardiac fibrosis but lipid droplets or mitochondrial changes were not reported. In conclusion, deficiencies in the one enzyme of mitochondrial fatty acid oxidation is not early lethal, but result in cardiomyopathies characterized with lipid accumulation and hypertrophy. Thus, defects in mitochondrial FA oxidation initiate the development of cardiac hypertrophy.

Impaired respiratory chain activity and cardiac outcomes. Normal function of the respiratory chain is critical for FA oxidation. Humans with deficiencies in respiratory chain complexes show cardiac hypertrophy [190-193] or dilated cardiomyopathy [186, 193]. After 2 weeks of age, mice with a heart-specific defect in mitochondrial transcription factor A (Tfam) had progressively decreasing rates in respiratory chain

enzyme activities and rates of mitochondrial ATP production [194]. In heart-specific Tfam-KO mice, mitochondrial DNA became depleted and the mice died between 10-12 weeks of age [172]. In Tfam-deficient hearts, mitochondrial mass increased late in the progression, but ATP production was not improved by the increased mitochondrial biogenesis. In fact, the authors suggested that the "observed switch in metabolism is unlikely to benefit energy homeostasis in the respiratory chain-deficient hearts and therefore likely aggravates the disease. It can thus be concluded that at least some of the secondary gene expression alterations in mitochondrial cardiomyopathy do not compensate but rather directly contribute to heart failure progression" [194]. Similar findings are present in people with mitochondrial myopathies, usually caused by defects in OX/PHOS genes; and these patients present with a range of symptoms often including muscle weakness and multi-system degeneration [195]. Such people have increases in mtDNA transcripts and nuclear OXPHOS gene transcripts and a variety of related genes involved in energy metabolism [192]. These changes suggest that tissues are attempting to compensate for the OXPHOS defects by stimulating mitochondrial biogenesis. Related to OX/PHOS function, a knockout of the heart/muscle isoform of the adenine nucleotide translocator (Ant1) resulted in cardiac hypertrophy with mitochondrial proliferation. ANT transports ATP from the mitochondria into the cytosol in exchange for ADP [196]. In conclusion, these data suggest that defects in oxidative phosphorylation result in cardiac hypertrophy due to defective energy production, despite increased mitochondrial biogenesis.

FA availability for heart and cardiac outcomes. FA availability for oxidation influences heart energy metabolism in normal and diabetic hearts. In this regard, the heart–specific deficiency of lipoprotein lipase (LPL) induced in mice at 8 weeks of age results in a virtually absent uptake of FA hydrolyzed from VLDL-TAG and overall FA

oxidation rates are reduced 50% [197]. The heart-specific LPL deficient mice develop cardiac hypertrophy and a 50% decline in fractional shortening. Acute deletion of cardiac lipoprotein lipase forces the heart to increase glucose uptake and oxidation, decrease FA uptake and oxidation, and eventually leads to decreased ejection fraction and cardiac hypertrophy indicating that lack of exogenous FA was severely detrimental to heart function [197, 198]. The deficiency of CD36/FAT, a plasma membrane protein that enhances FA uptake into cells, reduces free FA uptake into the heart by 50% but does not affect FA oxidation at the mitochondria [199]. CD36 null mice have enlarged hearts and impaired recovery from ischemia that is rescued by the addition of medium chain fatty acids, suggesting that fatty acid metabolism is critical for ischemia-reperfusion recovery [200]. These data suggest that diminished uptake of FA by the heart in CD36 null mice does not heavily impact heart function but diminished uptake of FA from circulating lipids, as in the LPL deficient hearts, leads to heart dysfunction. Thus, it appears that the uptake of extracellular FA is critical below a threshold.

Table 2.6. Genetic deficiencies and resulting cardiac outcome.

Gene	Function	Cardiac Outcome
OCTN1	Carnitine transporter	Hypertrophy, lipid accumulation
CPT1-inhibitors	Acyl-carnitine transferase	Hypertrophy
CACT	Carnitine transporter	Cardiomyopathy, lipid accumulation
MCAD	FA oxidation	Hypertrophy, lipid accumulation
VLCAD	FA oxidation	Hypertrophy, lipid accumulation, mitochondrial excess
MTP	FA oxidation	Arrhythmia
OX/PHOS	Electron transport chain	Hypertrophy, mitochondrial excess
ANT1	ATP transporter	Hypertrophy, mitochondrial excess
LPL	Endothelial Lipase	Hypertrophy
CD36	FA uptake/oxidation	Impaired ischemia recovery

The FA entering the cardiomyocytes must be “trapped” within the cell via activation with a CoA or by binding to carrier proteins. For example, the heart-specific fatty acid binding protein, H-FABP, knockout mouse has 80% reduction in heart FA

uptake with a concomitant 80% increase in glucose uptake. The H-FABP knockout mouse has cardiac hypertrophy and exercise intolerance possibly due to reduced rates of FA oxidation, however, FA oxidation was not assessed [201]. The cardiac-restricted knockout of PPARδ in mouse results in decreased FA oxidation and hypertrophy of the heart [202]. **While several signaling mechanisms have been linked to the induction of pathological hypertrophy; the mechanisms that lead hypertrophied hearts to fail remain unknown.**

Energy insufficiency in cardiac hypertrophy. The metabolic shift from FA oxidation towards increased glucose oxidation in the hypertrophic heart may ultimately result in reduced energy production. Reductions in heart phosopho-creatine/ATP ratios correlate with severity of heart failure [203]. However, whether cardiac energy demands are adequately met by increased rates of glucose oxidation in the hypertrophy state remains to be established. The activity of AMPK, due to a rise in the AMP/ATP ratio, is associated with cardiac hypertrophy [204]. Increased AMPK activity suggests that the increased rates of glucose oxidation are either mediated through increased AMPK activity, or that glucose oxidation does not supply sufficient ATP to prevent the activation of AMPK. AMPK activity has been shown to increase both FA and glucose uptake and oxidation; therefore it is not likely that AMPK is the mechanism by which glucose oxidation is preferentially increased in the hypertrophic heart. It is also unclear whether insufficient energy production is a causal factor in hypertrophy-related heart failure. However, heart failure does correlates with reductions in mitochondrial respiratory chain protein content and activity [205]. The mitochondrial dysfunction seen in heart failure is postulated to be due to oxidative stress and not due to changes in gene expression; however, the mechanism of increase in oxidative stress by increased glucose oxidation remains unclear. Furthermore, studies show that mitochondrial function in hypertrophied

hearts prior to heart failure is not impaired suggesting that mitochondrial dysfunction occurs in late stage heart failure [206].

Lipid Intermediates and signaling. Ventricular hypertrophy occurs in obese individuals and in these patients it is associated with myocardial lipid accumulation. Fatty heart is correlated with congestive heart failure and diabetes and is found in some mouse models of cardiac hypertrophy [207]. Cellular lipids accumulate in the form of triacylglycerol in intracellular lipid droplets. Triacylglycerol itself is not thought to be a lipotoxic molecule; however, the precursors for TAG synthesis have been shown to mediate cellular signaling pathways. Lipotoxicity is a term that refers to cell death due to the accumulation of lipids and lipid by-products and is a postulated mechanism for cardiac failure. Acyl-CoAs are the first molecule formed for the synthesis of TAG and the accumulation of lipids can lead to a rise in cellular acyl-CoAs, such as palmitoyl-CoA. Palmitoyl-CoA can condense with serine to form the molecule ceramide. Ceramide, in turn, may induce apoptosis by activating stress signals and/or upregulating inducible nitric oxide synthase. Another lipid intermediate is lysophosphatidic acid (LPA) which is an intermediate of complex lipid synthesis that is a known mediator of cellular signaling. In cardiomyocytes, LPA increases cell size and the expression of ANF, a hypertrophy marker. LPA has also been shown to stimulate the phosphorylation of Akt and the expression of p65 and NF-κB; whereas, the inhibition of PI3K, mTOR, and NF-κB prevented LPA-induced expression of ANF [208]. These data suggest that the lipid intermediate LPA may play a role in the signaling that mediates cardiac cell growth. Diacylglycerol (DAG) is another lipid intermediate known to activate protein kinase C (PKC) [209]. Cellular DAG levels are increased in response to signaling through the hypertrophic-inducing Gq protein-coupled receptor agonists angiotensin II, endothelin 1, and phenylephrine. PKC regulates numerous cellular functions including cell growth and

differentiation and PKC plays an important role in the development of cardiac hypertrophy and the progression to heart failure, thus DAG may mediate PKC signaling and cardiac function [210-212]. Additionally, DAG can be converted to phosphatidic acid (PA) by one of the eleven DAG kinase isoforms. PA has also been shown to act as a lipid second messenger by regulating PKC and phospholipase C isoforms that may be involved in mediating hypertrophic signaling [213], [214]. Thus, in models of increased cardiac lipid accumulation a rise in cellular lipid intermediates such as acyl-CoA, LPA, PA, and DAG could be expected. These lipid intermediates could thus act as ligands or second messengers that mediate the cellular signaling involved in the development of cardiac hypertrophy and heart failure.

Glycolytic intermediates and signaling. Glycolytic enzymes are associated with the sarcolemma and the sarcoplasmic reticular membranes, where the ATP generated by glycolysis is thought be important for supporting the activity of ion pumps and channels that regulate excitation-contraction coupling [215, 216]. The ATP generated by glycolytic metabolism may also be particularly important for maintaining intracellular Ca^{2+} homeostasis during ischemia-reperfusion potentially due to the anaerobic nature of glycolysis and due to the proximity of glycolytic enzymes to Ca^{2+} channels [217]. Glycolytic metabolism may play a regulatory role in Ca^{2+} homeostasis through direct interaction of glycolytic intermediates with Ca^{2+} channels. The ryanodine receptor/Ca^{2+}-release channel has increased activity due to exposure to glycolytic intermediates [218]. While direct interaction of glycolytic intermediates has not been shown, studies reveal that the intermediates are critical in regulating Ca^{2+} flux especially in conditions of low ATP supply potentially by serving as precursors to ATP synthesis at the sarcolemma [219]. These data suggest that cardiac glycolysis and glycolytic intermediates may serve as an energy source and regulator for Ca^{2+} homeostasis.

Glucose stimulates S6K phosphorylation in isolated working mouse hearts, indicating that increased glucose catabolism activates mTOR [220]. Further, in cardiomyocytes that are exposed to 2-deoxyglucose, which is converted to 2-deoxyglucose-6-phophate but not further metabolized, S6K is phosphorylated, whereas exposure to 3-O methylglucose, which cannot be converted to methylglucose-6-phosphate, does not phosphorylate S6K [220]. These data suggest that an increased glycolytic flux stimulates mTOR and that the shift to glycolytic metabolism causes cardiac hypertrophy. Potentially, the increase in glycolytic activity can induce hypertrophy and may lead to imbalances in Ca^{2+} homeostasis that influence heart failure.

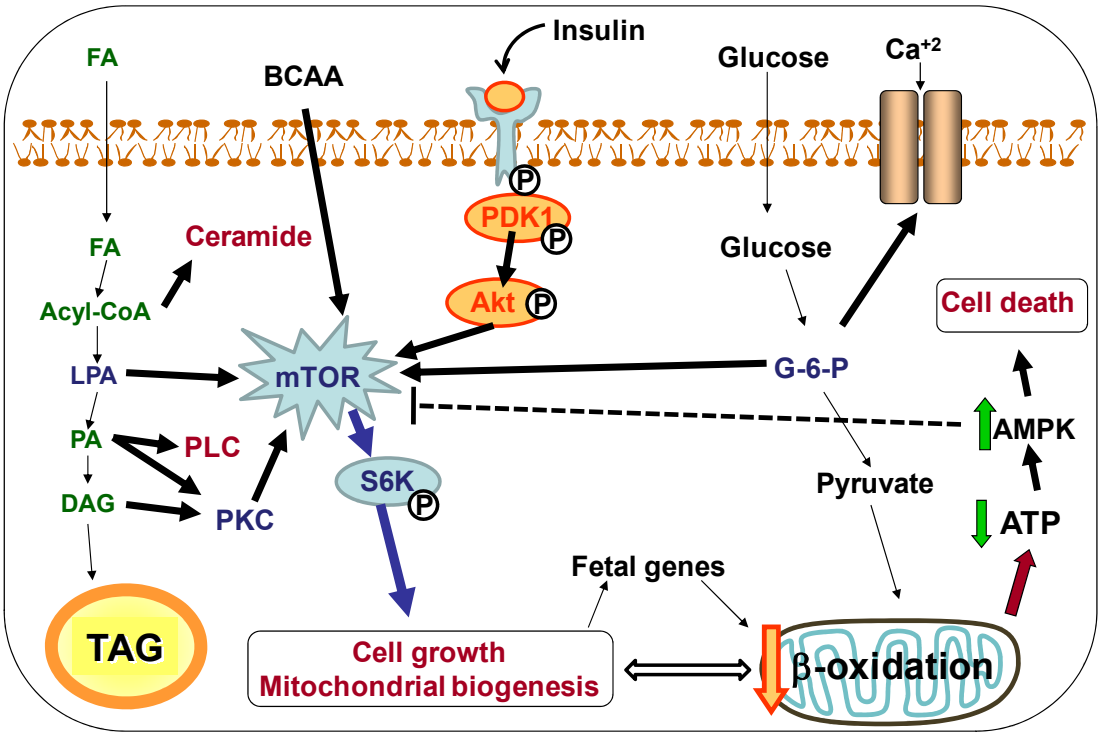

Figure 2.10. Potential mechanisms linking substrate metabolism to cardiac hypertrophy. Cardiac hypertrophy can occur due to mTOR activation. mTOR is predicted to be activated by many cellular signals including insulin signaling, glycolytic intermediates, lipogenic intermediates, and protein kinase C. It remains unclear how a shift away from FA oxidation would activate mTOR.

CHAPTER IV

THE ROLE OF ACSL1 IN CARDIAC METABOLISM AND FUNCTION

The aim 1 and 2 manuscript focused on the role of ACSL1 in adipocyte metabolism of adipose-specific ACSL1 knockout mice, *Acsl1*$^{A-/-}$. ACSL1 is the major ACSL isoenzyme expressed in adipose tissue where the primary fate of FA is storage as TAG, but ACSL1 is also the major ACSL isoenzyme in heart where the primary fate of FA is oxidation. The next chapter focuses on the cardiac-related phenotype of a multi-tissue tamoxifen-induced ACSL1 knock out mouse, *Acsl1*$^{T-/-}$. The data that follows also suggests that ACSL1 activates FA for oxidation in heart. These studies show that the reduction in FA oxidation causes cardiac hypertrophy through the activation of mTOR.

Mouse cardiac acyl-CoA synthetase-1 deficiency impairs fatty acid oxidation and induces hypertrophy and mitochondrial biogenesis.

Acyl-CoA synthetase-1 is required for cardiac FA oxidation

Authors:

Jessica M. Ellis[1], Shannon B. Mentock[1], Michael A. DePetrillo[1], Timothy R. Koves[2], Steven M. Watkins[3], Deborah M. Muoio[2], Gary W. Cline[4], Gerald I. Shulman[4,5], Monte S. Willis[6], and Rosalind A. Coleman[1]

[1]Department of Nutrition, University of North Carolina at Chapel Hill, 27599

[2]Department of Medicine, Duke University, Durham NC 27708

[3]Lipomics Technologies, Inc., 2545 Boatman Ave, West Sacramento, CA 95691

[4]Departments of Internal Medicine and Cellular & Molecular Physiology; and [5]Howard Hughes Medical Institute, Yale University School of Medicine, New Haven, CT 06520

[6]Department of Pathology, University of North Carolina at Chapel Hill, 27599

Corresponding author: Rosalind A. Coleman,

135 Dauer Drive, MHRC 2301, Department of Nutrition, CB# 7461, University of North Carolina at Chapel Hill, Chapel Hill, NC 27599, USA.

Tel: 919-966-7213

Fax: 919-843-8555

email: rcoleman@unc.edu

Conflicts of Interest: None

Abstract

Acyl-CoA synthetase isoform-1 (ACSL1) catalyzes the synthesis of acyl-CoA from long chain fatty acids and contributes the majority of long-chain acyl-CoA synthetase activity in the heart. To understand its functional role in heart, we studied mice lacking ACSL1 under temporal control (*Acsl1*$^{T-/-}$). Compared to littermate controls, heart ventricular ACSL activity was reduced more than 90%, acyl-CoA content was 65% lower, and long-chain acyl-carnitine content was 80-90% lower. The rate of [^{14}C]palmitate oxidation in heart homogenate and mitochondria was 90% lower than in controls, and maximal [^{14}C]pyruvate and [^{14}C]glucose oxidation were each 20% higher. Compared to controls, *Acsl1*$^{T-/-}$ hearts were hypertrophied, and the mitochondrial area was 54% greater than controls with twice as much mitochondrial DNA. The phosphorylation of S6 kinase, a target of mTOR kinase, increased 5-fold in *Acsl1*$^{T-/-}$ hearts, and the mRNA abundance of *Pgc1*α and *Errα*, increased by 100% and 41%, respectively; these S6K targets induced mitochondrial biogenesis. Our data suggest that ACSL1 is required to synthesize the acyl-CoAs that are oxidized in the heart, and that without ACSL1, diminished FA oxidation and compensatory catabolism of glucose and amino acids leads to mTOR activation, cardiac hypertrophy, and mitochondrial biogenesis without lipid accumulation or immediate cardiac dysfunction.

Keywords: oxidation, cardiac hypertrophy, acyl-CoA, mitochondrial biogenesis, mTOR

Non-standard Abbreviations and Acronyms: ACSL, long-chain acyl-CoA synthetase; ASM, acid soluble metabolites; FA, fatty acid; PC, phosphatidylcholine; PL, phospholipid; TAG, triacylglycerol; mTOR, mammalian target of rapamycin.

Introduction

Under fasting conditions 60 to 90% of heart ATP is provided by the mitochondrial oxidation of long-chain fatty acids (FA) [53, 221, 222]. Reduced cardiac FA oxidation and increased glucose utilization are a proposed consequence of pathological left ventricular hypertrophy (LVH) [223, 224]. However, when genes that encode enzymes of FA oxidation are knocked out in mice, LVH develops [225-228]. Thus, it remains unclear whether the shift in substrate use is a cause or consequence of cardiac hypertrophy and whether the increased use of glucose interferes with cardiac function.

ACSL isoenzymes convert FA to acyl-CoA in an ATP-dependent manner, simultaneously activating and trapping FA within cells [229]. Activation to acyl-CoA is required before FA can be either oxidized to provide ATP or esterified to synthesize triacylglycerol (TAG) or membrane phospholipids (PL). The activation of FA is catalyzed by one of a family of 5 long-chain acyl-CoA synthetases (ACSL), ACSL1, ACSL3, ACSL4, ACSL5, and ACSL6, which differ in substrate preference, enzyme kinetics, subcellular location, and tissue-specific expression [24]. Because amphipathic acyl-CoAs can move freely within a membrane monolayer or be transported to distant membranes, all acyl-CoAs should, theoretically, be metabolically equivalent, no matter which ACSL isoenzyme catalyzes their formation and no matter which subcellular organelle is the site of their synthesis. Yet, both loss-of-function and gain-of-function studies suggest that each ACSL isoenzyme has a distinct function in directing acyl-CoAs to one or more specific downstream pathways [16, 34, 36].

Although FA provide the major substrate for oxidation in heart, it is unknown whether ACSL activity affects FA oxidation rates or whether a particular ACSL isoenzyme activates FA destined for oxidation. Total ACSL activity of mouse embryonic (E16.5) heart increases

14-fold during the week after birth and 90-fold by adulthood [5]. This dramatic increase in ACSL activity parallels the transition of the developing heart's substrate preference from glucose prenatally to FA after birth. In mice, this transition is accompanied by a 6-fold increase in *Acsl1* mRNA abundance and a >90% decrease in the mRNA abundance of *Acsl3*, the predominant *Acsl1* in fetal heart [5]. In rats the increase in ACSL activity and *Acsl1* mRNA expression parallels the postnatal heart's increased workload, rate of ATP generation, oxidative preference for FA, and expression of FA oxidative genes [230]. Together, these data suggested that ACSL1 might be the major activator of the FA that are oxidized in postnatal cardiac tissue.

In order to understand the relationship between cardiac substrate use and hypertrophy, we created a mouse model that lacks acyl-CoA synthetase-1 (ACSL1) in multiple tissues, including heart. We reasoned that the absence of ACSL1 would enable us to learn whether a block in FA activation prevents potential lipotoxicity and abnormal heart function, and to determine the mechanism by which a shift in substrate use from FA to glucose causes cardiac hypertrophy.

Results

Cardiac ACSL activity and acyl-CoA content are reduced in mice that lack ACSL1

Mice with *Loxp* sequences inserted on either side of exon 2 in the *Acsl1* gene were backcrossed to the C57Bl/J6 strain six times [78], and then interbred with mice in which Cre expression, driven by chicken β-actin and cytomegalovirus enhancers, can be induced by tamoxifen (B6.Cg-Tg(CAG-cre/Esr1)5Amc/J; Jackson Labs, Bar Harbor, MA) to generate tamoxifen-inducible multi-tissue *Acsl1* knockout mice (*Acsl1*$^{T-/-}$). Tamoxifen was injected i.p. (3.5 mg/kg body wt) for 4 consecutive days when mice were 6-8 weeks old. Control littermates, which were also injected with tamoxifen, lacked the C*re* gene (*Acsl1*$^{flox/flox}$).

Compared to liver, kidney and adipose, the largest and most persistent reduction in total ACSL enzyme activity and ACSL1 protein was observed in *Acsl1*$^{T-/-}$ hearts (**Figure 1A, B, S1A, B**). Ten weeks after tamoxifen was injected, total ACSL activity in heart ventricles was 97% lower than controls (**Figure 1A**). The ACSL activity that remained in tissues was probably due to other ACSL isoenzymes, to residual ACSL1 activity in cells that had not been exposed to tamoxifen, or in liver, to hepatocytes that metabolize tamoxifen. The appearance, histology, and weights of the liver and adipose tissue did not differ between genotypes **(Table 2; data not shown**). Two weeks after the tamoxifen injection, heart *Acsl1* mRNA was nearly absent but 40% of ACSL1 protein remained (**Figure 1B**), suggesting that the half-life of ACSL1 may be as long as two weeks. By ten weeks after tamoxifen, virtually no ACSL1 protein was present. Other differences between the two time points included 37% lower *Acsl1*$^{T-/-}$ TAG and 2.5-fold higher FA concentrations in plasma, compared to controls at two weeks, but not at ten weeks after tamoxifen. In *Acsl1*$^{T-/-}$ hearts, loss of ACSL1 reduced the total pool of long-chain acyl-CoAs by 65% (**Figure 1D**), with 67-75% reductions in 16:0-, 16:1-, 18:1-, 18:2-, and 18:3-CoA species and a 26% reduction in 18:0-

CoA (**Figure 1E**). Expressed as a percentage of total acyl-CoA content, 18:0-CoA was twice as high in *Acsl1*$^{T-/-}$ hearts as in controls, and all other species except 16:0 were reduced ~20% (**Figure S1C**). Thus, aside from the relative increase in 18:0-CoA, lack of ACSL1 did not markedly change the FA composition of the acyl-CoA pool. These data indicate that ACSL1 is the major activator of long-chain FA in the heart, and that the knockdown of *Acsl1* was virtually complete and persistent in cardiac tissue for as long as 10 weeks. Despite the 65% reduction in long-chain acyl-CoA content in *Acsl1*$^{T-/-}$ hearts, total cardiac TAG content did not change, suggesting that ACSL1 does not limit the acyl-CoA pool used for the synthesis of TAG (**Figure 1F**).

ACSL1 is required for heart FA oxidation

To determine whether ACSL1 provides acyl-CoAs for FA oxidation, we assessed the rates of [1-^{14}C]palmitate incorporation into CO_2 and ASM, which are measures of complete and incomplete oxidation, respectively. Compared to controls, the rate of maximal FA oxidation in *Acsl1*$^{T-/-}$ heart homogenates was 95% lower (**Figure 2A**). Thus, the absence of ACSL1 nearly abolished FA oxidative capacity. In contrast, in *Acsl1*$^{T-/-}$ liver, in which ACSL1 protein and activity remained similar to that of controls (**Figure S1A,B**), the rate of [1-^{14}C]palmitate oxidation was unchanged (Figure 2A). The oxidation rates for the ACSL1 product [1-^{14}C]palmitoyl-CoA were similar between genotypes (**Figure 2B**), indicating that CPT1-mediated transport of acyl-CoA into the mitochondria and its subsequent oxidation to CO_2 was unimpaired and that the severe block in FA oxidation in *Acsl1*$^{T-/-}$ hearts was due to the lack of FA activation.

The 95% lower rates of FA oxidative capacity in *Acsl1*$^{T-/-}$ heart homogenates strongly suggested that ACSL1 activates the pool of FA that is directed towards mitochondrial oxidation. This interpretation is further supported by the presence of residual ACSL1 in

purified heart mitochondria two weeks after tamoxifen was injected (**Figure 2C**). At that time, when ~40% of ACSL1 protein still remained, [1-^{14}C]palmitate oxidation in *Acsl1*$^{T-/-}$ heart mitochondria was 40% lower than in controls (**Figure S1D**); however, 10 weeks after tamoxifen, when ACSL1 protein was absent, [1-^{14}C]palmitate oxidation was 90% lower than in controls (**Figure 2D**). These data showing that the rate of FA oxidative capacity and the amount of ACSL1 protein decreased in parallel, support the idea that ACSL1 is required to activate cardiac FA before they can be oxidized.

Cellular acyl-carnitines are markers of metabolite flux through degradative and oxidative pathways [136]. In *Acsl1*$^{T-/-}$ cardiac tissue, total free carnitine was 77% higher than in control hearts, indicating that carnitine was not limiting (**Figure 2E**), whereas acetyl-carnitine was 51% lower, consistent with reduced mitochondrial acetyl-CoA levels (**Figure 2F**). Confirming the impaired FA oxidation, nearly all medium-chain (8 to 12 carbons) acyl-carnitine species in *Acsl1*$^{T-/-}$ hearts were 60-80% lower than in controls (**Figure 2G**), and long-chain acyl-carnitines were 80-90% lower (**Figure 2H**). Total cholesteryl ester and diacylglycerol were reduced ~20% in *Acsl1*$^{T-/-}$ hearts, but total PL and TAG were unaffected (**Figure S2A,B,C**). Because the content of PL and TAG was normal in *Acsl1*$^{T-/-}$ hearts, but the abundance of nearly all acyl-carnitine species was reduced ~90%, it appears that ACSL1 activity does not affect the synthesis of acyl-CoAs used in the pathways of PL and TAG synthesis, but, instead, specifically provides the acyl-CoAs required for FA oxidation.

Pathological cardiac hypertrophy and mitochondrial biogenesis in the *Acsl1*$^{T-/-}$ mice

Compared to controls, the weights of *Acsl1*$^{T-/-}$ female and male hearts as a percent of body weight were 23% and 17% greater, respectively (**Figure 3A**). Cardiomyocyte area was 27% larger than controls (**Figure 3B**), and ventricular walls appeared thickened (**Figure 3C**). Echocardiography confirmed that *Acsl1*$^{T-/-}$ ventricular walls were 10-41% thicker than

controls (**Table 1**) with a 34% heavier left ventricular mass (**Figure 3D**). Analysis also showed that the *Acsl1*$^{T-/-}$ left ventricular inner diameter was ~30% smaller than controls, suggesting concentric ventricular hypertrophy (**Table 1**). Despite LVH, the percent fractional shortening and ejection fraction were similar to controls, indicating that cardiac function remained normal for at least 2 months after the ablation of *Acsl1* (**Figure 3E,F and Table 1**).

Upregulation of fetal genes occurs with pathological hypertrophy [231], thus, the 4- to 5-fold higher mRNA expression of the fetal genes, α-skeletal actin and brain natriuretic peptide, together with the 6-fold upregulation of *Acsl3,* the major *Acsl* mRNA expressed in fetal heart [5] (**Figure 1C**), is compatible with pathological hypertrophy (**Figure 3G**). Fibrosis was not present (data not shown). Thus, lack of ACSL1 for ten weeks severely impaired FA oxidation and induced ventricular hypertrophy with upregulation of fetal genes but without cardiac dysfunction or failure.

Electron microscopy showed that the mitochondrial area in *Acsl1*$^{T-/-}$ ventricles was 54% greater than in controls (**Figure 4A,B**). Confirming the enhanced mitochondrial biogenesis in *Acsl1*$^{T-/-}$ ventricles, the mitochondrial DNA abundance for NADH dehydrogenase subunit 1, cytochrome B, and cytochrome C oxidase 1 were at least 2-fold higher than controls (**Figure 4C**). Mitochondrial biogenesis is driven by several transcription factors, including PGC1α and ERRα [232]. In *Acsl1*$^{T-/-}$ ventricles the mRNA abundance of *Pgc1*α and *Err*α was 100% and 41% greater, respectively, than in controls (**Figure 4D**). Because FA oxidation was severely impaired, we suspected that an energy deficit might exist that would activate the energy-sensing enzyme, AMP-activated kinase (AMPK), which can upregulate *Pgc1*α. However, compared to controls, AMPK phosphorylation (Thr^{172}), was ~40% lower in *Acsl1*$^{T-/-}$ ventricles (**Figure 4E**). Myocardial ATP and AMP content did not differ between genotypes (**Figure S2D**), suggesting that glucose oxidation had increased sufficiently to maintain the cellular ATP/AMP ratio. Because long-chain acyl-CoAs

can indirectly reduce AMPK activation by allosterically interacting with LKB1/AMPKK, the decrease in AMPK phosphorylation may have resulted from the reduction in ventricular acyl-CoA content [61].

Increased glucose use in *Acsl1*$^{T-/-}$ hearts

Because the capacity of *Acsl1*$^{T-/-}$ hearts to oxidize FA was markedly impaired, yet cellular ATP content was preserved, we questioned whether the oxidative capacity for non-FA substrates had increased to compensate. In *Acsl1*$^{T-/-}$ heart homogenates, the maximal rate of [U-^{14}C]glucose incorporation into [^{14}C]CO_2 was 20% higher than in controls (**Figure 5A**), and in *Acsl1*$^{T-/-}$ ventricular mitochondria, the oxidation of [1-^{14}C]pyruvate to [^{14}C]CO_2 was 17% higher (**Figure 5B)**. Consistent with increased utilization of glucose, blood glucose in *Acsl1*$^{T-/-}$ plasma was 17% lower than in controls (**Table 2).** These findings suggested an increase in pyruvate dehydrogenase activity compatible with the increase in mitochondrial abundance. In addition, propionyl- and methyl-malonyl/succinyl-carnitines were 71% and 174% higher in *Acsl1*$^{T-/-}$ hearts (**Figure 5C**). These carnitine species are metabolites of glucose and of branched-chain and ketogenic amino acids, suggesting that oxidation of these alternate substrates had increased in *Acsl1*$^{T-/-}$ hearts. Confirming that protein catabolism provided an alternative fuel source, the total amino acid content in *Acsl1*$^{T-/-}$ hearts was 32% higher than in controls (**Figure 5D**). This increase in amino acid content was reflected by increases in nearly every amino acid species (**Figure 5E,F**). Together, these data strongly support the conclusion that reduced FA oxidation in *Acsl1*$^{T-/-}$ hearts leads to compensatory increases in glycolysis and protein catabolism.

mTOR stimulates hypertrophy and mitochondrial biogenesis in *Acsl1*$^{T-/-}$ hearts

The mammalian target of rapamycin, mTOR kinase, activates pathways that increase both cell growth and mitochondrial biogenesis [233, 234]. mTOR kinase activation is required for

both thyroid hormone-induced and spontaneous hypertensive rat cardiac hypertrophy [235, 236]. To determine whether mTOR was linked to the hypertrophy and mitochondrial biogenesis observed in *Acsl1*$^{T-/-}$ hearts, we quantified phosphorylation of the mTOR target, p70-S6 kinase (S6K). Compared to controls, S6K phosphorylation at Thr^{389} was 5-fold greater in *Acsl1*$^{T-/-}$ hearts (**Figure 5G**). These data strongly suggest that the cardiac hypertrophy in *Acsl1*$^{T-/-}$ mice was mediated by activation of the mTOR pathway. Possible causes of enhanced mTOR signaling include elevations in amino acid availability [237], enhanced glycolytic flux [238], elevated plasma insulin [239], and hypertension [240]. mTOR activation in *Acsl1*$^{T-/-}$ hearts probably resulted from a combination of several of these factors, including the 32% higher amino acid content (**Figure 5D**) and the increase in glucose oxidation. In addition, diminished AMPK activity, as measured by the ~40% reduction in *Acsl1*$^{T-/-}$ heart AMPK phosphorylation (**Figure 4E**), would relieve the inhibition of mTOR by AMPK [241]. Other activators of mTOR signaling were not present; neither plasma insulin nor the area under the curve during an insulin tolerance test differed between genotypes (**Table 2**), and hypertension was not present (**Table 2**). In summary, these data suggest that increased amino acid availability, decreased AMPK activity, and increased glycolytic flux activated mTOR in *Acsl1*$^{T-/-}$ hearts, and that enhanced mTOR activity resulted in mitochondrial biogenesis and cardiac hypertrophy.

PPARα transcription factor activity in nuclear extracts from control and *Acsl1*$^{T-/-}$ hearts was not different between genotypes (**Figure S2E**), but several PPARα/δ target genes were markedly upregulated in *Acsl1*$^{T-/-}$ hearts, including muscle carnitine palmitoyltransferase 1, cytosolic thioesterase 1, and *Acsl3* [242] (**Figure 5 H, I and 1C**). The increased mRNA abundance of mitochondrial β-oxidation genes could reflect either increased mitochondrial content in *Acsl1*$^{T-/-}$ hearts or the activation of PPARδ by mTOR [243].

Altered FA composition of *Acsl1*$^{T-/-}$ cardiac lipids

Despite the 90% loss of ACSL activity, *Acsl1*$^{T-/-}$ and control hearts contained similar amounts of TAG and PL (**Figure 1F, Figure S2A,B,C**). If all acyl-CoAs were metabolically equivalent, the composition of complex lipids would reflect changes in the acyl-CoA pool. However, despite the fact that the *Acsl1*$^{T-/-}$ hearts contained twice as much 18:0-CoA as controls (as a percentage of total long-chain acyl-CoAs) (**Figure S1C**), the amount of 18:0 did not change in the TAG, PE, and PS fractions of *Acsl1*$^{T-/-}$ hearts and was significantly lower in the CL and PC fractions (**Figure S3A-J**). *Acsl1*$^{T-/-}$ 18:1-CoA content was ~60% lower than in controls and, as a percent of total long-chain acyl-CoAs, was 10-20% lower (**Figure 1E, Figure S1C**), however, the total content of 18:1 was not altered in the TAG, PE, and PS fractions, and was increased in the CL and PC fractions. As a percent of total esterified FA, 18:1 was increased in TAG, PE, CL, and PC, but not in PS (**Figure S3A-J**). These data indicate that the FA composition of TAG and PL in *Acsl1*$^{T-/-}$ heart did not reflect the changes in the acyl-CoA pool and suggest that other ACSL isoenzymes contributed the acyl-CoAs that were esterified in pathways of glycerollipid synthesis.

Discussion

The primary finding of this study is that ACSL1 provides the FA used for cardiac oxidation, and that in the absence of ACSL1, the heart compensates by increasing the oxidation of glucose and amino acids. Normally, FA provide 60 to 90% of the heart's energy requirements, and glucose and lactate oxidation provide the remaining ATP [221, 222]. The use of these three energy sources is controlled by substrate availability, physiological conditions, and transcriptional and hormonal regulation. Our data suggest that, in addition, the activity of the ACSL1 isoform controls the use of FA as an oxidative substrate.

Whether a shift from lipolytic to glycolytic oxidation is a cause or a consequence of cardiac hypertrophy has remained unclear. Data from human deficiencies in FA oxidation and rodent models with genetically or chemically impaired FA oxidative capacity support the interpretation that reduced FA oxidation causes cardiac hypertrophy. For example, in humans, defects in the Na^+-carnitine co-transporter (OCTN2) cause a cardiomyopathy characterized by cardiac lipid accumulation and hypertrophy [244]. Similarly, the juvenile visceral steatosis mouse mimics human systemic carnitine deficiency because it has a spontaneous deficiency of OCTN2 that results in cardiac lipid accumulation and hypertrophy and a 2-fold increase in cardiac mitochondrial area [225]. Similarly, inhibition of CPT1 and acyl-carnitine synthesis in rats leads to cardiac hypertrophy [226], and mice deficient in long-chain acyl-CoA dehydrogenase (LCAD) [227] or very-long-chain acyl-CoA dehydrogenase (VLCAD) [228] also develop cardiac hypertrophy, increased mitochondrial biogenesis, and TAG accumulation. In VLCAD deficient mice, AMPK is activated and whole body fat oxidation is increased [60].

When ACSL1 is overexpressed 12-fold in mouse heart, left ventricular mass doubles by 3 weeks of age, and heart failure, characterized by a 50% reduction in percent fractional shortening, occurs by 4 weeks of age [245]. Rates of FA oxidation were not assessed in these hearts, but heart TAG and phosphatidylcholine content was 12-fold and 1.5-fold higher, respectively, than in controls. These data suggest that when ACSL1 is markedly overexpressed, the acyl-CoAs produced are used to synthesize TAG and PL. In this model, ACSL1 overexpression probably trapped high amounts of acyl-CoA within cardiomyocytes, without a concomitant increase in demand for oxidation. Thus, similar to VLCAD and LCAD null mice, in which mitochondrial FA oxidation is partially prevented [227, 228], excess and potentially toxic acyl-CoAs are esterified to form TAG. In contrast to these models, lack of ACSL1 prevents FA activation, thereby both blocking FA metabolism and preventing FA from being trapped as acyl-CoA within cells. The reduction in ACSL activity allows non-activated FA to leave cells, thereby decreasing the apparent rate of FA uptake and amount of FA retained [35]. The *Acsl1*$^{T-/-}$ mice have severely impaired cardiac FA oxidation that results in hypertrophy, but without TAG accumulation.

The fact that cardiac content of PL and TAG was unchanged in *Acsl1*$^{T-/-}$ hearts despite a 97% reduction in ACSL activity, suggests that ACSL1 does not substantially contribute to the synthesis of acyl-CoAs that are incorporated into glycerolipids. If the metabolic fate of a cellular acyl-CoA were non-specific, then a 65% decrease in long-chain acyl-CoA content should diminish both oxidation and TAG synthesis equally. The normal content of TAG, the 80-90% reduction in long-chain acyl-carnitines, and the 90% decrease in palmitate oxidative capacity support the conclusion that ACSL1 channels FA specifically towards oxidation, and that acyl-CoAs synthesized by other ACSL isoenzymes are used for complex lipid synthesis, but not for oxidation.

A major regulator of cell size is the kinase mTOR which activates S6K to initiate transcriptional activity that induces cell growth [246]. Activated mTOR is present in several models of cardiac hypertrophy and is likely to be an important signal in the pathway that mediates hypertrophy. For example, S6K phosphorylation is increased in the hypertrophic hearts of spontaneous hypertensive rats (SHR), and treatment with the mTOR inhibitor rapamycin attenuates the hypertrophy without altering the hypertension [240]. Similarly, rapamycin inhibits thyroid hormone-induced S6K phosphorylation and cardiac hypertrophy [236]. Exercise-induced cardiac hypertrophy in mice also increases S6K phosphorylation [247], whereas mouse hearts lacking acetyl-CoA carboxylase 2 (ACC2) have reduced S6K phosphorylation and smaller hearts [248]. These data strongly suggest that mTOR activation mediates cell growth in several models of cardiac hypertrophy and that when mTOR is inhibited, the hypertrophy reverses or diminishes.

Several mechanisms could enhance mTOR activation in *Acsl1*$^{T-/-}$ hearts, including elevated amino acid content and diminished AMPK activity. AMPK phosphorylates the tumor suppressor complex that coverts GTP-Rheb to GDP-Rheb and inactivates mTOR [241]. Thus, a lower content of activated AMPK would potentially relieve this inhibition to allow greater mTOR activity. A third mechanism for activating mTOR is observed in isolated working mouse hearts, in which the metabolism of glucose has increased [238]. In these hearts, the initial phosphorylation of glucose appears to be critical for S6K phosphorylation; S6K phosphorylation occurred after exposing cardiomyocytes to 2-deoxyglucose, which can be phosphorylated, but not after exposure to 3-O methylglucose, which cannot. Our data suggest that the shift from FA to glucose oxidation, the consequent increase in glycolytic flux, the increase in amino acid availability, and the reduction in AMPK phosphorylation all contributed to mTOR activation in *Acsl1*$^{T-/-}$ hearts. mTOR then increased the mRNA expression of *Pgc1*α and *Err*α, resulting in mitochondrial biogenesis [249].

Because the ACSL reaction converts ATP to AMP, it has been proposed that ACSL-generated AMP is a major activator of AMPK during lipolysis in 3T3-L1 adipocytes [51]. AMPK is not activated when ACSL1 is overexpressed in mouse hearts [250]. In *Acsl1*$^{T-/-}$ hearts, AMP content was not diminished, yet AMPK phosphorylation was 40% lower than in controls, diminishing AMPK activation (Figure 4E). In *Acsl1*$^{T-/-}$ heart mitochondria, the oxidation of palmitate, but not palmitoyl-CoA, was impaired, indicating that ACSL1 was required to activate FA for oxidation and that CPT1 activity for acyl-CoA was normal. Thus, the block in FA occurred because ACSL1 did not provide an acyl-CoA substrate.

In summary, the loss of ACSL1 in mouse heart results in severely impaired FA oxidation, a compensatory increase in glucose oxidation, and cardiac hypertrophy without systolic dysfunction or lipid accumulation. The 5-fold increase in S6K phosphorylation suggests that the activation of the mTOR pathway initiates the observed cardiac hypertrophy and mitochondrial biogenesis in *Acsl1*$^{T-/-}$ hearts. In support of the role of ACSL1 in activating FA for oxidation, mice with an adipose-specific knockout of ACSL1 had reduced FA oxidation rates in white and brown adipocytes and were severely cold intolerant [251]. Like ACSL1 in adipose, it appears that ACSL1 functions in cardiac tissue to activate FA destined for β-oxidation. In this model, the shift in substrate use from FA to glucose causes the ensuing cardiac hypertrophy, although cardiac function was not impaired during the time period studied.

Methods:

Animal Treatment: All protocols were approved by the University of North Carolina Institutional Animal Care and Use Committee. Mice were housed in a pathogen-free barrier facility (12 h light/dark cycle) with free access to water and food (Prolab RMH 3000 SP76 chow). When the mice were 6-8 weeks old, tamoxifen (Sigma, St. Louis MO) (75 mg/kg BW), dissolved in corn oil (20 mg/ml), was injected i.p. for 4 consecutive days into both *Acsl1*$^{T-/-}$ and littermate *Acsl1*$^{flox/flox}$ control mice. Tissues were removed and snap frozen in liquid nitrogen. To isolate mitochondria, hearts were removed, rinsed in PBS, minced and homogenized with 10 up-and-down strokes, using a motor-driven Teflon pestle and glass mortar in ice-cold buffer (0.2 mM EDTA, 0.25 M sucrose, 10 mM Tris HCl, pH7.8, protease inhibitor (Roche, Florence, SC)). Homogenates were centrifuged at 1,000 x g for 10 min at 4°C, the supernatant was spun at 12,000 x g for 15 min at 4°C, and the resulting pellet was washed once and resuspended in oxidation buffer. Protein content was determined by the BCA assay (Pierce, Rockford, IL) with BSA as the standard. Plasma was collected from mice in 5% 0.5 M EDTA. Plasma TAG, β-hydroxybutyrate (Stanbio, Boerne, TX), cholesterol, FFA, glucose (Wako, Richmond, VA), and free and total glycerol (Sigma) were measured with colorimetric assays. Insulin tolerance tests were performed by i.p. injection with insulin (0.5 U/kg body wt) and tail blood glucose was measured at baseline, 15, 30, 60, and 120 min using a One Touch Ultra glucometer (Lifescan, Inc., Milpitas, CA). Blood pressure was measured by CODA High-Throughput Non-Invasive Tail Blood Pressure System (Kent Scientific, Torrington, CT).

ACSL assay: ACSL initial rates were measured with 50 μM [1-^{14}C]palmitic acid (Perkin Elmer, Waltham, MA), 10 mM ATP, and 0.25 mM CoA in total membrane fractions (0.5-4.0 μg) or in ventricular mitochondria [147].

RT-PCR: Total RNA was isolated from ventricles (RNeasy Fibrous Tissues Kit, Qiagen, Alameda, CA), and cDNA was synthesized (Applied Biosystems High Capacity cDNA RT Kit). Total DNA was isolated using the QIAmp DNA Micro Kit (Qiagen). DNA or cDNA was amplified by real-time PCR using SYBR Green (Applied Biosystems, Foster City, CA) detection with primers specific to the gene of interest. Results were normalized to the housekeeping gene *Gapdh* for mRNA and H19 for DNA and expressed as arbitrary units of $2^{-\Delta\Delta CT}$ relative to the control group.

Immunoblots: Total protein lysates were isolated in lysis buffer (20 mM Tris base, 1% Triton-X-100, 50 mM NaCl, 250 mM sucrose, 50 mM NaF, 5 mM $Na_2P_2O_7$, plus protease inhibitor (#11836153 Roche. Florence, SC)). Total membrane fractions were isolated in Medium I (10 mM Tris, pH7.4, 1 mM EDTA, 0.25 M sucrose, 1 mM dithiothreitol). Equal amounts of protein (40-60 µg) were loaded and resolved on 10% SDS polyacrylamide gels and transferred to nitrocellulose membranes. Blots were probed with antibodies against ACSL1 (#4047, Cell Signaling, Danvers, MA), P-AMPK (#2535), and P-p70 S6K (#9234) and were then stripped and reprobed with either total AMPKα (#2532) or p70 S6K (9202). Purity of mitochondrial fractions was verified by immunoblot with antibodies against the mitochondrial protein VDAC (Abcam, Cambridge MA, ab16816) and the ER protein calnexin (Abcam, ab13504).

Histology: Hearts were gravity perfused and fixed for 24 h in 4% paraformaldehyde-PBS and transferred to 70% ethanol. Fixed tissues were embedded in paraffin, serial sectioned, and stained with hematoxylin and eosin or Masson's trichrome. For lectin staining, paraformaldehyde-fixed cardiac tissue was deparaffinized, hydrated, and incubated with *Triticum vulgaris* lectin TRITC conjugate (Sigma). Sections were subsequently examined by

fluorescence microscopy. For electron micrograph analysis, animals were euthanized and the hearts perfused with a freshly made solution containing 2% paraformaldehyde and 2.5% glutaraldehyde in 0.15 M sodium phosphate buffer, pH 7.4. Cardiac tissue was imaged using a LEO EM910 transmission electron microscope at 80kV (LEO Electron Microscopy, Thornwood, NY) and photographed using a Gatan Bioscan Digital Camera (Gatan, Inc., Pleasanton, CA). Mitochondrial area and myocyte size were quantified using NIH ImageJ Software.

.Echocardiograms: Mouse echocardiograms were performed on unanaesthetized mice with the VisualSonics Vevo 770 (Toronto, Ontario, Canada) ultrasound biomicroscopy system. M-mode images of the left ventricle were analyzed using VisualSonics software.

Fatty acid oxidation: Freshly isolated ventricles and liver were minced and homogenized with 10 up-and-down strokes using a motor-driven Teflon pestle and glass mortar in ice-cold buffer (100 mM KCl, 40 mM Tris·HCl, 10 mM Tris base, 5 mM $MgCl_2 \cdot 6H_2O$, 1 mM EDTA, and 1 mM ATP (pH = 7.4)) at a 20-fold dilution (wt/vol) [154]. Oxidation was measured in a 200 µl reaction mixture containing 100 mM sucrose, 10 mM Tris·HCl, 10 mM KPO_4, 100 mM KCl, 1 mM $MgCl_2 \cdot 6H_2O$, 1 mM L-carnitine, 0.1 mM malate, 2 mM ATP, 0.05 mM coenzyme A, and 1 mM dithiothreitol (pH = 7.4) with either: 8 µM [1-^{14}C]palmitate (0.1 µCi/reaction) and 100 µM sodium palmitate complexed to BSA; 16 µM [1-^{14}C]pyruvate (0.1 µCi/reaction) and 200 µM pyruvate; 4 µM [1-^{14}C]palmitoyl-CoA (0.04 µCi/reaction) and 50 µM palmitoyl-CoA or 8 µM [U-^{14}C]glucose (0.1 µCi/reaction) and 200 µM glucose. Oxidation studies measured the production of ^{14}C-labeled carbon dioxide (CO_2) and acid soluble metabolites (ASM) for 30 min without substrate competition in a two-well oxidation system: one well contained the reaction mixture with the tissue homogenate and the adjoining well contained 1N NaOH. The reaction was terminated by adding 70% perchloric acid to the assay well and then incubated for one h to drive the CO_2 into the NaOH. Radioactivity of ASM in the

supernatant of the reaction mixture and CO_2 was determined by liquid scintillation. Fatty acid oxidation was quantified using the following formula: ([(dpm-BL)/SA] / [g of tissue wet wt x time (min) of reaction incubation]),where BL is the dpm of blank wells and SA is the FA specific radioactivity.

Tissue lipid and nucleotide content: Acyl-carnitines were quantified by liquid chromatography and tandem mass spectrometry [252]. Complex lipid content was analyzed by Lipomics Technologies, Inc (West Sacramento, CA) [253]. Acyl-CoA and diacylglycerol composition and content were assessed from whole heart extracted with internal standards [254]. After separation, purification, and elution, lipid metabolite extracts were separated by high performance liquid chromatography, and individual and total lipid species were analyzed by liquid chromatography/tandem mass spectrometry [254]. Frozen heart was homogenized in 0.4 M perchlorate and neutralized in 4M K_2CO_3 as described [255]. Nucleotides were separated by HPLC [256] using a Varian Prostar solvent delivery system (PS-210 Varian, Palo Alta, CA) and a Luna 5u C18 100A column (Phenomenex, Torrance, CA). Peaks were detected using a Gilson 118 UV detector (Middleton, WI).

PPARα activity: Nuclear fractions were isolated from fresh hearts (Nuclear Extraction Kit, Cayman Chemicals, Ann Arbor, MI) and used with the PPARα Complete Transcription Factor Assay Kit (Cayman Chemicals, Ann Arbor, MI) according to the manufacturer's protocol.

Acknowledgements:

Sources of Funding: NIH grants DK59935 (RAC), DK40936 (GIS), and the UNC NORC DK056350, a grant from the American Diabetes Association (DMM) an NIH Predoctoral Training grant T32-HL069768 (JME), and pre-doctoral (JME) fellowship from the American Heart Association Mid-Atlantic Division.

Figure 1 (4.1). ACSL activity and acyl-CoA content are reduced in mice that temporally lack ACSL1.

Total ACSL activity (A) and ACSL1 protein (B) in control and *Acsl1*$^{T-/-}$ ventricles 2 and 10 wk after tamoxifen, n=5-7. C) Acsl isoenzyme mRNA abundance in ventricles 2 and 10 wk after tamoxifen in control and *Acsl1*$^{T-/-}$ mice, n=6. Heart total (D) and individual long-chain acyl-CoA content (E) in control and *Acsl1*$^{T-/-}$ mice 10 weeks after tamoxifen, n=7-8. F) Heart TAG content in control and *Acsl1*$^{T-/-}$ mice 10 weeks after tamoxifen, n=7-8. Data represent mean ± SEM; *, P≤0.05 versus control; #, P≤0.05 2 wk versus 10 wk after tamoxifen within genotype.

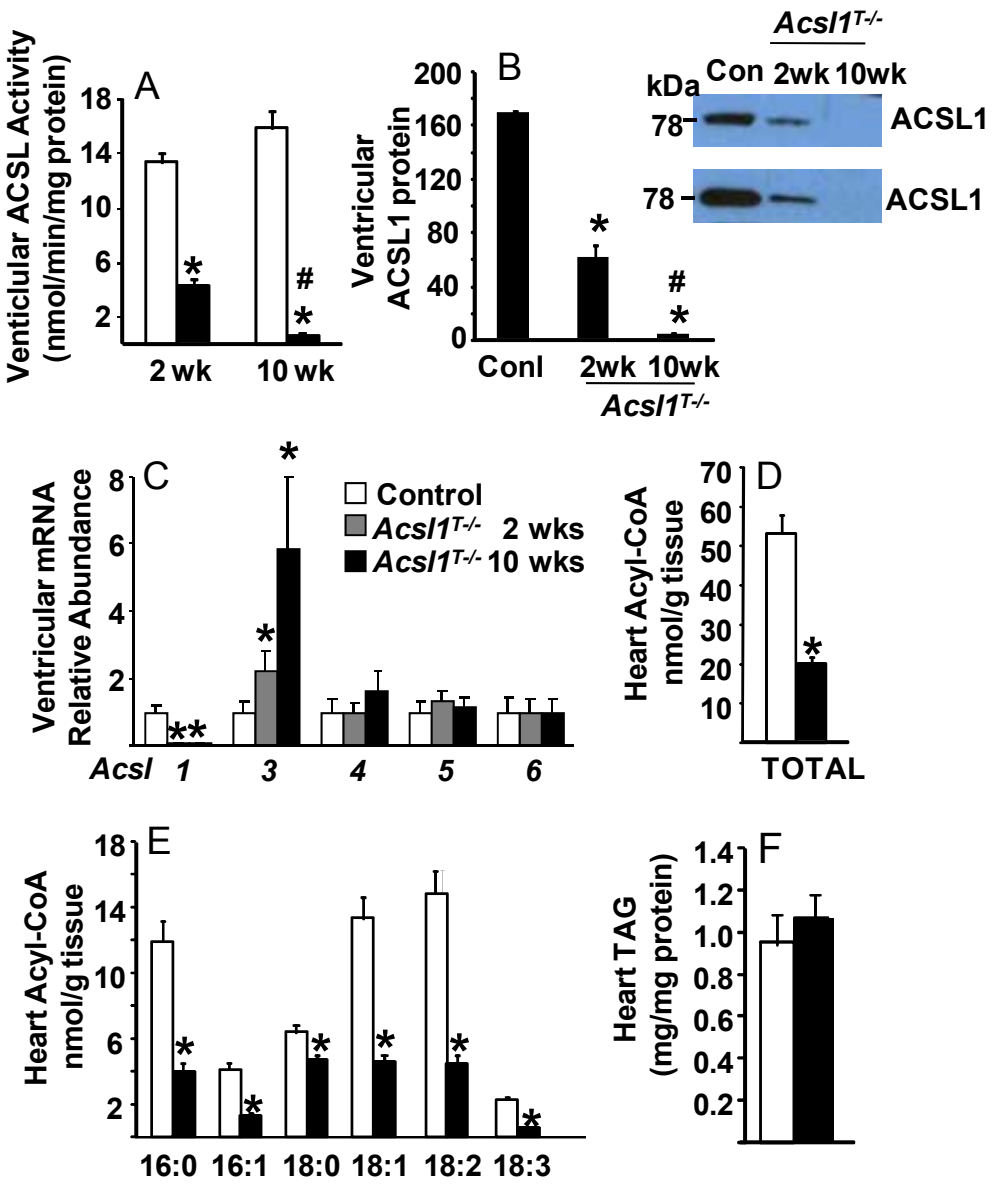

Figure 2 (4.2). *Acsl1*$^{T-/-}$ hearts have impaired FA oxidation

A) [1-^{14}C]Palmitate oxidation to CO_2 and acid soluble metabolites (ASM) in heart and liver homogenates and B) heart [1-^{14}C]palmitoyl-CoA oxidation into CO_2 from control (C) and *Acsl1*$^{T-/-}$ (T$^{-/-}$) mice, n=5-6. C) Representative immunoblots against ACSL1, VDAC, and calnexin in control and *Acsl1*$^{T-/-}$ mitochondrial fractions 2 and 10 weeks after tamoxifen. D) [1-^{14}C]Palmitate oxidation to CO_2 and ASM from control (C) and *Acsl1*$^{T-/-}$ (T$^{-/-}$) ventricular mitochondria, n=5-6. E) Free, F) acetyl-, G) medium-chain, and H) long-chain acyl-carnitines in control and *Acsl1*$^{T-/-}$ hearts, n=5-7. Data represent mean ± SEM; *, P≤0.05 versus control.

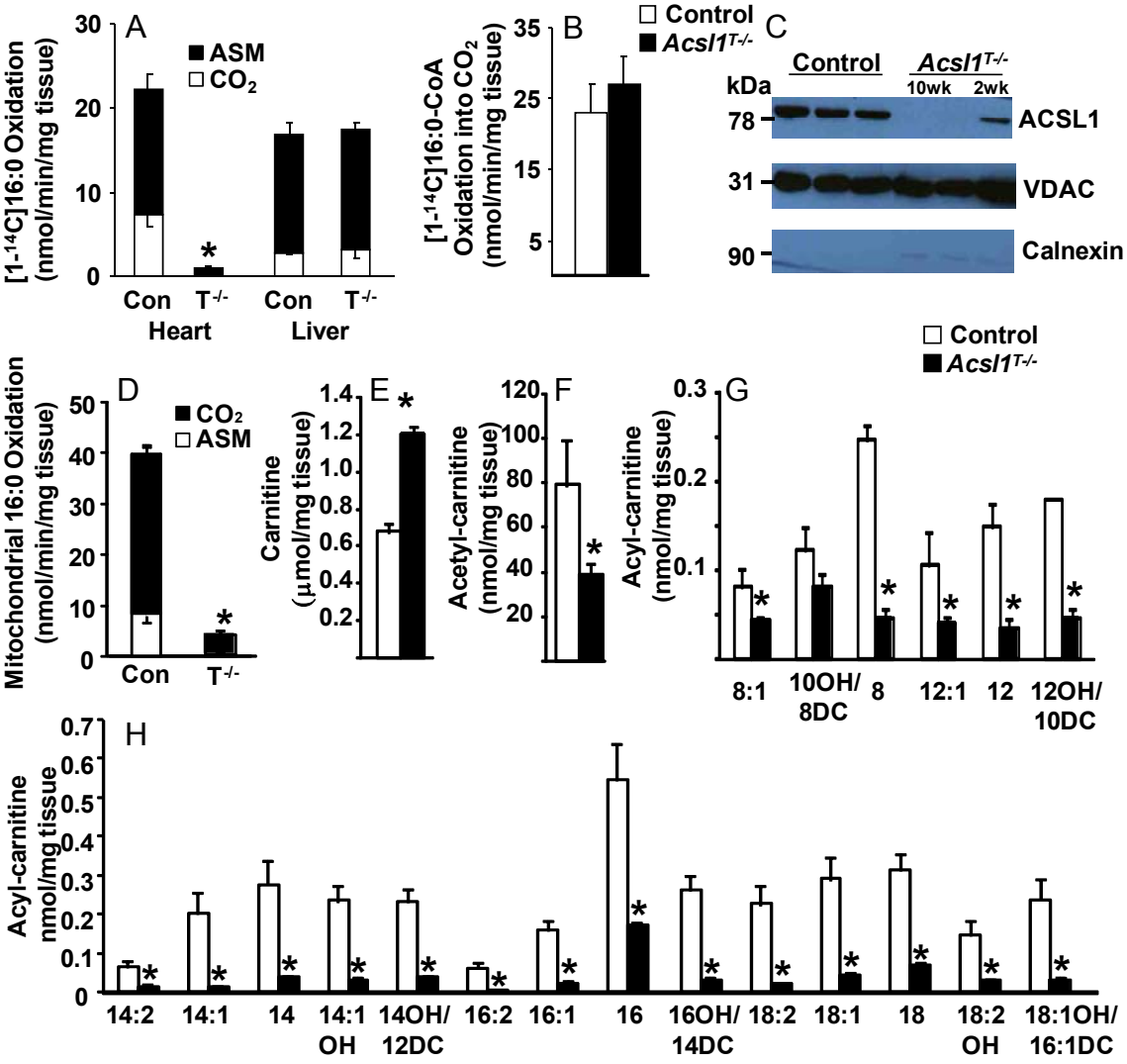

Figure 3 (4.3). *Acsl1*$^{T-/-}$ mice develop cardiac hypertrophy

A) Wet weight of control and *Acsl1*$^{T-/-}$ female and male hearts expressed as a percent of body weight, n=10-20. B) Quantification of cardiomyocyte area from lectin-stained control and *Acsl1*$^{T-/-}$ male hearts, n=3. C) Representative H&E stained control and *Acsl1*$^{T-/-}$ hearts. D) Echocardiography calculation of left ventricular (LV) mass over body mass from male control and *Acsl1*$^{T-/-}$ mice, n=8-10. E) Representative echocardiogram M-mode images and F) percent fractional shortening (%FS) in control and *Acsl1*$^{T-/-}$ male mice, n=8-10. G) mRNA abundance of fetal gene markers, α-skeletal actin (*αSkAc*) and brain natriuretic peptide (*Bnp*) in control and *Acsl1*$^{T-/-}$ hearts, n=6. Data represent mean ± SEM; *, P≤0.05 versus control.

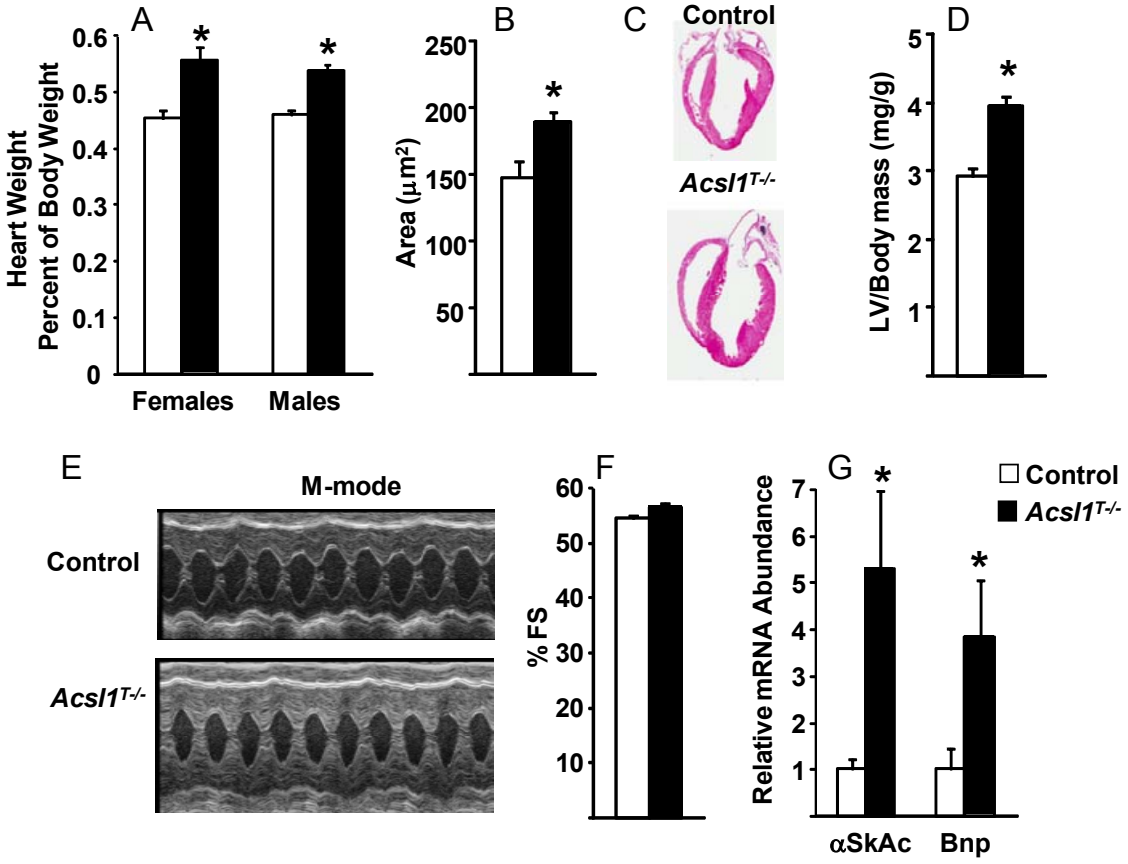

Figure 4 (4.4). Mitochondrial excess in *Acsl1*$^{T-/-}$ hearts

A) Representative electron microscopy images (8000X, scale bar = 2μm) and B) quantification of mitochondrial area from control and *Acsl1*$^{T-/-}$ male 10 wk ventricles, n=3. C) Quantification of the mitochondrial DNA genes, cytochrome C oxidase 1 (Co1), cytochrome B (Cytb), and NADH dehydrogenase subunit 1 (Nd1) relative to nuclear DNA in male and female control and *Acsl1*$^{T-/-}$ 10 wk ventricles, n=6. D) mRNA abundance of Pgc1α and Errα in control and *Acsl1*$^{T-/-}$ ventricles 2 wk after tamoxifen, n=6. E) Quantification of AMPK phosphorylation at Thr^{172} over total AMPK in control and *Acsl1*$^{T-/-}$ 10 wk ventricles, n=5-7. Data represent mean ± SEM; *, P≤0.05 versus control.

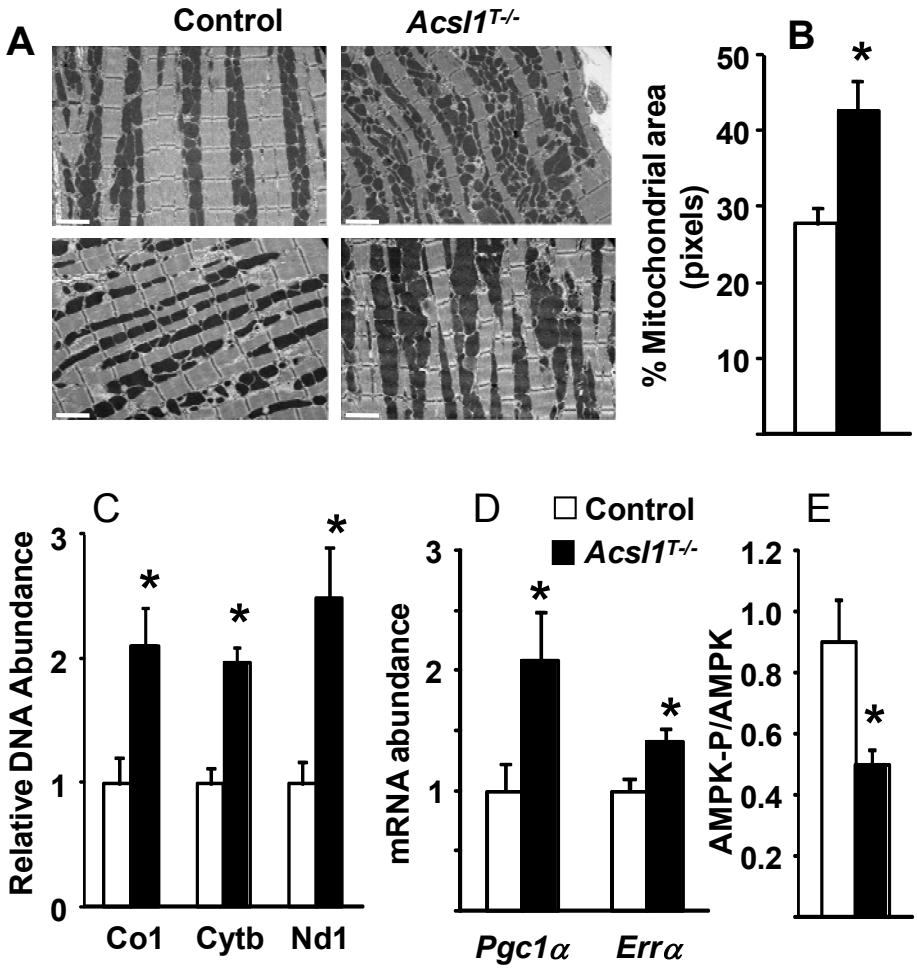

Figure 5 (4.5). Glucose oxidation, amino acid catabolism, and S6 kinase activation are increased in *Acsl1*$^{T-/-}$ hearts

A) [U-^{14}C]Glucose oxidation to CO_2 in heart homogenates from control and *Acsl1*$^{T-/-}$ mice, n=5-6. B) [1-^{14}C]Pyruvate to CO_2 in heart mitochondria from control and *Acsl1*$^{T-/-}$ mice, n=3-4. C) Short-chain acyl-carnitines in control and *Acsl1*$^{T-/-}$ hearts, n=5-7. D) Total amino acids and E,F) individual amino acids in control and *Acsl1*$^{T-/-}$ hearts, n=5-7. G) Representative immunoblots and quantification of p70S6K phosphorylation at Thr^{389} per total p70S6K in control and *Acsl1*$^{T-/-}$ ventricles, n=8-10. H,I) mRNA abundance of Cte1, mCpt1, Mcad, Cd36, Fas, Atps, and Pparα in control and *Acsl1*$^{T-/-}$ ventricles, n=6. Data represent mean ± SEM; *, P≤0.05 versus control.

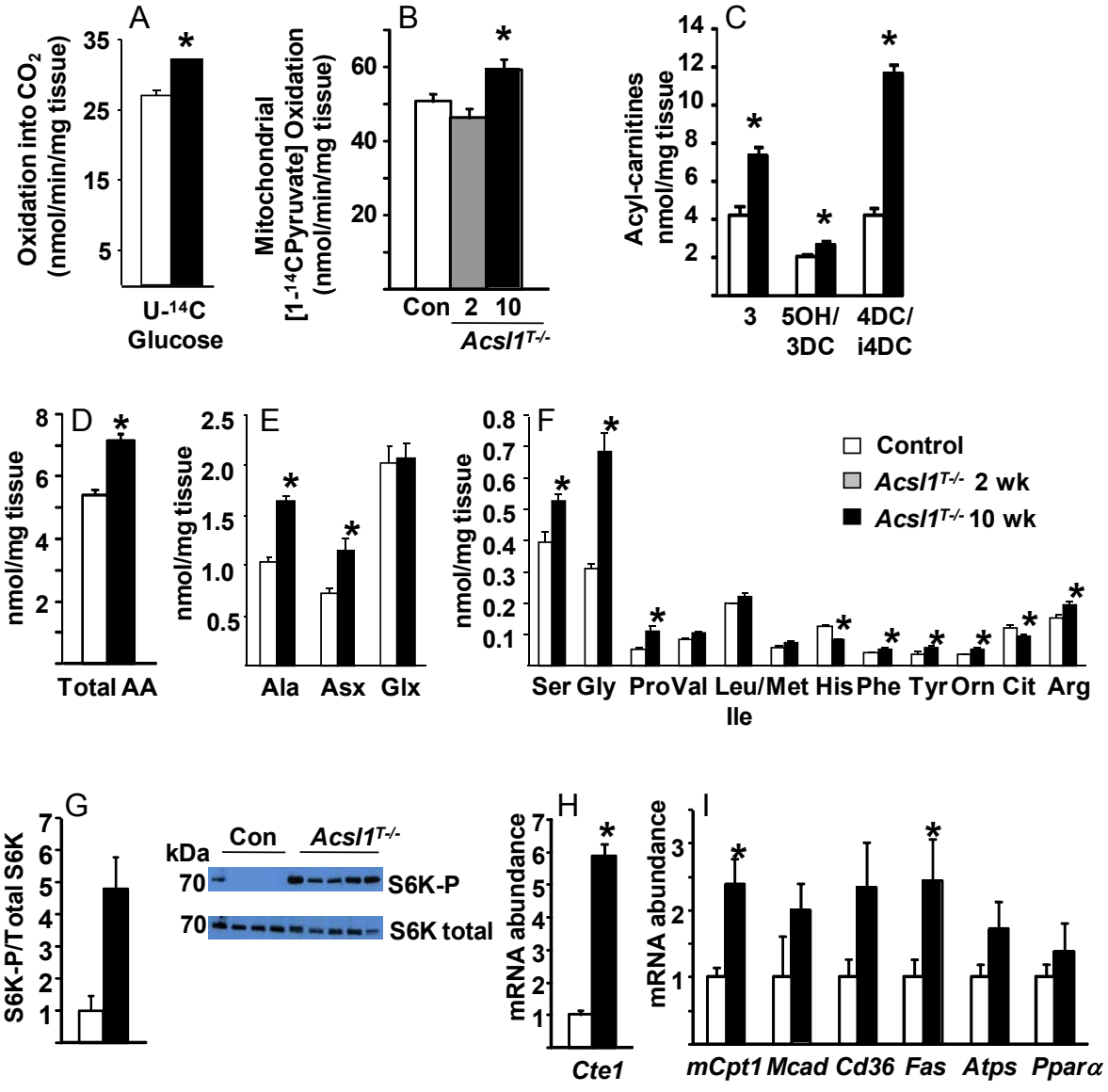

Figure 6 (4.6). Overview of metabolic disturbance and pathway activation in the *Acsl1*$^{T-/-}$ heart.

The loss of ACSL1 prevents uptake and activation of FA for FA oxidation, but not for TAG and PL synthesis. The inability of *Acsl1*$^{T-/-}$ heart to oxidized FA is compensated for by increased glucose and amino acid catabolism. The shift in oxidative metabolism results in the activation of the mTOR pathway that causes mitochondrial biogenesis and hypertrophy in *Acsl1*$^{T-/-}$ heart.

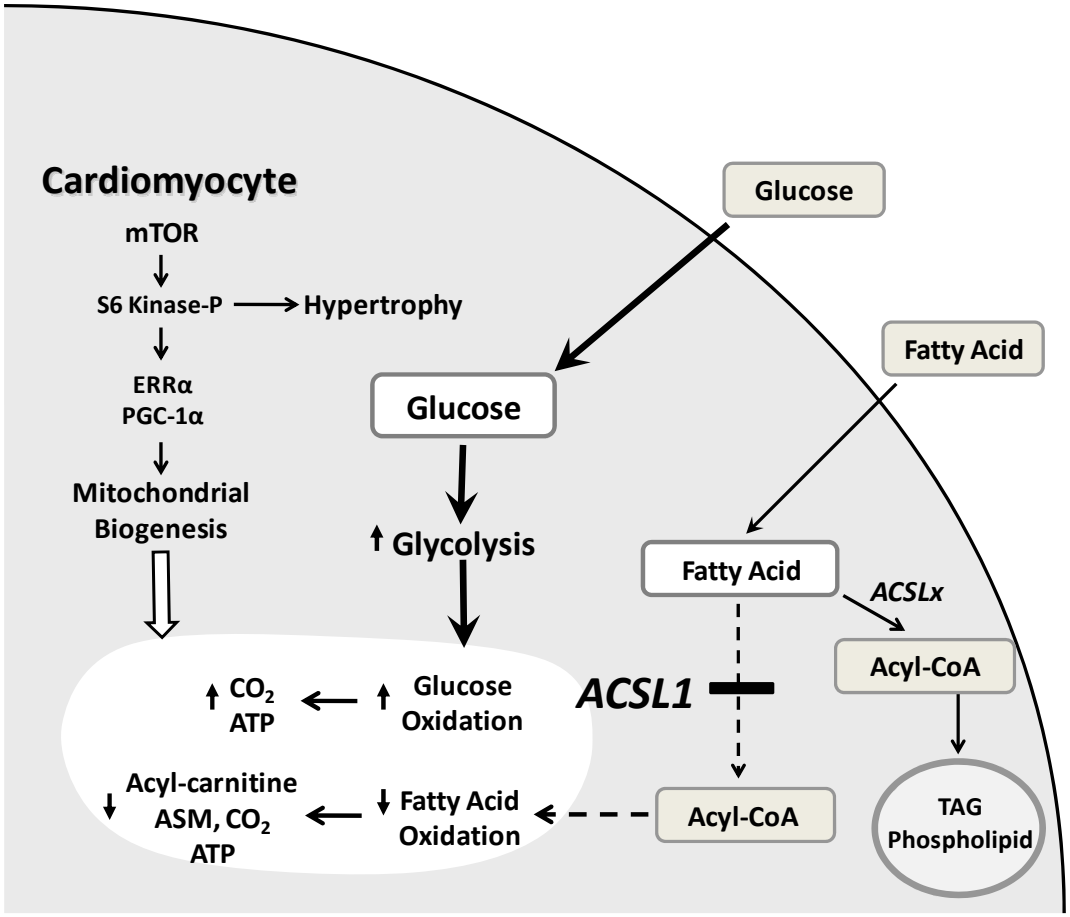

Table I. Echocardiogram diameter and functional characteristics

Transthoracic echocardiogram imaging was performed on conscious control and *Acsl1*$^{T-/-}$ male mice 10 weeks after tamoxifen. M-mode images were analyzed, n=6-8. Data represent mean ± SEM *, P≤0.05 versus control. IVS, interventricular septum; LVID, left ventricular inner diameter; LVPW, left ventricular posterior wall; %EF, percent ejection fraction; LV, left ventricular; d, diastole; s, systole.

	Control	***Acsl1*$^{T-/-}$**
IVS,d	0.98 ± .02	1.29 ± .02*
LVID,d	2.88 ± .06	2.47* ± .06*
LVPW,d	0.86 ± .01	1.23* ± .02
IVS,s	1.67 ± .03	1.89* ± .04
LVID,s	1.31 ± .04	1.08* ± .03
LVPW,s	1.48 ± .03	1.80* ± .04
% EF	86.6 ± .50	88.3 ± .51
LV Mass (mg)	86.5 ± 3.57	115.4* ± 4.24

Table 2. Body weight, adipose weight, plasma metabolites, and blood pressure in male mice

Male control and *Acsl1*$^{T-/-}$ mice 2 and 10 weeks after tamoxifen body and adipose weight, plasma metabolites, and area under the curve in response to insulin tolerance tests, n=15-8. Data represent mean ± SEM; *, P≤0.05 versus control; †, P≤0.05 2 week versus 10 week within genotype. G-WAT, gonadal white adipose tissue; TAG, plasma triacylglycerol; FA, plasma fatty acids; ITT, insulin tolerance test; AUC, area under the curve.

	2 weeks		10 weeks	
	Control	*Acsl1*$^{T-/-}$	Control	*Acsl1*$^{T-/-}$
Body Weight	25.5 ± 1.5	23.3 ± 1.7	31.4† ± 0.8	30.1† ± 0.4
G-WAT (% of BW)	0.87 ± 0.1	0.92 ± 0.1	1.7† ± 0.2	1.8† ± 0.2
TAG (mg/dL)	47.2 ± 3	29.7 ± 2.0*	36.7† ± 5	33.8 ± 2
FA (mmol/L)	0.08 ± .03	0.28 ± .04*	0.08 ± .01	0.09† ± .01
Glucose (mg/dL)	136 ± 8	131 ± 9	164 ± 3.6	136* ± 5.3
Insulin (ng/mL	-	-	2.73 ± 0.8	1.67 ± .2
ITT (AUC)	-	-	4981 ± 298	4828 ± 357
Systolic (mm Hg)	-	-	155 ± 4.0	158 ± 3.4
Diastolic (mm Hg)	-	-	120 ± 4.3	125 ± 3.6

Supplementary Figure 1 (4.7). ACSL activity and ACSL1 protein loss in *Acsl1*$^{T-/-}$ liver, kidney, and adipose tissue and *Acsl1*$^{T-/-}$ heart acyl-CoA composition and loss of FA oxidation over time.

A) Total ACSL activity in control and *Acsl1*$^{T-/-}$ 2 and 10 wk after tamoxifen and B) representative immunoblot against ACSL1 protein in liver, kidney, gonadal adipose (WAT), and brown adipose (BAT), 10 wk after tamoxifen, n=5-7. C) Heart long-chain acyl-CoA content as a relative percentage in control and *Acsl1*$^{T-/-}$ mice 10 weeks after tamoxifen, n=7-8. D) [1-^{14}C]Palmitate oxidation to CO_2 and ASM from control (C) and *Acsl1*$^{T-/-}$ ($T^{-/-}$) ventricular mitochondria 2 and 10 wk after tamoxifen, n=5-6. Data represent mean ± SEM; *, P≤0.05 versus control.

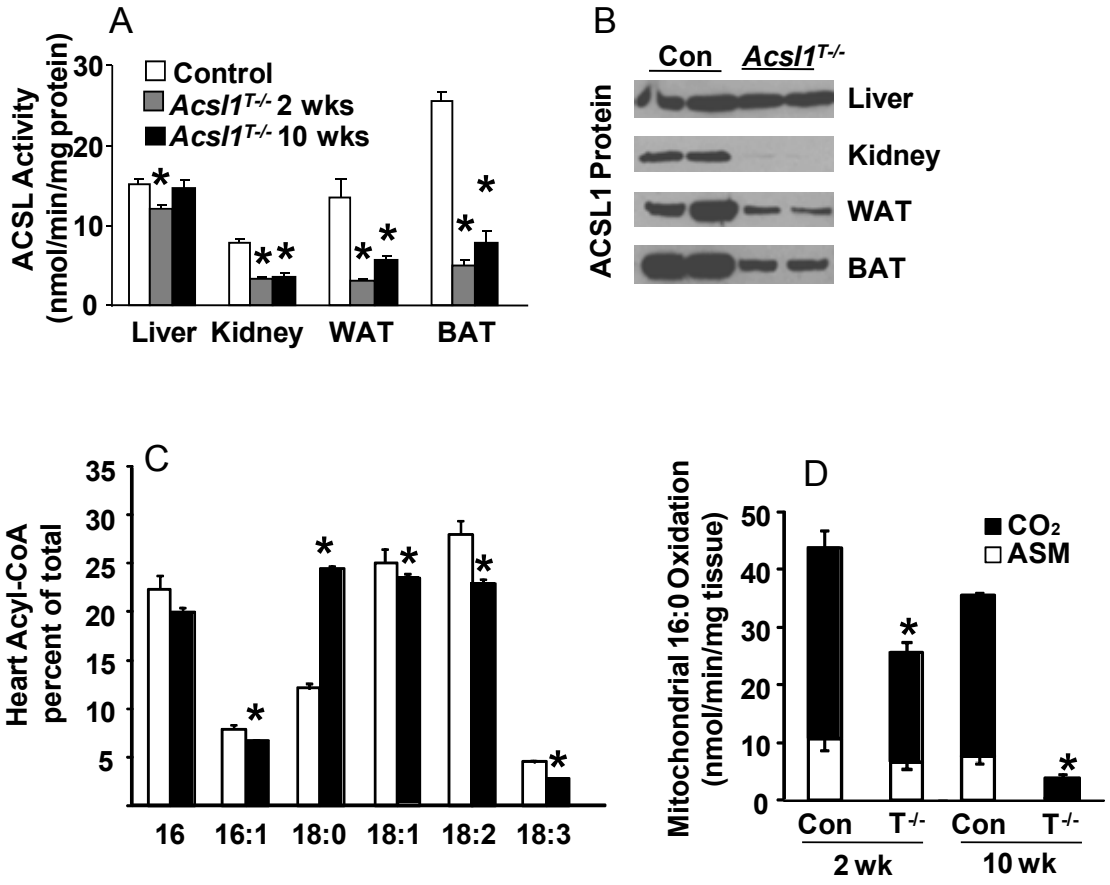

Supplementary Figure 2 (4.8). Heart lipid content, fibrosis, and PPARα transcriptional activity are normal in *Acsl1*$^{T-/-}$mice.

A,B,C) Lipid content of control and *Acsl1*$^{T-/-}$ male heart 10 wk after tamoxifen, n=8. D)Myocardial ATP and AMP content determined by HPLC in control and *Acsl1*$^{T-/-}$ hearts. E) PPARα transcription factor activity in nuclear extracts from control and *Acsl1*$^{T-/-}$ heart, n=6-8. Data represent mean ± SEM; *, P≤0.05 versus control. TAG, triacylglycerol; CL, cardiolipin; CE cholesterol ester; DAG, diacylglycerol; PC, phosphatidylcholine; PE, phosphatidylethanolamine.

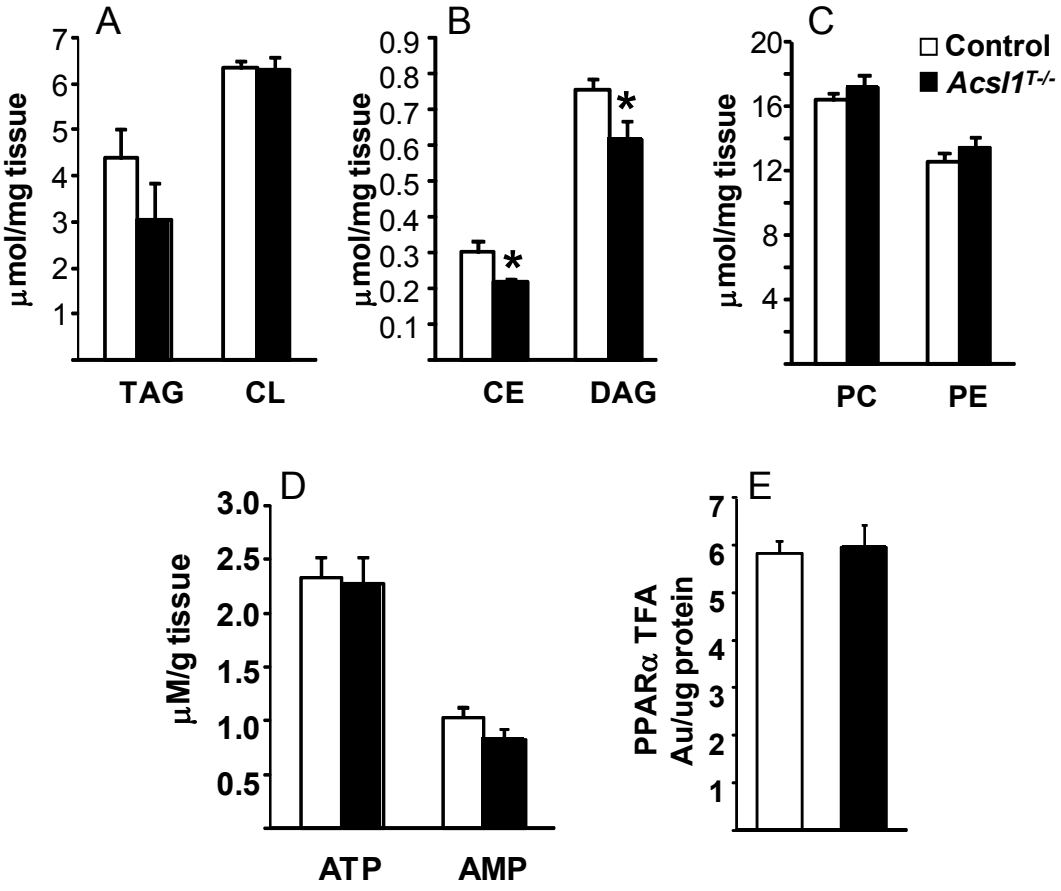

Supplementary Figure 3 (4.9). Lipid composition of heart from *Acsl1*$^{T-/-}$ mice

Heart long-chain FA species content as percent of total FA and in total nmol in the TAG (A,B), CL (C,D), PC (E,F), PE (G,H), and PS (I,J) fractions from control and *Acsl1*$^{T-/-}$ hearts, n=8Data represent mean ± SEM; *, P≤0.05 versus control. TAG, triacylglycerol; CL, cardiolipin; PC, phosphatidylcholine; PE, phosphatidylethanolamine; PS, phosphatidylserine.

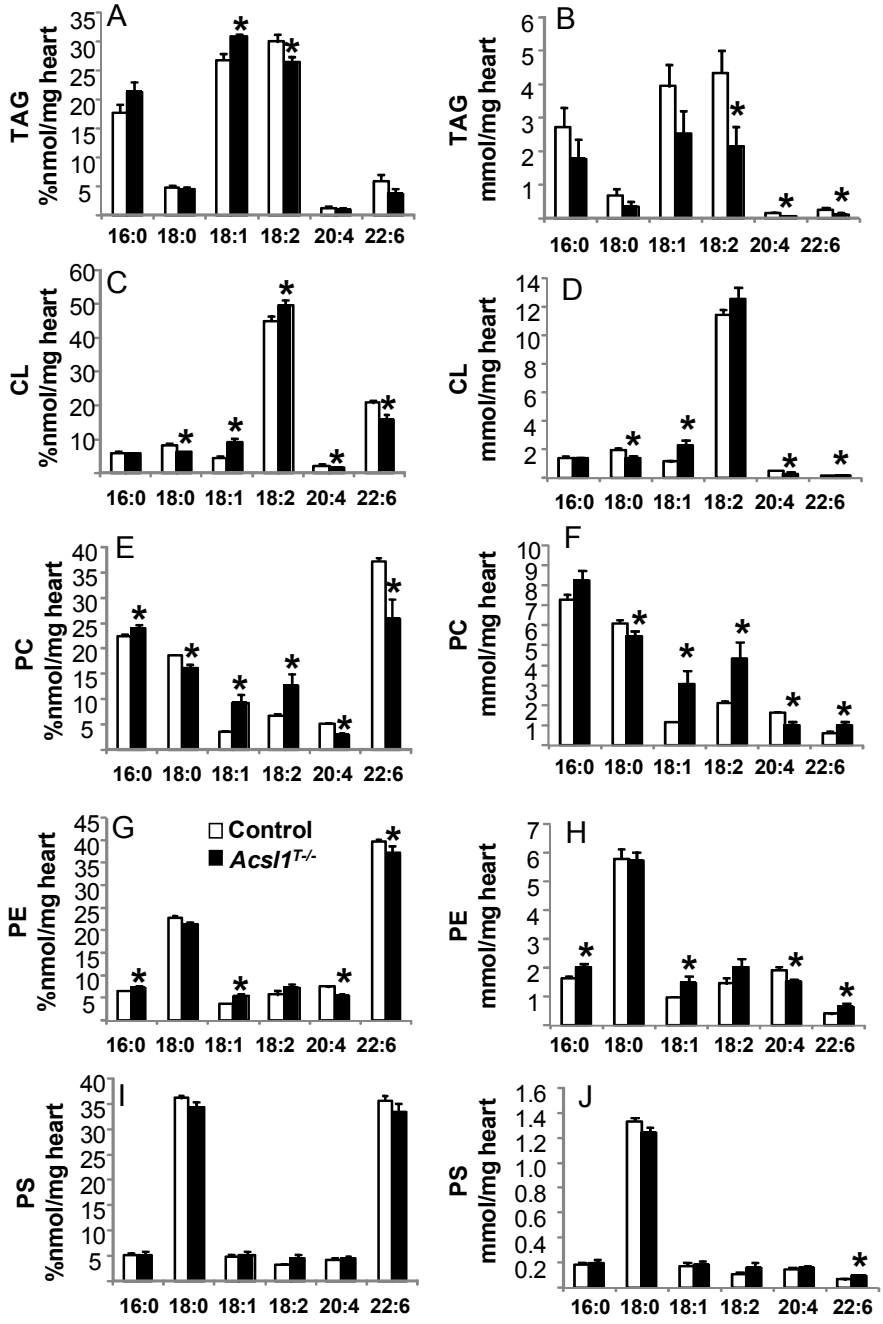

CHAPTER V

THE LACK OF ACSL1 SPECIFICALLY IN CARDIOMYOCYTES

The previous manuscript described the cardiac phenotype of a "total" body ACSL1 knock out in which the lack of ACSL1 in peripheral tissues and in non-cardiomyocyte cells within the heart may have influenced circulating metabolites and the ensuing cardiac phenotype. To confirm that lack of ACSL1 specifically in cardiomyocytes results in impaired cardiac FA oxidization and leads to hypertrophy, we generated a tamoxifen-inducible ventricular cardiomyocyte-specific ACSL1 knockout mouse, *Acsl1*$^{H-/-}$. The cardiac hypertrophy and severe defect in FA oxidation persisted in the *Acsl1*$^{H-/-}$ mouse, suggesting that ACSL1, specifically in cardiomyocytes, is required for FA oxidation and that without ACSL1, hypertrophy ensues. Thus, the goal of Aim3D has been completed. However, to further explore the role of ACSL1 in cardiomyocytes, we will characterize the response of *Acsl1*$^{H-/-}$ mice to various challenges, including high-fat diet-induced cardiac TAG-accumulation and insulin resistance, recovery from ischemic injury, oxidation of FA and glucose in isolated working heart, gene expression by microarray, and the rates of FA and glucose uptake. While the proposed Aim has been completed, the chapter that follows is a manuscript in preparation because the physiological experiments proposed above are ongoing.

Lack of ACSL1-mediated FA oxidation impairs recovery from ischemia and prevents high-fat diet induced cardiac steatosis

Authors:

Jessica M. Ellis[1], Trisha Grevengoed[1], Timothy R. Koves[2], Steven M. Watkins [3], Deborah M. Muoio, Gary W. Cline[4], Gerald I. Shulman[4], Monte S. Willis[5], and Rosalind A. Coleman[1]

[1]Department of Nutrition, University of North Carolina at Chapel Hill, 27599

[2]Department of Medicine, Duke University, Durham NC, 27703

[3]Lipomics Technologies, Inc., 2545 Boatman Ave, West Sacramento, CA 95691

[4]Departments of Internal Medicine and Cellular & Molecular Physiology; and [3]Howard Hughes Medical Institute, Yale University School of Medicine, New Haven, CT 06520

[5]Department of Pathology, University of North Carolina at Chapel Hill, 27599

Corresponding author: Rosalind A. Coleman,

135 Dauer Drive, Department of Nutrition, CB# 7461, University of North Carolina at Chapel Hill, Chapel Hill, NC 27599, USA.

Tel: 919-966-7213

Fax: 919-843-8555

email: rcoleman@unc.edu

Abstract:

Long chain acyl-CoA synthetases (ACSL) catalyze the conversion of long chain fatty acids into their acyl-CoA derivatives. Although ACSL1 is the most abundant of the five ACSL isoenzymes in the heart, its role in cardiac FA metabolism remains unclear. In mice with a heart-specific loss of ACSL1 under temporal control (*Acsl1*$^{H-/-}$), heart total long-chain acyl-CoA synthetase activity was reduced more than 90%, compared to littermate controls. ACSL1 deficiency reduced the content of acyl-CoA by 30% and palmitate and oleate oxidation was ~90% lower than in control hearts. *Acsl1*$^{H-/-}$ hearts developed hypertrophy, evidenced by increased heart weight and left ventricular wall diameter. The lack of ACSL1 increased cell death 24 hours after cardiac ischemia. *Acsl1*$^{H-/-}$ mice, compared to controls, were resistant to high-fat diet induced weight gain and the accumulation of cardiac TAG. These data suggest that cardiac ACSL1 catalyzes the initial step for FA retention and activation specifically for FA oxidation and that without ACSL1, diminished FA oxidative capacity leads to cardiac hypertrophy, increased cell death after ischemia and resistance to high-fat diet induced TAG accumulation.

Introduction:

The current epidemic of obesity is characterized by imbalances in lipid storage and lipid oxidation for energy that can lead to diseases such as diabetes and cardiovascular disease. In the heart, long-chain fatty acids (FA) of 14-20 carbons are the major substrates for energy production [168, 169]. The complete oxidation of fatty acids and glucose via mitochondrial oxidative phosphorylation accounts for greater than 90% of heart ATP production [257]. When cardiac FA oxidative metabolism is impaired genetically, pathological cardiac hypertrophy develops [173]. Pathological hypertrophy is defined by increased cardiomyocyte size accompanied by alterations in cell function and cell metabolism. Hypertrophy may initially be a positive adaptation to a disease state, but with time, may result in a decline in cardiac function. In the Framingham heart study, left ventricular hypertrophy (LVH) was identified in ~18% of the total population and in ~42% of the population over the age of 70 [170, 171]. LVH is independently associated with increasing age, blood pressure, obesity, valve disease, and myocardial infarction [171].

Ventricular hypertrophy occurs in obese individuals and in these patients it is associated with myocardial lipid accumulation [258]. Fatty heart is correlated with congestive heart failure and diabetes and is found in some mouse models of cardiac hypertrophy [207]. Cellular lipids accumulate in the form of triacylglycerol in intracellular lipid droplets. Triacylglycerol itself is not thought to be a lipotoxic molecule; however, the precursors for TAG synthesis have been shown to mediate cellular signaling pathways that can induce cell death [259]. Lipotoxicity is a term that refers to cell death due to the accumulation of lipids and lipid by-products and is a postulated mechanism for cardiac failure. Acyl-CoAs are the first molecule formed for the synthesis of TAG and the accumulation of lipids can lead to a rise in cellular acyl-CoAs. In models of increased cardiac lipid accumulation a rise in cellular lipid intermediates such as acyl-CoA, LPA, PA,

and DAG could be expected. These lipid intermediates could act as ligands or second messengers that mediate the cellular signaling involved in the development of cardiac cell death.

Injury sustained after an ischemic event postulated to be caused by the rapid reversion back to aerobic mitochondrial metabolism leading to increased oxidative stress and mitochondrial Ca^{+2} flux that leads to cell death by increasing the membrane permeability transition [260]. Inhibiting mitochondrial oxidation improves the acute recovery of isolated perfused hearts and cardiomyocytes [260]. However, long-term (24 hour) recovery after ischemia is improved by PPARα agonists and impaired in PPARα cardiac deficient mice [261, 262]. These data suggest that acute recovery from ischemia is improved by a slower transition to mitochondrial oxidative metabolism, but that the long-term recovery after ischemia-reperfusion is improved by mitochondrial oxidative metabolism.

ACSL isoenzymes convert FA to acyl-CoA in an ATP-dependent manner, simultaneously activating and trapping the FA within the cell. The conversion of FA to acyl-CoA is postulated to regulate the rate of cellular FA uptake by a process described as vectoral acylation [35, 73, 229, 263]. Activation to acyl-CoA is also required before FA can be oxidized to provide ATP or esterified for energy storage as TAG or for the synthesis of membrane phospholipids. The activation of FA is catalyzed by one of a family of 5 long-chain acyl-CoA synthetases (ACSL), ACSL1, ACSL3, ACSL4, ACSL5, and ACSL6, which differ in substrate preference, enzyme kinetics, subcellular location, and tissue-specific expression [24]. Because, theoretically, amphipathic acyl-CoAs can move freely within a membrane monolayer or be transported to distant membranes, all acyl-CoAs should be metabolically equivalent, no matter which ACSL isoenzyme catalyzes their formation and no matter which subcellular organelle forms the site of their synthesis. Yet, both loss-of-function and gain-of-function studies suggest that each of ACSL isoenzyme may have a distinct

function in directing acyl-CoAs to one or more specific downstream pathways and in regulating rates of FA uptake [34, 36].

FA are the major substrate for energy production preferred by the adult heart. The low total ACSL activity of embryonic (E16.5) heart increases 14-fold in the week after birth and is 90-fold higher in the adult heart together with increases in *Acsl1* mRNA [5]. The increase in ACSL activity and *Acsl1* mRNA expression parallels the heart's increased workload, rate of ATP generation, oxidative preference for FA, and expression of FA oxidative genes. We previously reported that ACSL1 is critical for FA oxidative metabolism in the heart of a multi-tissue ACSL1 knockout mouse, the *Acsl1*$^{T-/-}$ mouse [264]. Here we report severe decreases in FA oxidation in the tamoxifen-inducible ventricular cardiomyocyte-specific Acsl1 knockout mouse, *Acsl1*$^{H-/-}$. The lack of ACSL1 specifically in ventricular cardiomyocytes impairs FA oxidation and recovery from ischemia, and it protects from high-fat diet-induced TAG accumulation.

Results:

Generation of *Acsl1*$^{H-/-}$ mice

Mice with *Loxp* sequences inserted on either side of exon 2 in the *Acsl1* gene[9] were backcrossed to the C57Bl/J6 strain six times and then interbred with mice in which Cre expression is driven by α-myosin heavy chain promoter is induced by tamoxifen (B6.Cg-Tg(Myh6-cre/Esr1)1Jmk/J, Jackson Labs) to generate tamoxifen-inducible heart-specific *Acsl1* knockout mice (*Acsl1*$^{H-/-}$). Tamoxifen was injected i.p. (3.5 mg/kg body wt) for 4 consecutive days when mice were 6-8 weeks old. Control littermates, which were also injected with tamoxifen, lacked the C*re* gene (*Acsl1*$^{flox/flox}$). Data were collected 2 and 10 weeks after tamoxifen was injected.

The α-MHC promoter is expressed in ventricular but not atrial cardiomyocytes. Consequently, *Acsl1*$^{H-/-}$ heart atrial ACSL activity was similar to controls whereas *Acsl1*$^{H-/-}$ heart ventricle ACSL activity was 90% lower (**Fig 1A**). Real-time PCR showed nearly absent expression of *Acsl1* mRNA in *Acsl1*$^{H-/-}$ ventricles, and 50% lower in Acsl5 mRNA expression (**Fig 1B**). ACSL1 protein was absent in *Acsl1*$^{H-/-}$ ventricles, but was similar to controls in liver and skeletal muscle (**Fig 1C**). In *Acsl1*$^{H-/-}$ hearts, loss of ACSL1 reduced the total long-chain acyl-CoA pool by 30%, with 30-43% reductions in 16:0-, 16:1-, 18:1-, 18:2-, and 18:3-CoA species and no change in 18:0-CoA (**Fig. 1D,E**). Expressed as a percentage of total acyl-CoA content, only 18:3 was significantly reduced and was 12% less than controls, thus, the total acyl-CoA pool was reduce but the FA composition of the acyl-CoA pool is not changed by the lack of ACSL1. These data suggest that ACSL1 is the major activator of long-chain FA in the heart but that other ACS enzymes provide up to 70% of the long-chain acyl-CoA pool.

ACSL1 is required for heart FA oxidation

To determine whether ACSL1 provided acyl-CoAs for FA oxidation, the rates of [1-^{14}C]palmitate incorporation into CO_2 and ASM, which are measures of complete and incomplete oxidation, respectively, were measured in heart homogenates from *Acsl1*$^{H-/-}$ and control mice. Compared to controls at 10 weeks after tamoxifen, the rate of FA oxidation in *Acsl1*$^{H-/-}$ heart homogenates was 92% lower (**Fig. 2A**). Thus, the lack of ACSL1 nearly abolished FA oxidation. [1-^{14}C]Pyruvate incorporation into CO_2 in *Acsl1*$^{H-/-}$ heart homogenates was similar to controls, showing that mitochondrial oxidation was normal for this non-FA substrate (**Fig 2B**). These data show that FA oxidation was severely impaired in hearts that lacked ACSL1.

Cardiac hypertrophy of *Acsl1*$^{H-/-}$ hearts

As a percent of body weight, the wet weights of *Acsl1*$^{H-/-}$ male and female hearts were 25% and 20% greater, respectively, than controls (**Fig 3A**). The left ventricular (LV) masses calculated from echocardiograph M-mode images were 34% heavier (**Fig 3B**). M-mode imaging showed the diameters of the *Acsl1*$^{H-/-}$ LV posterior wall (LVPW,d) and the interventricular septum (IVS,d) in diastole were 32% wider than controls, the LV inner diameter (LVID) was 13% smaller in *Acsl1*$^{H-/-}$ hearts, and the LV volume was 32% lower (**Table 1**). The percent fractional shortening and the ejection fraction of the *Acsl1*$^{H-/-}$ hearts were similar to measurements in controls, indicating that cardiac function remained normal despite ventricular hypertrophy (**Table 1**). Histological analysis of *Acsl1*$^{H-/-}$ hearts showed minimal fibrosis (data not shown). I the *Acsl1*$^{H-/-}$ hearts, the higher mRNA expression of the fetal gene markers, α-skeletal actin and brain natriuretic peptide, suggests that the hypertrophy was pathological (**Fig 3D**). The mitochondrial area, appearance, and mitochondrial DNA abundance were similar between genotypes (**Fig 3E,F,G**). Thus, lack of

ACSL1 impaired FA oxidation and induced ventricular hypertrophy without cardiac dysfunction or failure.

Acsl1$^{H-/-}$ mice are resistant to high-fat diet induce obesity

Female *Acsl1*$^{H-/-}$ mice were fed a 60%-high fat diet for 10 weeks to determine if whether ACSL1 is required for high-fat diet-induced accumulation of cardiac TAG and insulin resistance. *Acsl1*$^{H-/-}$ mice fed the high-fat diet *ad libitum*, gained 3 g less than controls (25.7 g versus 22.7 g) (**Fig. 4A**). *Acsl1*$^{H-/-}$ mice fed the high-fat diet, compared to littermate controls, accumulated less adipose mass. Gonadal and inguinal adipose depots were 36% and 20% less, respectively (**Fig. 4B,C**). Food intake, whole-body energy expenditure, and ambulatory movement across three planes were similar between genotypes (**Fig. S1A-D**). Despite the reduced accumulation of adipose mass in the high-fat diet fed *Acsl1*$^{H-/-}$ mice, after 8 weeks on the high-fat diet, compared to littermates on the control diet, the area under the curve for a glucose tolerance test was ~77% greater in both genotypes (**Fig. 4D**). Plasma TAG and FA were not different between genotypes on either diet; however, high-fat diet feeding raised plasma cholesterol ~18% in both genotypes (**Table 1**). *Acsl1*$^{H-/-}$ blood glucose was ~19% lower than controls fed either diet (**Table 1**). Control cardiac TAG increased 24% with high-fat diet feeding, whereas no change in cardiac TAG was observed in the *Acsl1*$^{H-/-}$ mice (**Fig 4E**). Despite the lack of TAG accumulation in *Acsl1*$^{H-/-}$ hearts, the heart weight was 25% greater than controls fed either diet. *Acsl1*$^{H-/-}$ heart weight was 28% and 41% greater when normalized to body weight on the low-fat and high-fat diets, respectively (**Fig 4F**).

Increased ischemia-induced cell death in the *Acsl1*$^{H-/-}$ hearts

To test the role of ACSL1 in recovery from ischemia-reperfusion injury, control and *Acsl1*$^{H-/-}$ left anterior descending arteries were occluded for 30 minutes followed by reperfusion. Cell death was assessed by triphenyltetrazolium chloride staining in hearts 24-hours later. Both the control and *Acsl1*$^{H-/-}$ mice had similar areas at risk (AAR) from the ischemia event, however, in control hearts, 30% of the AAR was infarct (dead) whereas in *Acsl1*$^{H-/-}$ hearts, 45% was infarct (**Fig. 5A**). The 150% greater area infarct in *Acsl1*$^{H-/-}$ heart suggests that ACSL1 is critical for full recovery from ischemia. These data suggest that ACSL1 and the ability of the heart to oxidize FA are beneficial for the long-term recovery of cardiac tissue after an ischemia-reperfusion study.

Discussion

The primary finding of this study is that ACSL1 is required for FA oxidation by cardiomyocytes. The knockout of ACSL1 reduced the cardiac content of long-chain acyl-CoA by 30%. If the metabolic fate of a cellular acyl-CoA were non-specific, one would expect to find diminished availability of acyl-CoAs for both the oxidation and the synthesis of complex lipids. However, the normal content of glycerolipids, and the 80-90% reduction in palmitate oxidation support the conclusion that ACSL1 channels FA specifically towards oxidation, and that acyl-CoAs synthesized by other ACSL isoenzymes were available and sufficient for complex lipid synthesis, but not for oxidation.

The effects of a multi-tissue tamoxifen inducible ACSL1 knockout mouse, *Acsl1*$^{T-/-}$, on heart function and metabolism have been investigated. The *Acsl1*$^{T-/-}$ hearts have severely impaired FA oxidation, mitochondrial biogenesis, and develop left ventricular (LV) hypertrophy. However, the lack of ACSL1 in peripheral tissues and in non-cardiomyocyte cells within the heart may have influenced circulating metabolites and the ensuing cardiac phenotype. To confirm that lack of ACSL1 specifically in ventricular cardiomyocytes caused defects in FA oxidation and cardiac hypertrophy similar to that observed in the *Acsl1*$^{T-/-}$ hearts, we generated a tamoxifen-inducible ventricular cardiomyocyte-specific ACSL1 knockout mouse, *Acsl1*$^{H-/-}$. Total ACSL activity in the *Acsl1*$^{T-/-}$ heart was reduced 97% and reduced 90% in the *Acsl1*$^{H-/-}$ suggesting that at least 90% of total ventricular ACSL activity is catalyzed by ACSL1 specifically in cardiomyocytes. The rate of [1-^{14}C]palmitate oxidation was reduced ~90% in both *Acsl1*$^{T-/-}$ and *Acsl1*$^{H-/-}$ heart homogenates, confirming that ACSL1 specifically and uniquely directs FA towards oxidation in cardiac tissue. Although, both the *Acsl1*$^{H-/-}$ and *Acsl1*$^{T-/-}$ hearts had 90% or greater loss in total ACSL activity, the long-chain acyl-CoA content was reduced 65% in *Acsl1*$^{T-/-}$ but only 30% in *Acsl1*$^{H-/-}$, suggesting that

ACSL1 expressed in non-cardiomyocytes and in *Acsl1*$^{H-/-}$ atria contribute to ~30% of cardiac acyl-CoA content.

Both *Acsl1*$^{T-/-}$ and *Acsl1*$^{H-/-}$ mice have enlarged hearts, compared to controls, with LV that are 20-35% heavier, have 10-40% increased LV wall diameter, and are dilated due to ~30% smaller LV inner diameter. The ejection fraction and fractional shortening are similar to controls, thus neither *Acsl1*$^{T-/-}$ nor *Acsl1*$^{H-/-}$ mice show systolic dysfunction. The *Acsl1*$^{T-/-}$ hearts upregulated of several fetal genes, including α-skeletal actin, *Acsl3*, and brain natrietic peptide, suggesting that the cardiac hypertrophy was pathological; however, the *Acsl1*$^{H-/-}$ hearts upregulated α-skeletal actin only casting doubt on the pathological nature of hypertrophy in *Acsl1*$^{H-/-}$ heart. Cardiac gene expression for several PPARα/δ regulated genes also deviated between the models. Specifically, carnitine-palmitoyl transferase 1 and medium-chain acyl-CoA dehydrogenase were upregulated in *Acsl1*$^{T-/-}$ hearts, whereas medium-chain acyl-CoA dehydrogenase and *Ppar*α were downregulated in *Acsl1*$^{H-/-}$ hearts. These data suggest that the upregulation of PPAR regulated genes in *Acsl1*$^{T-/-}$ hearts is not due to the lack of ACSL1 in cardiomyocytes, but that the peripheral effect of multi-tissue ACSL1 knockout influences cardiac PPAR regulation. Conversely, the PPARα target, cytosolic thioesterase 1 (*Cte1*) is ~6-fold upregulation in both *Acsl1*$^{T-/-}$ and *Acsl1*$^{H-/-}$ hearts. *Cte1* is also upregulated in brown adipose tissue of the adipose-specific knockout, *Acsl1*$^{A-/-}$, and in the liver of the liver-specific ACSL1 knockout, *Acsl1*$^{L-/-}$, thus the lack of ACSL1 in multiple cell types leads to the upregulation of *Cte1*. It remains unclear why CTE1 would be upregulated in the absence of ACSL1 particularly because CTE1 catalyzed the reverse reaction (acyl-CoA → FA) of ACSL1. Microarray analysis was performed on *Acsl1*$^{H-/-}$ and control hearts 2 and 10 weeks after tamoxifen to gain better insight into the temporal alterations in gene expression that occur when ACSL1 is lost specifically in cardiomyocytes.

Another discrepancy between the *Acsl1*$^{T-/-}$ and *Acsl1*$^{H-/-}$ hearts is the mitochondrial excess found in the *Acsl1*$^{T-/-}$ but not in *Acsl1*$^{H-/-}$ heart. The mitochondrial area measured from TEM images in *Acsl1*$^{T-/-}$ hearts, compared to controls, showed a 54% increase in mitochondria, and the ratio of mitochondria-specific DNA to nuclear DNA was 2-fold greater. In *Acsl1*$^{H-/-}$ hearts, mitochondrial area was 35% greater than controls, although this was not statistically significant at p=0.055, and the ratio of mitochondrial DNA to nuclear DNA was similar between *Acsl1*$^{H-/-}$ and controls. These data suggest that factors other than the lack of ACSL1 in cardiomyocytes drove mitochondrial biogenesis in *Acsl1*$^{T-/-}$ hearts. In summary, the data show that ACSL1 activates FA specifically for oxidation in cardiomyocytes and the shift away from FA oxidation leads to cardiac hypertrophy.

Methods:

Animal Treatment: *Acsl1*$^{H-/-}$ and littermate *Acsl1*$^{flox/flox}$ control mice were housed in a pathogen-free barrier facility (12 h light/dark cycle) in accordance with the UNC IACUC, with free access to water and food (Prolab RMH 3000 SP76 chow). When the mice were 6-8 weeks old, tamoxifen (3 mg /40 g body wt), dissolved in corn oil (20 mg/ml), was injected i.p. for 4 consecutive days. For the high-fat diet study, mice were given a control low-fat diet, D12450B, or a 60%-high-fat diet, D12492 (Research Diets Inc.) *ad libitum* beginning three days after the final tamoxifen injection. Tissues were removed and snap frozen in liquid N_2. Protein content was determined by the BCA assay (Pierce) with bovine serum albumin as the standard. Plasma was collected from mice in 5% 0.5 M EDTA. Plasma TAG, β-hydroxybutyrate (Stanbio), cholesterol, fatty acid, glucose (Wako), and free and total glycerol (Sigma) were measured with colorimetric assays. Insulin tolerance tests were performed by i.p. injection with insulin (5 U/kg body wt) and tail blood glucose was measured at baseline, 15, 30, 60, and 120 min using a One Touch Ultra glucometer (Lifescan, Inc). Rates of O_2 consumption were determined in Oxymax chambers (Columbus Instruments) after mice were acclimated overnight. Data were averaged from two day and two night cycles per mouse.

ACSL assay: ACSL initial rates were measured with 50 μM [1-^{14}C]palmitic acid, 10 mM ATP, and 0.25 mM CoA in total membrane fractions (0.5-4.0 μg) or in ventricular mitochondria [147][24].

RT-PCR: Total RNA was isolated from ventricles (Qiagen RNeasy Fibrous Tissues Kit), and cDNA was synthesized (Applied Biosystems High Capacity cDNA RT Kit), or total DNA was isolated (QIAmp DNA Micro Kit, Quiagen), and the reaction was performed using SYBR Green (Applied Biosystems) detection with primers specific to the gene of interest with equal

amounts of cDNA (10 ηg/reaction), and detected using a Taq-man thermocycler (BioRad). Results were normalized to the housekeeping gene *Gapdh* and expressed as arbitrary units of $2^{-\Delta CT}$.

Immunoblots: Protein isolated in lysis buffer (20 mM Tris base, 1% Triton-X-100, 50 mM NaCl, 250 mM sucrose, 50 mM NaF, 5 mM $Na_2P_2O_7$, plus protease inhibitor (#11836153 Roche)) or total membrane fractions isolated in Medium I (10 mM Tris, pH7.4, 1 mM EDTA, 0.25 M sucrose, 1 mM dithiothreitol) were equally loaded (40-60 µg) and electrophoresed on 10% SDS polyacrylamide gels, then transferred to PVDF membrane, blocked with 5% milk-TBST-1% or 5% BSA-TBST-1% for 1 h, incubated with anti-ACSL1 primary antibody (Cell Signaling Technologies, ACSL1 Antibody #4047) overnight at 4°C, washed, and incubated with secondary antibody for 1 h at room temperature (Cell Signaling Technologies, goat anti-rabbit). Protein was visualized with the Western Blot R-Probe Kit (Pierce).

Histology: Hearts were gravity perfused and fixed for 24 h in 4% paraformaldehyde-PBS, then transferred to 70% ethanol. Tissue was then embedded in paraffin, serial sectioned, and stained with hematoxylin and eosin or Masson's trichrome. For electron micrograph analysis, animals were euthanized and the hearts perfused with a freshly made solution containing 2% paraformaldehyde and 2.5% glutaraldehyde in 0.15 M sodium phosphate buffer, pH 7.4. Cardiac tissue was imaged using a LEO EM910 transmission electron microscope at 80kV (LEO Electron Microscopy, Thornwood, NY) and photographed using a Gatan Bioscan Digital Camera (Gatan, Inc., Pleasanton, CA). Quantification was performed using Image J Software.

Echocardiograms: Mouse echocardiograms were performed on unanaesthetized mice with the Visual Sonics Vevo 770 ultrasound biomicroscopy system. M-mode images of the left ventricle were analyzed using Visual Sonics software.

Left Anterior Descending Coronary Artery (LAD) Ligation. Mice were anesthetized with isoflorane. An endotracheal tube was inserted and connected to a Harvard rodent volume-cycled ventilator. The chest cavity was opened by a 0.5 cm incision of the left third intercostal space. Ligation was performed with a suture passed with a tapered needle underneath the LAD artery about 1mm lower than the tip of the left auricle. The artery was compressed by tightening the ligature, producing myocardial blanching and electrocardiographic (ECG) S-T segment elevation. After occlusion for 30 minutes, blood flow was restored by removing the ligature. Mice were anesthetized and killed 24 hours after ligation. Evans blue was perfused through non-ischemic heart, removed, and cut into sections. The sections were stained with triphenyltetrazolium chloride and fixed in 4% paraformaldehyde. Sections were photographed and the area at risk and area ischemic were calculated using image J software, NIH.

Fatty acid oxidation: Freshly isolated ventricles were minced, then homogenized with 10 up-and-down strokes, using a motor-driven Teflon pestle and glass mortar in ice-cold buffer (100 mM KCl, 40 mM Tris·HCl, 10 mM Tris base, 5 mM $MgCl_2 \cdot 6H_2O$, 1 mM EDTA, and 1 mM ATP (pH = 7.4)) at a 20-fold dilution (wt/vol) [265]. Oxidation was measured in a 200 µl reaction mixture containing 100 mM sucrose, 10 mM Tris·HCl, 10 mM KPO_4, 100 mM KCl, 1 mM $MgCl_2 \cdot 6H_2O$, 1 mM L-carnitine, 0.1 mM malate, 2 mM ATP, 0.05 mM coenzyme A, and 1 mM dithiothreitol (pH = 7.4) with either 8 µM [1-^{14}C]palmitate and 100 µM sodium palmitate complexed to BSA or with 16 µM [1-^{14}C]pyruvate and 200 µM pyruvate. Oxidation studies measured the production of ^{14}C-CO_2 and acid soluble metabolites (ASM) for 30 min in a two-well oxidation system. One well contained the reaction mixture and tissue homogenate and the adjoining well contained 1N NaOH. The reaction was terminated by adding 70% perchloric acid to the assay well, and cells were incubated for one h to drive the CO_2 into the $NaOH$. Radioactivity of ASM in centrifuged fractions and CO_2 was determined by liquid

scintillation counting using 4 ml of Ecolite (Molecular Products). Fatty acid oxidation was quantified using the following formula: ([(dpm-BL)/SA] ÷ [g of tissue wet wt/well x min of reaction incubation]) x 60 min/h, where BL is the dpm of blank wells and SA is the FA specific radioactivity [265].

Tissue Lipid: Acyl-carnitines were quantified by liquid chromatography and tandem mass spectrometry [252]. Acyl-CoA and DAG composition and content were assessed from whole heart homogenized with appropriate internal standards in specific organic reagents [254]. After separation, purification, and elution, lipid metabolite extracts were separated by high performance liquid chromatography, and individual and total lipid species were analyzed by liquid chromatography/tandem mass spectrometry.

Figures:

Figure 1 (5.1). Generation of mice that temporally lack ACSL1 specifically in ventricles **A**) Total ACSL activity with [1-^{14}C]palmitate in control and *Acsl1*$^{H-/-}$ atria and ventricles 10 wk after tamoxifen, n=5-7. **B**) Representative immunoblot against ACSL1 protein in heart, liver, and gastrocnemius (gastroc) muscle 10 weeks after tamoxifen. **C**) Acsl isoenzyme mRNA abundance in heart 10 wk after tamoxifen in control and *Acsl1*$^{H-/-}$ mice, n=6. Heart total (**D**) and long-chain acyl-CoA content (**E**) in control and *Acsl1*$^{H-/-}$ mice 10 weeks after tamoxifen, n=7-8. Data represent mean ± SEM; *, P≤0.05 versus control.

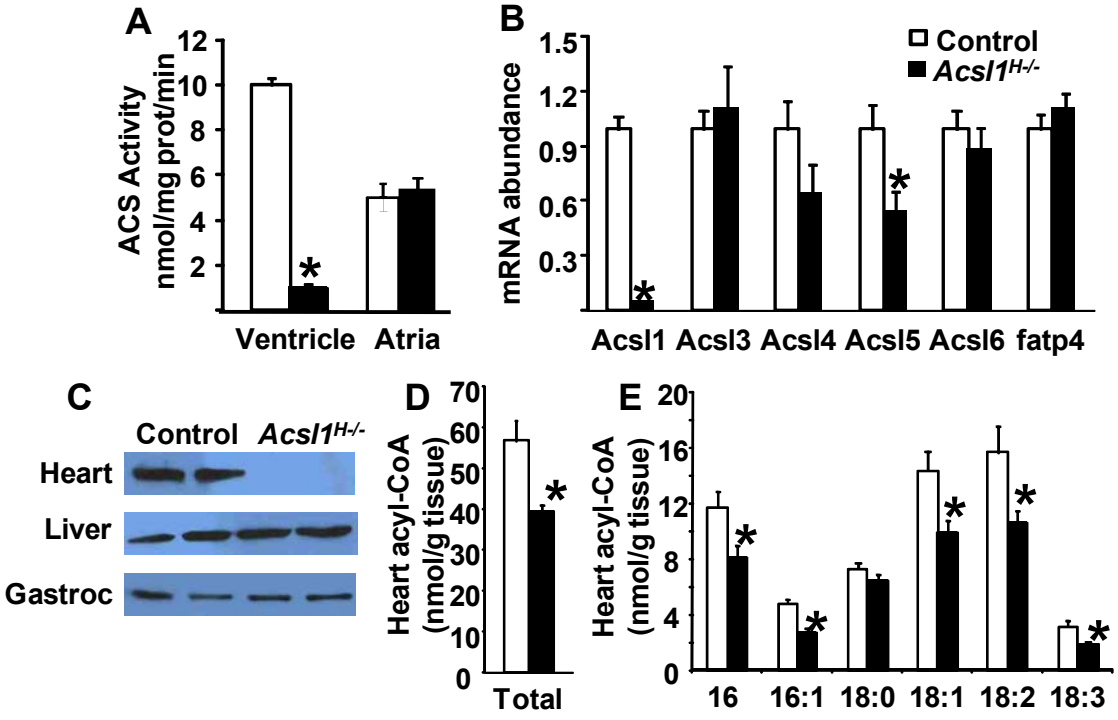

Figure 2.(5.2). *Acsl1*$^{H-/-}$ hearts have impaired FA oxidation
A) [1-^{14}C]Palmitate and **B**) [1-^{14}C]Oleate oxidation in CO_2 and acid soluble metabolites (ASM) in heart homogenates from control and *Acsl1*$^{H-/-}$ mice, n=5-6. **C**) [1-^{14}C]Pyruvate oxidation in CO_2 in heart homogenates from control and *Acsl1*$^{H-/-}$ mice, n=5-6. Data represent mean ± SEM; *, P≤0.05 versus control.

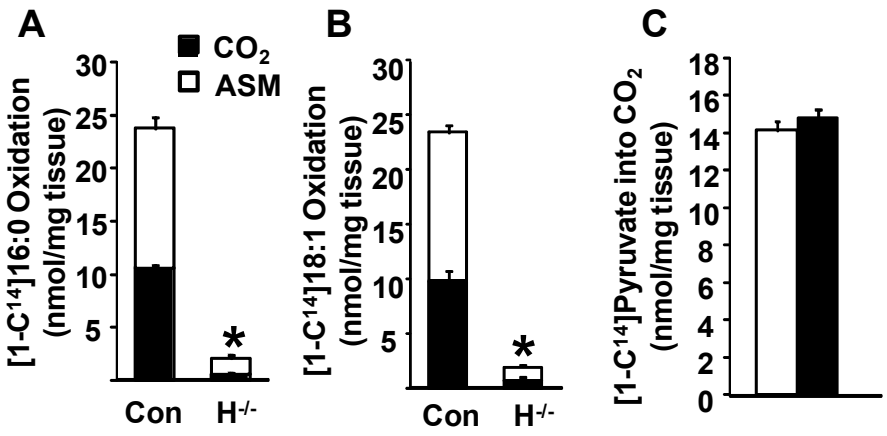

Figure 3 (5.3). *Acsl1*$^{H-/-}$ mice develop cardiac hypertrophy

A) Wet weight of control and *Acsl1*$^{H-/-}$ male and female hearts expressed as a percent of body weight, n=10-20. **B**) Echocardiography calculation of left ventricular (LV) mass in control and *Acsl1*$^{H-/-}$ male mice, n=8-10. **C**) Representative H&E stained control and *Acsl1*$^{H-/-}$ hearts. **D**) mRNA abundance of fetal gene markers, a-skeletal actin (*αSka*) and brain natriuretic peptide (*Bnp*) control and *Acsl1*$^{H-/-}$ hearts, n=6. **E**) Representative electron microscopy images and **F**) quantification of mitochondrial area from control and *Acsl1*$^{H-/-}$ ventricles, n=3. **G**) Quantification of the mitochondrial DNA genes, NADH dehydrogenase subunit 1 (Nd1), cytochrome B (cytb), and cytochrome C oxidase 1 (Co1) relative to nuclear DNA in control and *Acsl1*$^{H-/-}$ 10 week ventricles, n=6. Data represent mean ± SEM *, P≤0.05 versus control.

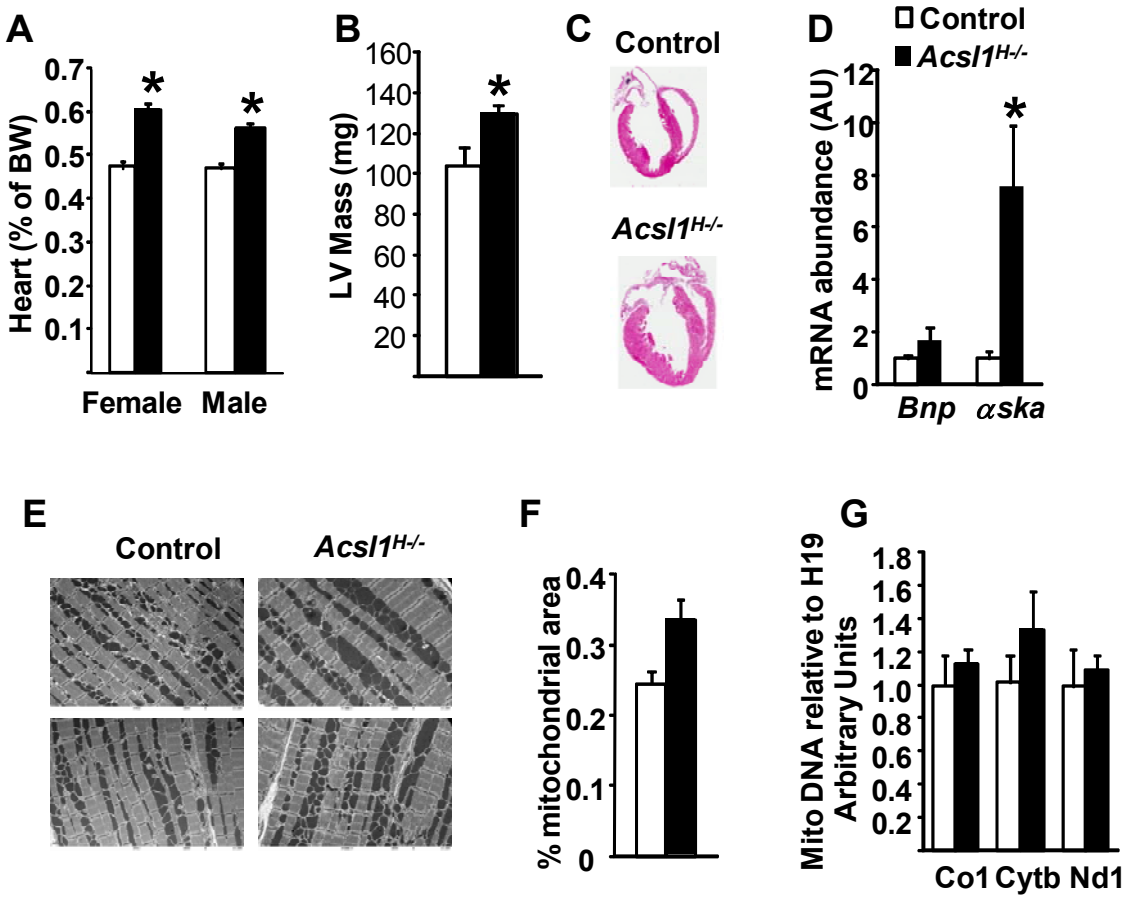

Figure 5 (5.4). *Acsl1*$^{H-/-}$ mice are resistant to high-fat diet induced obesity and cardiac TAG accumulation

A) Body weight over 10 weeks on low-fat diet or 60%-high-fat diet in control and *Acsl1*$^{H-/-}$ mice, n=10-15. **B**) Inguinal and **C**) gonadal adipose depot mass in control and *Acsl1*$^{H-/-}$ mice after 10 weeks on the diet, n=10-15. **D**) Blood glucose and **E**) area under the curve (AUC) during a glucose tolerance test in control and *Acsl1*$^{H-/-}$ mice after 8 weeks on the diet, n=10-15. **F**) Heart weight and **G**) heart TAG content in control and *Acsl1*$^{H-/-}$ mice after 10 weeks on the diet, n=8-15. Data represent mean ± SEM *, P≤0.05 versus control.

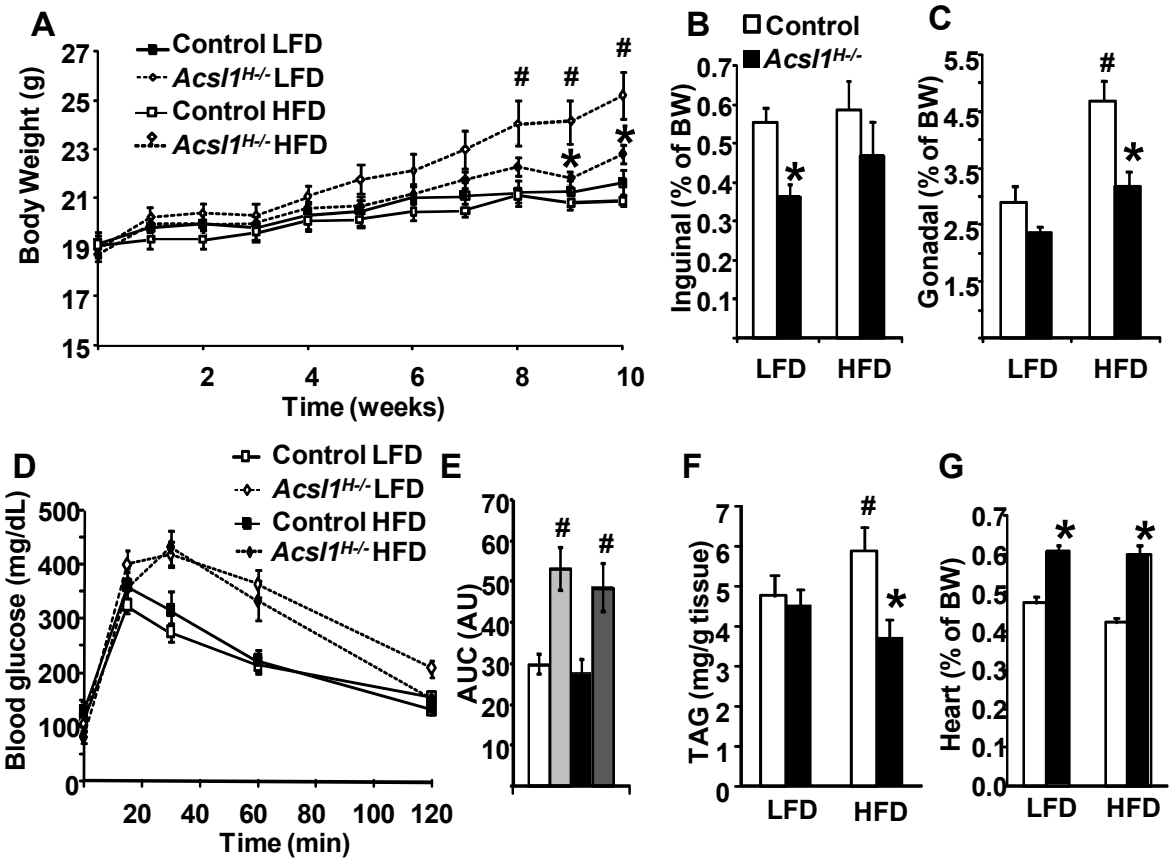

Figure 5 (5.5). Improved acute but impaired long-term recovery from ischemia in *Acsl1*$^{H-/-}$ heart

A) Quantification of area at risk (AAR) and area of infarct (AI) in control and *Acsl1*$^{H-/-}$ hearts 24 h after a 30 min of ischemia, n=6-8. **B**) Representative images of hearts stained with Evans blue and triphenyltetrazolium chloride 24 h after 30 min of ischemia. Data represent means ± SEM *, P≤0.05 versus control.

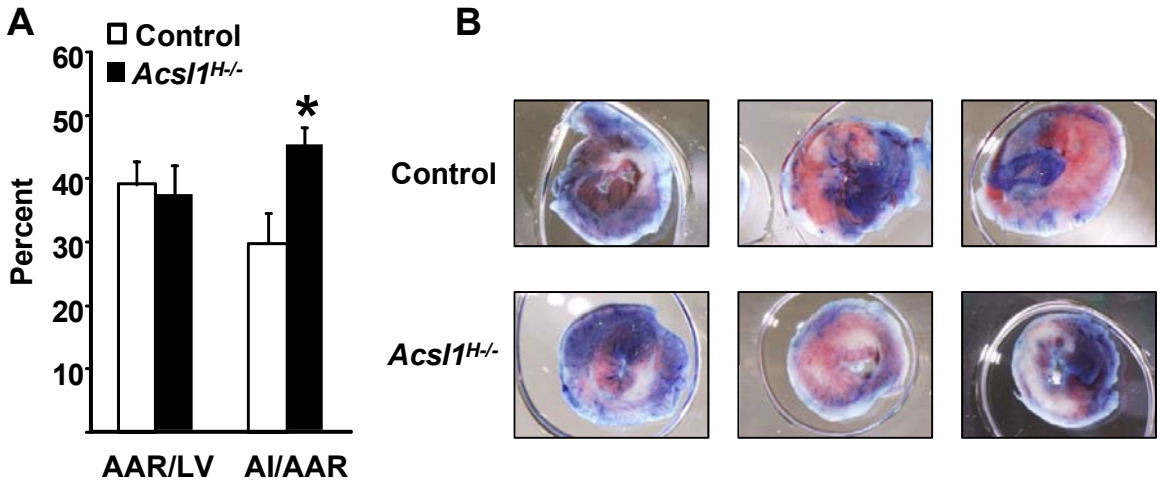

Table 1 (5.I). Echocardiogram diameter and functional characteristics in *Acsl1*$^{H-/-}$
Transthoracic echocardiogram imaging was performed on conscious control and *Acsl1*$^{H-/-}$ male mice 2 and 10 weeks after tamoxifen. M-mode images were analyzed, n=6-8. Data represent mean ± SEM *, P≤0.05 versus control.

	Control 2 wks	*Acsl1*$^{H-/-}$ 2 wks	Control 10 wks	*Acsl1*$^{H-/-}$ 10 wks
IVS,d	0.96 ± 0.02	1.02 ± 0.02	0.99 ± 0.02	1.3 ± 0.05*
LVID,d	3.0 ± 0.13	2.9 ± 0.04	3.13 ± 0.19	2.7 ± 0.11*
LVPW,d	0.97 ± 0.01	0.97 ± 0.01	0.93 ± 0.01	1.2 ± 0.04*
IVS,s	1.69 ± 0.06	1.64 ± 0.05	1.68 ± 0.05	1.9 ± 0.05*
LVID,s	1.34 ± 0.08	1.33 ± 0.03	1.43 ± 0.09	1.2 ± 0.03*
LVPW,s	1.53 ± 0.05	1.44 ± 0.05	1.53 ± 0.04	1.66 ± 0.03*
% EF	87 ± 0.9	86.1 ± 0.5	86 ± 0.7	86 ± 1.1
% FS	55 ± 1.0	54 ± 0.7	54 ± 0.9	54 ± 1.4
LV Mass, mg	96 ± 6.7	97 ± 3	104 ± 9	129 ± 4.7*

Table 2 (5.2). Plasma metabolites in control and *Acsl1*$^{H-/-}$ mice fed control and high-fat diet.

Female control and *Acsl1*$^{H-/-}$ plasma glucose, fatty acid (FA), cholesterol, glycerol, and triacylglycerol (TAG) 4 hour fasted values after 10 weeks on the diets, n=8-12. Data represent mean ± SEM *, P≤0.05 genotype effect within diet; #, P≤0.05 diet effect within genotype.

	Control LFD	***Acsl1*$^{H-/-}$ LFD**	**Control HFD**	***Acsl1*$^{H-/-}$ HFD**
Glucose (mg/dL)	160 ± 7	132 ± 5*	163 ± 10	129 ± 4*
FA (mEq/L)	0.23 ± .04	0.23 ± .04	0.28 ± .04	0.28 ± .05
Cholesterol (mg/dL)	81 ± 2	84 ± 5	96 ± 4#	100 ± 3#
Glycerol (mg/dL)	1.2 ± .2	1.3 ± .2	1.4 ± .2	1.1 ± .2
TAG (mg/dL)	39 ± 4	35 ± 5	31 ± 4	39 ± 5

Figure S1 (5.6). Normal RER, food intake and activity in *Acsl1*$^{H-/-}$ mice

Female control and *Acsl1*$^{H-/-}$ mice, on the high-fat or low-fat diet for 9 weeks, **A,B**) respiratory exchange ratio, **C**) activity and **D**) food intake across three planes were measured in the CLAMS system. Data represent mean ± SEM *, P≤0.05 genotype effect within diet; #, P≤0.05 diet effect within genotype.

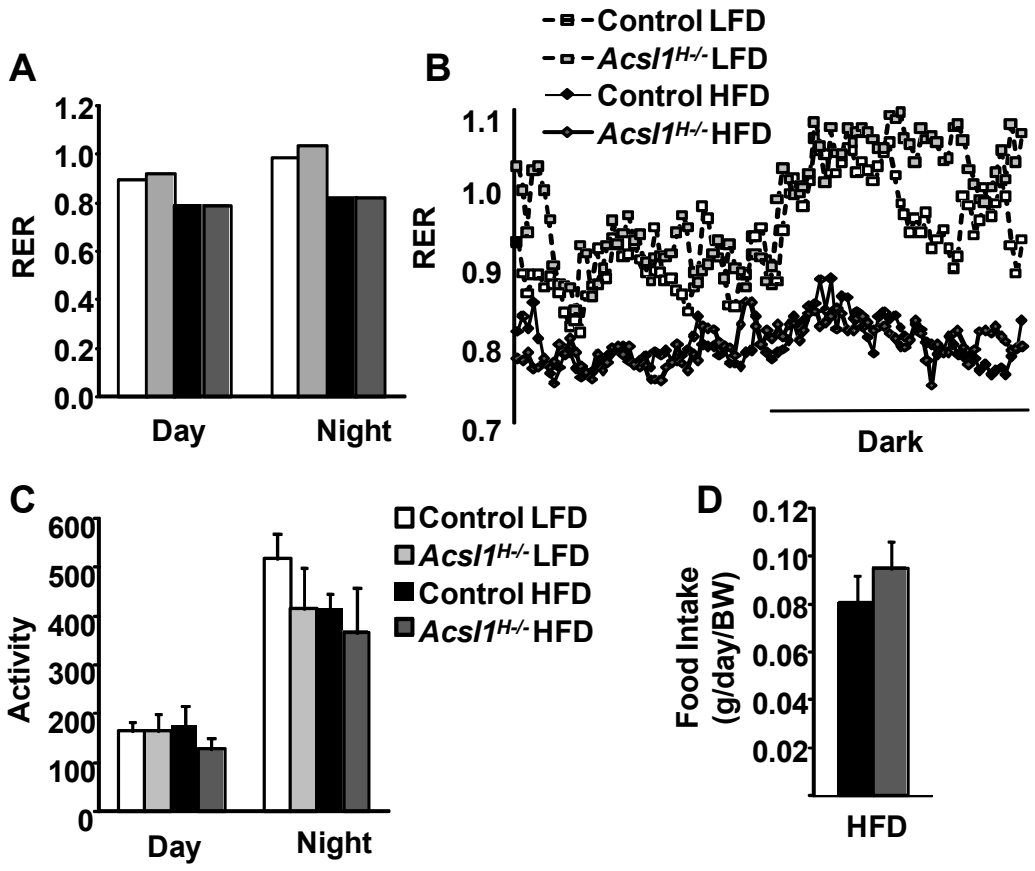

CHAPTER VI

SYNTHESIS

Overview of research findings

The major finding of this dissertation is that ACSL1 is the ACSL isoenzyme that channels FA towards oxidative metabolism in adipose tissue and heart. These findings are the result of investigating the metabolism and overt phenotypes in mouse models that lack ACSL1 in specific tissues. ACSL1 was previously thought to provide acyl-CoA for the synthesis of TAG in adipose tissue, and its role in cardiac metabolism remained unclear. This dissertation provides evidence for the new-found role that ACSL1 plays as the first enzyme for the FA oxidative pathway. These data also suggest that ACSL1 is critical for regulation of whole body adipose mass, thermogenesis, and cardiac metabolism and growth.

DIRECTIONS FOR FUTURE RESEARCH

How does FA channeling occur via acyl-CoA synthetases?

ACSL1 protein-protein interaction

This dissertation work has elucidated a function for ACSL1 in specifically channeling FA toward oxidation in several tissues. However, it remains unclear exactly how the ACSL1 enzyme could be shuttling its product towards a single metabolic pathway. The acyl-CoA produced by the ACS reaction has both hydrophobic and hydrophilic properties that should allow it to move freely within membranes and/or bind to proteins such as acyl-CoA binding proteins; thus all acyl-CoAs should theoretically be free to enter any downstream metabolic pathway. We predict that the different ACSL isoenzymes have interact with other proteins, thereby placing the acyl-CoA in direct contact with proteins that take it to specific metabolic pathways. For example, we hypothesize that in muscle tissues, ACSL1 is likely to interact with proteins such as M-CPT1 that would use the acyl-CoA as substrate to form an acyl-carnitine that would be transported into the mitochondria for the oxidative metabolism. The proteins that ACSL1 and other ACSLs interact with are likely to vary by tissue and cell type. Experiments are required to identify the specific protein-protein interactions of ACSL1 in different tissues and cell types and under different hormonal and physiological conditions.

Members of the Coleman Lab, specifically Dr. Jennifer Frahm and Dr. Lei Li, have recently generated data using mass spectrometry technologies that show ACSL1 interacting with several mitochondrial oxidative proteins. More studies are required to explore how the protein-protein interactions of ACSL1 facilitate channeling, control enzyme activity, and regulate metabolic flux. These studies would include identifying the protein-interacting

domains of ACSL1, mutating or truncating theses domains, and assessing enzyme activity and rates of FA oxidation in the mutants.

ACSL subcellular location

The subcellular location of the ACSL isoenzymes likely facilitates the proteins' role in cellular metabolism. For example an acyl-CoA formed at the mitochondria would preferentially be oxidized, whereas an acyl-CoA formed at the ER would be used for complex lipid synthesis. Although the ACSL1 protein is found in specific cell fractions in various tissue (see background), fractionation methods are often flawed because of the difficulty in obtaining highly pure fractions. Confocal microscopy of endogenous protein is a more reliable method to identify subcellular location, however, confocal microscopy for ACSL isoenzymes has not been conducted due to the poor quality and specificity of the endogenous ACSL isoenzymes-specific antibodies. Future studies should include the design and synthesis of highly-specific antibodies to all the endogenous ACSL isoenzymes, followed by confocal microscopy studies to identify the isoenzymes' subcellular locations in multiple tissues and cell lines. Confocal microscopy can also be used to study the movement of ACSL isoenzymes from one organelle to another.

What is the role of ACSL1 in the ER?

While isolating mitochondria from heart for the oxidation studies, I observed ACSL1 protein in both the mitochondrial and the microsomal fractions. Although my microsomal fractions were not devoid of mitochondrial proteins, it is likely that some ACSL1 protein resides in the non-mitochondrial organelles. Confocal microscopy, with a good endogenous ACSL1 antibody, is required to identify ACSL1 cellular localization. However, if ACSL1 is expressed at the ER, what is the role of ER ACSL1, and are the rates of TAG synthesis and/or omega oxidation reduced in *Acsl1*$^{T-/-}$ and *Acsl1*$^{H-/-}$ hearts?

The rate of labeled FA incorporation into cardiac TAG could be measured in several systems. First, HL-1 cardiomyocyte-like cells with ACSL1 knocked down could be used to study rates of TAG synthesis. However, HL-1 cells may not exactly mimic the metabolism of a contracting mouse heart, and these cells are difficult to transfect with siRNA (against Acsl1). Secondly, isolated primary cardiomyocytes from control and *Acsl1*$^{H-/-}$ mice could be used to study rates of TAG synthesis. However, primary cardiomyocyte isolation is technically difficult, and these cells can only be obtained from the glucose-oxidizing fetal heart. A third system would be to isolate whole working heart in the Langendorff perfusion apparatus to study rates of FA oxidation and TAG synthesis. Working heart is the preferred method, due to the intactness of the heart; however, our lab does not have the equipment necessary to perform these studies. We are collaborating with Dr. Mark Jeffrey at UT-Southwestern who will study the rates of fatty acid and glucose oxidation in whole working hearts in the Langendorff apparatus. These studies of oxidative, but not anabolic metabolism of ^{13}C-labeled glucose and FA are on-going in control and *Acsl1*$^{H-/-}$ isolated working hearts. Lastly, to measure rates of TAG synthesis in the heart we plan to intravenously inject labeled FA and collect heart to extract lipids and quantify the amount of labeled FA that was incorporated into lipids. The latter experiments will be performed with the assistance of Dr. Terry Combs and Trisha Grevengoed.

If ACSL1 does not affect rates of TAG synthesis, why is it present at the ER? As discussed previously, ACSL1 could facilitate the oxidation of FA through the ER omega-oxidation pathway. The product of omega oxidation is a dicarboxylic acid, a molecule identified by mass spectrometry as an indicator of the flux of FA through the omega oxidation pathway. If the amount of dicarboxylic FA were reduced similar to the reduction in acyl-carnitines, it would suggest that ACSL1 also regulates FA oxidation at the ER. ER-localized ACSL1 may also be a “reserve” site if, with stimuli, ACSL1 would move to the mitochondria to facilitate FA oxidative metabolism.

ACSL1 protein regulatory mechanisms

Until now, the regulation of ACSL isoenzymes has been inferred from mRNA expression. However, the activity and function of ACSL isoenzymes is likely to be regulated post-translationally, by acetylation, phosphorylation, protein-protein interactions, and intracellular location. The mechanisms that would activate or inhibit ACSL1 *in vivo* are unknown. Recent mass spectrometry data from the Coleman lab shows that ACSL1 is phosphorylated and acetylated at multiple sites. These phosphorylation and acetylation sites may regulate enzyme activity, perhaps in response to various hormonal or other signaling stimuli. Research is ongoing in the Coleman lab to determine how mutations that mimic or inhibit the phosphorylation and acetylation affect ACSL1 activity. The data generated will be critical for understanding the regulatory mechanisms on ACSL1 protein.

Why do brown adipocytes that lack ACSL1 release less glycerol?

While performing labeling and lipolytic experiments in control and *Acsl1*$^{A-/-}$ brown adipocyte cells, we observed approximately 50% less glycerol released under lipolytic conditions. The appropriate experiment to determine why glycerol released is blunted in the knock out cells would be to use labeled glycerol and trace its metabolism with and without lipolytic stimuli. We hypothesize that due to reduced rates of FA oxidation in the *Acsl1*$^{A-/-}$ cells, the glycerol may either be oxidized to compensate or be used to form complex lipids from FA taken up by the cell but not oxidized.

De novo synthesis in ACSL1 knockout tissues

TAG content in WAT and in cold-exposed BAT is greater in the *Acsl1*$^{A-/-}$ mice; however, I did not measure the rates of FA synthesis in these tissues. Overexpression of GLUT4 in mouse tissues activates CHREBP that upregulates *de novo* FA synthesis genes.

It is possible that glucose uptake and oxidation are increased in ACSL1 knock out tissues to compensate for impaired FA oxidative metabolism, and that the glucose intermediates that act as signals to activate CHREBP in GLUT4-overexpressing tissues are present in ACSL1 knock out tissues. We have not investigated mTOR activation in white adipose in the *Acsl1*$^{A-/-}$ mice. The increased flux of glucose oxidative metabolism in ACSL1 knockout tissue may activate mTOR, as it appears to do in the heart (see pg 97 and 112). Adipose activation of mTOR is linked to ChREBP activation and upregulation of *de novo* FA synthesis genes. If rates of FA synthesis are increased in the *Acsl1*$^{A-/-}$ adipose, this could be the cause of increased white adipose mass. Opposing this idea is the finding that the mRNA abundance of fatty acid synthetase is not increased in *Acsl1*$^{A-/-}$ gonadal adipose. To confirm that FA synthesis is not increased, the incorporation of radiolabeled acetate or glucose into lipid can be measured in control and ACSL1 knockout primary isolated adipocytes and primary pre-adipocytes, as well as in working heart, and/or cardiomyocytes that express or lack ACSL1.

Acsl1$^{A-/-}$ macrophage affects

Although the FABP4 promoter used to express Cre recombinase in the *Acsl1*$^{A-/-}$ mice is known to be expressed in macrophages, we have yet to measure the change in ACSL1 protein, activity, or mRNA in *Acsl1*$^{A-/-}$ macrophages. Dr. Karin Bornfeldt used our Acsl1 floxed mice to create a macrophage-specific *Acsl1* knockout (*Acsl1*^{MACKO}). Although her data have not yet been published, Dr. Bornfeldt and her colleagues found that compared to controls, *Acsl1*^{MACKO} bone-marrow derived macrophages have a reduced inflammatory response to M1 (LPS and IFN-γ) activation. However, no differences in circulating inflammatory molecules were observed in *Acsl1*^{MACKO} mice. The *Acsl1*^{MACKO} thioglycollate-elicited macrophages, compared to controls, had reduced rates of oleate incorporation into TAG and CE; however, *Acsl1*^{MACKO} macrophages had normal TAG and CE content. The only phenotype observed of *Acsl1*^{MACKO} macrophages *in vivo* was reduced atherosclerotic plaque

formation when *Acsl1*^{MACKO} bone marrow was transplanted into *Ldlr*$^{-/-}$ mice infected with the islet-killing and diabetic-inducing lymphocytic choriomeningitis virus (LCMV). Thus, type-1 diabetic LDLR$^{-/-}$ mice with *Acsl1*^{MACKO} macrophages were resistant to atherosclerosis. However, LDLR$^{-/-}$ mice expressing *Acsl1*^{MACKO} macrophages in the non-diabetic state did not have resistance to atherosclerotic plaque formation. These findings suggest that macrophages deficient in Acsl1 in the *Acsl1*$^{A-/-}$ mice do not modulate the observed phenotype of increased fat mass, cold intolerance, and impaired mitochondrial FA oxidation.

Acsl1$^{A-/-}$ rate of adipocyte differentiation

The *Acsl1*$^{A-/-}$ mice have increased fat mass, but we failed to show increased adipocyte cell size by histology. Thus, the question remains concerning how the rate of adipocyte differentiation is affected in *Acsl1*$^{A-/-}$ mice. My experience with primary pre-adipocyte cultures, suggests that animal-to-animal and isolation-to-isolation variation is too great to reliably measure differences in adipocyte differentiation. To study the rates of adipocyte differentiation, I would propose to isolate pre-adipocytes from mice with floxed *Acsl1* and expressing the ubiquitous tamoxifen-inducible *Cre Recombinase* , then expose the cells, from the same mouse, to media with vehicle or tamoxifen (to induce the knockout) and measure the rates of differentiation.

mTOR and ACSL1, what is the link and what does it mean?

Data presented in this dissertation suggests that the kinase, mTOR, is activated in Acsl1 knockout hearts. mTOR has been highlighted as a major signaling molecule in the pathogenesis of cardiac hypertrophy and mitochondrial excess. The question remains, is mTOR activation the mechanism through which hypertrophy and mitochondrial biogenesis occurs? In other words, would rapamycin treatment attenuate or reverse the hypertrophy and the high mitochondrial content observed in ACSL1 knockout mice?

How is mTOR stimulated in ACSL1-knockout heart?

Another question remains, what are the stimuli that activates mTOR in the ACSL1 knockout mice? Known stimulators of mTOR in heart include: insulin signaling, IGF signaling, glycolytic metabolites (particularly glucose-6-phosphate), inhibited AMPK activity, PKC, PLC, and the MAPK/ERK pathway (phenylephrine induced). Cardiac mTOR is activated by several known stimulators of cardiac hypertrophy, including angiotensin II, pressure overload, hypertension, thyroid hormone, and phenylephrine. Thus, mTOR seems the likely mechanism through which hypertrophy is induced in these models. However, each of the models activates a different pathway upstream of mTOR; thus, the stimulators of mTOR vary depending on the model. It remains to be elucidated which of the known stimuli activates mTOR in the ACSL1 knockout mice and why that stimulus is present.

In adipocyte lipolysis stimulated by isoproterenol, the AMP generated from the ACSL1 enzymatic reaction has been implicated in activating AMPK [266]. Further research is required to assess cellular AMP levels and the activation of AMPK in ACSL1 knockout tissues. AMPK phosphorylation was decreased in *Acsl1*$^{T-/-}$ hearts but preliminary experiments show that total cardiac AMP and ATP levels are not different between genotypes.

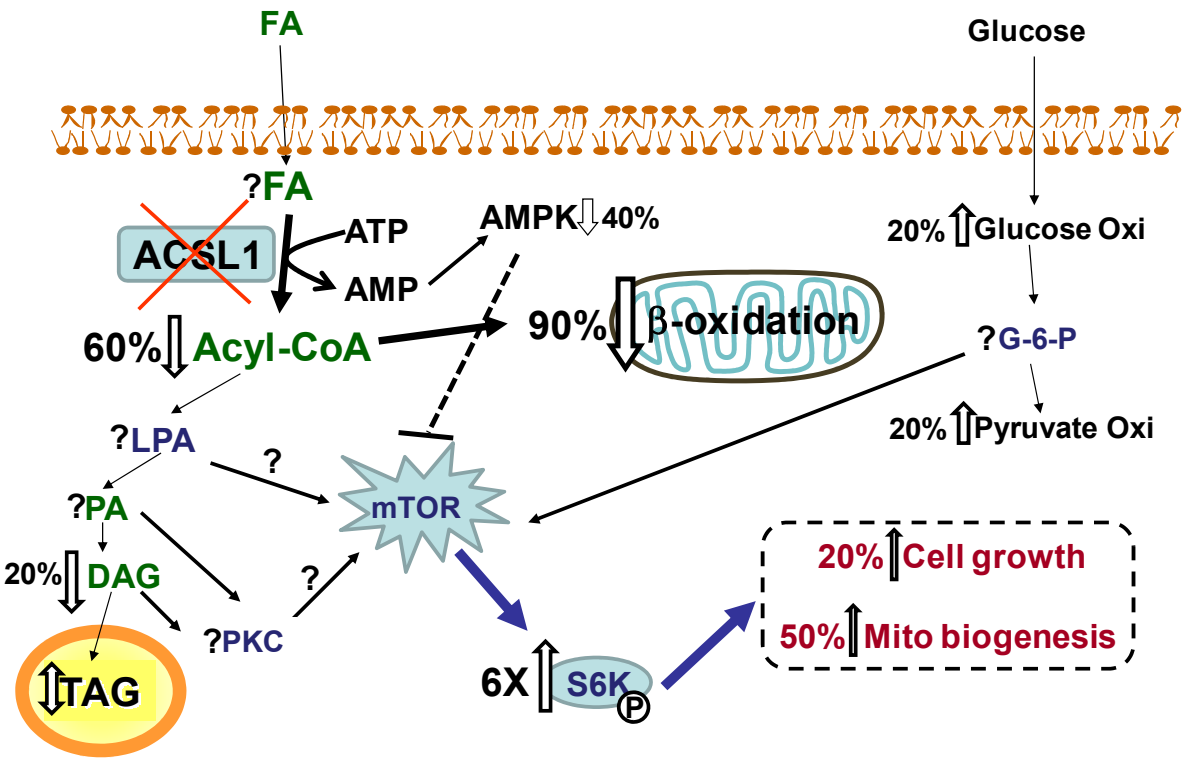

Figure 6.1. Potential links between ACSL1 knockout and mTOR activation.
The lack of ACSL1 reduces the conversion of long-chain FA to acyl-CoA by ~90% and reduces the oxidation of FA by ~90% in *Acsl1*$^{H-/-}$ and *Acsl1*$^{T-/-}$ hearts. Both *Acsl1*$^{H-/-}$ and *Acsl1*$^{T-/-}$ hearts become enlarged, but the two transgenic hearts have unique gene expression profiles and mitochondrial content. *Acsl1*$^{H-/-}$ and *Acsl1*$^{T-/-}$ both have reduced DAG, and DAG can activate mTOR through PKC. However, because DAG is reduced in the *Acsl1*$^{H-/-}$ and *Acsl1*$^{T-/-}$ hearts, PKC activation by DAG is not likely to be the mechanism that activates mTOR. AMPK can inhibit mTOR activity; however, because AMPK phosphorylation is increased in *Acsl1*$^{H-/-}$ but decreased in *Acsl1*$^{T-/-}$ hearts, AMPK activation and relief of mTOR inhibition is probably not the mechanism that allows cell growth in the *Acsl1*$^{H-/-}$ hearts. In both transgenic models the reduction in cardiac FA oxidation is compensated for by increased glucose uptake and oxidation. Glucose intermediates can activate mTOR in cardiomyocytes, thus an increase in glycolytic metabolism may mediate mTOR-driven cardiac hypertrophy.

Continuation of *Acsl1*$^{H-/-}$ studies:

The objective to confirm the impaired FA oxidation and hypertrophy in the heart of a heart-specific ACSL1 knockout mouse has been completed. Our original intention was to include FA oxidation measurements in heart homogenates and the cardiac phenotyping data from the *Acsl1*$^{H-/-}$ mice with the manuscript on the *Acsl1*$^{T-/-}$ mice. However, rather than combining this data into one manuscript, we have opted to perform additional studies on the *Acsl1*$^{H-/-}$ mice to further determine how the lack of ACSL1 affects heart metabolism and function.

The following list briefly describes the additional questions being asked, the methods used to answer these questions, and progress made towards the completion of the experiment:

Are *Acsl1*$^{H-/-}$ mice resistant to high-fat diet induced obesity?

Method: *Acsl1*$^{H-/-}$ and control mice have been placed on a 60%-high-fat diet for 10 weeks. Cardiac TAG content and insulin-stimulated signaling will be determined. We expect to find that TAG does not accumulate in the *Acsl1*$^{H-/-}$ mice because the lack of ACSL1 reduces uptake and retention of FA.

Progress: See manuscript 3. Diet studies have been performed and data collection for heart insulin signaling is underway. We hypothesize that *Acsl1*$^{H-/-}$ mice will be resistant to high-fat diet-induced TAG accumulation in the heart, because ACSL1 reduces the rate of FA uptake, retention of the excess dietary FA, see next question.

Does ACSL1 affect the rate of FA uptake by the heart?

Method: Radiolabeled bromo-palmitate, 2-deoxy-glucose, and palmitate will be injected into control and *Acsl1*$^{H-/-}$ mice intravenously. Hearts and plasma will be extracted 30 minutes later and the total radioactivity in the heart will be counted. For the labeled FA substrates, total lipid will be extracted and by chromatographed to quantify label incorporated into complex lipids. My expectation is that uptake and retention of the bromolyated FA will be reduced in the *Acsl1*$^{H-/-}$ heart because the rate of FA conversion to an acyl-CoA, and thus trapping within the cell, will be reduced. The rate of FA incorporation into complex lipids will be normal in the *Acsl1*$^{H-/-}$ heart because ACSL1 channels FA towards oxidation, not towards lipid synthesis. Glucose uptake will be increased in the *Acsl1*$^{H-/-}$ hearts because the oxidation of glucose is increased to compensate for the reduced FA oxidative capacity.

Progress: In the planning stage

How does the lack of ACSL1 change transcriptional activity?

Method: Control and *Acsl1*$^{H-/-}$ ventricle mRNA will be analyzed by microarray studies. These data will be mostly exploratory, but we expect that we will see changes because we have QRT-PCR data that show *Acsl1*$^{H-/-}$ ventricles upregulate the fetal gene program and down-regulate several PPAR-regulated genes.

Progress: Microarrays have been run in collaboration with Dr. Cam Patterson. Analysis is underway.

How are the rates of FA and glucose oxidation changed in *Acsl1*$^{H-/-}$ whole heart?

Method: use of the "gold standard" Langendorff perfusions to measure the rate of FA and glucose oxidation in whole working hearts of control and *Acsl1*$^{H-/-}$ mice.

Progress: Mice were shipped to UT Southwestern and the Langendorff perfusions have been performed with 13C-labeled substrate. The tissue is awaiting mass spectrometry analysis and data analysis will follow. This has been performed in collaboration with Dr. Mark Jeffrey We expect to see reduced oxidation of the FA substrate and increased oxidation of the glucose substrate in *Acsl1*$^{H-/-}$ hearts to corroborate data we have generated in cardiac homogenate and mitochondrial preparations.

Public Health Significance

FA metabolism plays a central role in obesity and obesity-related complications. Understanding the metabolisms that underlie disease will aid in treating disease. Because ACSL1 had previously been postulated to activate FA for lipid synthesis in adipose tissue, drugs to inhibit ACSL1 to reduce obesity had been considered. However, the data presented in this dissertation provide novel evidence that ACSL1 activates FA destined for oxidation. Thus, a drug that activates ACSL1 has the potential to increase caloric expenditure through thermogenesis and the catabolism of fat. Data presented in this dissertation show that ACSL1 is critical for FA oxidation. The knockout of adipose ACSL1 in mouse results in increased adipose mass, and the knockout of cardiac ACSL1 results in cardiac hypertrophy. Thus, SNPs in ACSL1 may be correlated with obesity and idiopathic hypertrophies in human populations.

REFERENCES

1. Soukas, A., et al., *Distinct transcriptional profiles of adipogenesis in vivo and in vitro.* J. Biol. Chem., 2001. **276**: p. 34167-34174.

2. Gerhold, D.L., et al., *Gene expression profile of adipocyte differentiation and its regulation by peroxisome proliferator-activated receptor-{gamma} agonists.* Endocrinology, 2002. **143**(6): p. 2106-2118.

3. Marszalek, J.R., et al., *Acyl CoA synthetase 2 (ACS2) over-expression enhances fatty acid internalization and neurite outgrowth.* J. Biol. Chem., 2004. **279**: p. 23882-23891.

4. Coleman, R.A., et al., *Selective changes in microsomal enzymes of triacylglycerol, phosphatidylcholine, and phosphatidylethanolamine biosynthesis during differentiation of 3T3-L1 preadipocytes.* J. Biol. Chem., 1978. **253**: p. 7256-7261.

5. de Jong, H., et al., *Ontogeny of mRNA expression and activity of long-chain acyl-CoA synthetase (ACSL) isoforms in Mus musculus heart.* Biochim. Biophys. Acta., 2007. **1771**: p. 75-82.

6. Durgan, D.J., et al., *Distinct transcriptional regulation of long-chain acyl-CoA synthetase isoforms and cytosolic thioesterase 1 in the rodent heart by fatty acids and insulin.* Am. J. Physiol. Heart Circ. Physiol., 2006. **290**: p. H2480-2497.

7. CDC, *State-specific prevalence of obesity among adults*, CDC, Editor. 2007, MMWR p. 765-8.

8. Hisanaga, Y., et al., *Structural basis of the substrate-specific two-step catalysis of long chain fatty acyl-CoA synthetase dimer.* J. Biol. Chem., 2004. **279**: p. 31717-31726.

9. Kochan, G., et al., *Structural snapshots for the conformation-dependent catalysis by human medium-chain acyl-coenzyme a synthetase ACSM2A.* J Mol Biol, 2009. **388**(5): p. 997-1008.

10. Watkins, P.A., et al., *Evidence for 26 distinct acyl-CoA synthetase genes in the human genome.* J Lipid Res, 2007. **48**(12): p. 2736-50.

11. Starai, V.J., et al., *Sir2-dependent activation of acetyl-CoA synthetase by deacetylation of active lysine.* Science, 2002. **298**(5602): p. 2390-2.

12. North, B.J. and D.A. Sinclair, *Sirtuins: a conserved key unlocking AceCS activity.* Trends Biochem Sci, 2007. **32**(1): p. 1-4.

13. Schwer, B., et al., *Calorie restriction alters mitochondrial protein acetylation.* Aging Cell, 2009. **8**(5): p. 604-6.

14. Distler, A.M., J. Kerner, and C.L. Hoppel, *Post-translational modifications of rat liver mitochondrial outer membrane proteins identified by mass spectrometry.* Biochim. Biophys. Acta., 2007. **1774**: p. 628-636.

15. Jump, D.B., *Dietary polyunsaturated fatty acids and regulation of gene transcription.* Curr. Opin. Lipidol., 2002. **13**: p. 155-164.

16. Bu, S.Y., M.T. Mashek, and D.G. Mashek, *Suppression of long chain acyl-CoA synthetase 3 decreases hepatic de novo fatty acid synthesis through decreased transcriptional activity.* J Biol Chem, 2009. **284**(44): p. 30474-83.

17. Mashek, D.G., et al., *Revised nomenclature for the mammalian long chain acyl-CoA synthetase gene family.* J. Lipid. Res., 2004. **45**: p. 1958-1961.

18. Coleman, R.A., T.M. Lewin, and D.M. Muoio, *Physiological and nutritional regulation of enzymes of triacylglycerol synthesis.* Ann. Rev. Nutr, 2000. **20**: p. 77-103.

19. Mannaerts, G.P., et al., *Evidence that peroxisomal acyl-CoA synthetase is located at the cytoplasmic side of the peroxisomal membrane.* Biochem. J., 1982. **204**: p. 7-23.

20. Kim, J.-H., T.M. Lewin, and R.A. Coleman, *Expression and characterization of recombinant rat acyl-CoA synthetases 1, 4, and 5: Selective inhibition by triacsin C and thiazolidinediones.* J. Biol. Chem., 2001. **276**: p. 24667-24673.

21. Lewin, T.M., et al., *Acyl-CoA synthetase isoforms 1, 4, and 5 are present in different subcellular membranes in rat liver and can be inhibited independently.* J. Biol. Chem., 2001. **276**: p. 24674-24679.

22. Van Horn, C.G., et al., *Characterization of recombinant long-chain rat acyl-CoA synthetase isoforms 3 and 6: Identification of a novel variant of isoform 6.* Biochemistry, 2005. **44**: p. 1635-1642.

23. Richards, M.R., et al., *Fatty acid transport protein 1 and long-chain acyl coenzyme A synthetase 1 interact in adipocytes.* J. Lipid Res., 2006. **47**: p. 665-672.

24. Coleman, R.A., et al., *Do acyl-CoA synthetases regulate fatty acid entry into synthetic versus degradative pathways?* J. Nutr., 2002. **132**: p. 2123-2126.

25. Watkins, P.A., *Very-long-chain acyl-CoA synthetases.* J Bio Chem, 2008. **283**(4): p. 1773-1777.

26. Soupene, E. and F.A. Kuypers, *Mammalian long-chain acyl-CoA synthetases.* Exp Biol Med (Maywood), 2008. **233**(5): p. 507-21.

27. Mashek, D.G. and R.A. Coleman, *Cellular fatty acid uptake: the contribution of metabolism.* Curr. Opin. Lipidol., 2006. **17**: p. 274-278.

28. Yao, H. and J. Ye, *Long chain acyl-CoA synthetase 3-mediated phosphatidylcholine synthesis is required for assembly of very low density lipoproteins in human hepatoma Huh7 cells.* J. Biol. Chem., 2008. **283**: p. 849-854.

29. Yao, H. and J. Ye, *Long chain acyl-CoA synthetase 3-mediated phosphatidylcholine synthesis is required for assembly of very low density lipoproteins in human hepatoma huh7 cells.* J Bio Chem, 2008. **283**(2): p. 849-854.

30. Fujimoto, Y., et al., *Identification of major proteins in the lipid droplet-enriched fraction isolated from the human hepatocyte cell line HuH7.* Biochim. Biophys. Acta, 2004. **1644**: p. 47-59.

31. Caviglia, J.M., et al., *Rat long chain acyl-CoA synthetase 5, but not 1, 2, 3, or 4, complements Escherichia coli fadD.* J. Biol. Chem., 2004. **279**: p. 11163-11169.

32. Muoio, D.M., et al., *Acyl-CoAs are functionally channeled in liver: potential role of acyl-CoA synthetase.* Am. J. Physiol. Endocrinol. Metab., 2000. **279**(6): p. E1366-1373.

33. Li, L.O., et al., *Overexpression of rat long chain acyl-CoA synthetase 1 alters fatty acid metabolism in rat primary hepatocytes.* J. Biol. Chem., 2006. **281**: p. 37246-37255.

34. Mashek, D.G., et al., *Rat long chain acyl-CoA synthetase 5 increases fatty acid uptake and partitioning to cellular triacylglycerol in McArdle -RH7777 cells.* J. Biol. Chem., 2006. **281**: p. 945-950.

35. Tong, F., et al., *Fatty acid transport by vectorial acylation in mammals: roles played by different isoforms of rat long-chain acyl-CoA synthetases.* Arch. Biochem. Biophys., 2006. **447**: p. 46-52.

36. Li, L.O., et al., *Overexpression of rat long chain acyl-CoA synthetase 1 alters fatty acid metabolism in rat primary hepatocytes.* J. Biol. Chem., 2006. **281**(48): p. 37246-55.

37. Zhou, Y., et al., *Transcriptional activation of hepatic ACSL3 and ACSL5 by oncostatin m reduces hypertriglyceridemia through enhanced beta-oxidation.* Arterioscler Thromb Vasc Biol, 2007. **27**(10): p. 2198-205.

38. Souza, S.C., et al., *Modulation of hormone-sensitive lipase and protein kinase A-mediated lipolysis by perilipin A in an adenoviral reconstituted system.* J. Biol. Chem., 2002. **277**: p. 8267-8272.

39. Lobo, S., B.M. Wiczer, and D.A. Bernlohr, *Functional analysis of long-chain acyl-coa synthetase 1 in 3T3-L1 adipocytes.* J Biol Chem, 2009. **284**: p. 18347-18356.

40. Forner, F., et al., *Proteome differences between brown and white fat mitochondria reveal specialized metabolic functions.* Cell Metab, 2009. **10**(4): p. 324-35.

41. Wiczer, B.M. and D.A. Bernlohr, *A novel role for fatty acid transport protein 1 in the regulation of tricarboxylic acid cycle and mitochondrial function in 3T3-L1 adipocytes.* J Lipid Res, 2009. **50**(12): p. 2502-13.

42. Sebastian, D., et al., *Novel role of FATP1 in mitochondrial fatty acid oxidation in skeletal muscle cells.* J Lipid Res, 2009. **50**(9): p. 1789-99.

43. Jia, Z., et al., *The fatty acid transport protein (FATP) family: very long chain acyl-CoA synthetases or solute carriers?* J Mol Neurosci, 2007. **33**(1): p. 25-31.

44. Tomoda, H., et al., *Evidence for an essential role of long chain acyl-CoA synthetase in animal cell proliferation.* J. Biol. Chem., 1991. **266**: p. 4214-4219.

45. Mashima, T., et al., *Acyl-CoA synthetase as a cancer survival factor: its inhibition enhances the efficacy of etoposide.* Cancer Sci, 2009. **100**(8): p. 1556-62.

46. Mashima, T., et al., *Promotion of glioma cell survival by acyl-CoA synthetase 5 under extracellular acidosis conditions.* Oncogene, 2009. **28**(1): p. 9-19.

47. Pei, Z., et al., *Acyl-CoA synthetase VL3 knockdown inhibits human glioma cell proliferation and tumorigenicity.* Cancer Res, 2009.

48. Ellis, J.M., et al., *Acyl-coenzyme A synthetases in metabolic control.* Current Opinion in Lipidology, 2010. **21**(3): p. 212-217.

49. Gonzalez, A.A., et al., *Metabolic adaptations to fasting and chronic caloric restriction in heart, muscle, and liver do not include changes in AMPK activity.* Am J Physiol Endocrinol Metab, 2004. **287**(5): p. E1032-7.

50. Mulligan, J.D., et al., *Upregulation of AMPK during cold exposure occurs via distinct mechanisms in brown and white adipose tissue of the mouse.* J Physiol, 2007. **580**(Pt. 2): p. 677-84.

51. Gauthier, M.S., et al., *AMP-activated protein kinase is activated as a consequence of lipolysis in the adipocyte: potential mechanism and physiological relevance.* J Biol Chem, 2008. **283**(24): p. 16514-24.

52. Wiczer, B.M., et al., *FATP1 mediates fatty acid-induced activation of AMPK in 3T3-L1 adipocytes.* Biochem Biophys Res Commun, 2009. **387**(2): p. 234-8.

53. Clark, H., D. Carling, and D. Saggerson, *Covalent activation of heart AMP-activated protein kinase in response to physiological concentrations of long-chain fatty acids.* Eur J Biochem, 2004. **271**(11): p. 2215-24.

54. Steinberg, G.R. and B.E. Kemp, *AMPK in health and disease.* Physiol Rev, 2009. **89**(3): p. 1025-78.

55. Fediuc, S., M.P. Gaidhu, and R.B. Ceddia, *Regulation of AMP-activated protein kinase and acetyl-CoA carboxylase phosphorylation by palmitate in skeletal muscle cells.* J Lipid Res, 2006. **47**(2): p. 412-20.

56. Maeda, K., et al., *Adipocyte/macrophage fatty acid binding proteins control integrated metabolic responses in obesity and diabetes.* Cell Metab, 2005. **1**(2): p. 107-19.

57. Za'tara, G., et al., *AMPK activation by long chain fatty acyl analogs.* Biochem Pharmacol, 2008. **76**(10): p. 1263-75.

58. Watt, M.J., et al., *Beta-adrenergic stimulation of skeletal muscle HSL can be overridden by AMPK signaling.* Faseb J, 2004. **18**(12): p. 1445-6.

59. Watt, M.J., et al., *Fatty acids stimulate AMP-activated protein kinase and enhance fatty acid oxidation in L6 myotubes.* J Physiol, 2006. **574**(Pt 1): p. 139-47.

60. Zhang, D., et al., *Resistance to High-Fat Diet-Induced Obesity and Insulin Resistance in Mice with Very Long-Chain Acyl-CoA Dehydrogenase Deficiency.* Cell Metabolism, 2010. **11**(5): p. 402-411.

61. Taylor, E.B., et al., *Long-chain acyl-CoA esters inhibit phosphorylation of AMP-activated protein kinase at threonine-172 by LKB1/STRAD/MO25.* Am J Physiol Endocrinol Metab, 2005. **288**(6): p. E1055-61.

62. Færgeman, N.J. and J. Knudsen, *Role of long-chain fatty acyl-CoA esters in the regulation of metabolism and in cell signalling.* Biochem. J., 1997. **323**: p. 1-12.

63. Teng, A.C., et al., *Functional characterization of a promoter polymorphism that drives ACSL5 gene expression in skeletal muscle and associates with diet-induced weight loss.* Faseb J, 2009. **23**(6): p. 1705-9.

64. Perera, F., et al., *Relation of DNA methylation of 5'-CpG island of ACSL3 to transplacental exposure to airborne polycyclic aromatic hydrocarbons and childhood asthma.* PLoS One, 2009. **4**(2): p. e4488.

65. Meloni, I., et al., *The XLMR gene ACSL4 plays a role in dendritic spine architecture.* Neuroscience, 2009. **159**: p. 657-669.

66. Zeman, M., et al., *Fatty acid CoA ligase-4 gene polymorphism influences fatty acid metabolism in metabolic syndrome, but not in depression.* Tohoku J Exp Med, 2009. **217**(4): p. 287-93.

67. Kotronen, A., et al., *Genetic variation in the ADIPOR2 gene is associated with liver fat content and its surrogate markers in three independent cohorts.* Eur J Endocrinol, 2009. **160**(4): p. 593-602.

68. Klar, J., et al., *Mutations in the fatty acid transport protein 4 gene cause the ichthyosis prematurity syndrome.* Am J Hum Genet, 2009. **85**(2): p. 248-53.

69. Herrmann, T., et al., *Mice with targeted disruption of the fatty acid transport protein 4 (Fatp 4, Slc27a4) gene show features of lethal restrictive dermopathy.* J Cell Biol, 2003. **161**(6): p. 1105-15.

70. Suzuki, H., et al., *Structure and regulation of rat long-chain acyl-CoA synthetase.* J. Biol. Chem., 1990. **265**: p. 8681-8685.

71. Gargiulo, C.E., S.M. Stuhlsatz-Krouper, and J.E. Schaffer, *Localization of adipocyte long-chain fatty acyl-CA synthetase at the plasma membrane.* J. Lipid. Res., 1999. **40**: p. 881-892.

72. Chiu, H.-C., et al., *A novel mouse model of lipotoxic cardiomyopathy.* J. Clin. Invest., 2001. **107**: p. 813-822.

73. Milger, K., et al., *Cellular uptake of fatty acids driven by the ER-localized acyl-CoA synthetase FATP4.* J. Cell Sci., 2006. **119**: p. 4678-4688.

74. Fujimoto, Y., et al., *Involvement of ACSL in local synthesis of neutral lipids in cytoplasmic lipid droplets in human hepatocyte HuH7*. 2007. p. 1280-1292.

75. Sleeman, M.W., et al., *Association of acyl-CoA synthetase-1 with GLUT4-containing vesicles.* J. Biol. Chem., 1998. **273**: p. 3132-3135.

76. Brasaemle, D.L., et al., *Proteomic analysis of proteins associated with lipid droplets of basal and lipolytically stimulated 3T3-L1 adipocytes.* J. Biol. Chem., 2004. **279**: p. 46835-46842.

77. Parkes, H.A., et al., *Overexpression of acyl-CoA synthetase-1 increases lipid deposition in hepatic (HepG2) cells and rodent liver in vivo.* Am. J. Physiol. Endocrinol. Metab., 2006. **291**: p. E737-744.

78. Li, L.O., et al., *Liver-specific loss of long chain acyl-CoA synthetase-1 decreases triacylglycerol synthesis and beta-oxidation and alters phospholipid fatty acid composition.* J Biol Chem, 2009. **284**(41): p. 27816-26.

79. Doege, H. and A. Stahl, *Protein-mediated fatty acid uptake: novel insights from in vivo models.* Physiology (Bethesda), 2006. **21**: p. 259-68.

80. Schaffer, J.E. and H.F. Lodish, *Expression cloning and characterization of a novel adipocyte long chain fatty acid transport protein.* Cell, 1994. **79**: p. 427-436.

81. Watkins, P.A., et al., *Evidence for 26 distinct acyl-coenzyme A synthetase genes in the human genome.* J. Lipid Res., 2007. **48**(12): p. 2736-50.

82. Kim, J.K., et al., *Inactivation of fatty acid transport protein 1 prevents fat-induced insulin resistance in skeletal muscle.* J. Clin. Invest., 2004. **113**: p. 756-763.

83. Mashek, D.G., L.O. Li, and R.A. Coleman, *Rat long chain acyl-CoA synthetase mRNA, protein and activity vary in tissue distribution and in response to diet.* J. Lipid Res., 2006. **47**: p. 2004-2010.

84. Kansara, M.S., et al., *Physiological concentrations of insulin and T3 stimulate 3T3-L1 adipocyte acyl-CoA synthetase gene transcription.* Am. J. Physiol., 1996. **270**: p. E873-E881.

85. Martin, G., et al., *Coordinate regulation of the expression of the fatty acid transport protein and acyl-CoA synthetase genes by PPARα and PPARγ activators.* J. Biol. Chem., 1997. **272**: p. 28210-28217.

86. Shimomura, I., et al., *Rapid enhancement of acyl-CoA synthetase, LPL, and GLUT-4 mRNAs in adipose tissue of VMH rats.* Amer. J. Physiol., 1996. **270**: p. E995-E1002.

87. Hall, M. and E.D. Saggerson, *Reversible inactivation by noradrenaline of long-chain fatty acyl-CoA synthetase in rat adipocytes.* Biochem. J., 1985. **226**: p. 275-282.

88. Shimomura, I., et al., *Marked reduction of acyl-CoA synthetase activity and mRNA in intra-abdominal visceral fat by physical exercise.* Am. J. Physiol., 1993. **265**: p. E44 - 50.

89. Coleman, R.A. and E.B. Haynes, *Selective changes in microsomal enzymes of triacylglycerol and phosphatidylcholine synthesis in fetal and postnatal rat liver: Induction of microsomal sn-glycerol 3-P and dihydroxyacetone-P acyltransferase activities.* J. Biol. Chem., 1983. **258**: p. 450-465.

90. Oikawa, E., et al., *A novel acyl-CoA synthetase, ACS5, expressed in intestinal epithelial cells and proliferating preadipocytes.* J. Biochem., 1998. **124**: p. 679-685.

91. Young C. Cho, C.R.J., *PPARgamma1 synthesis and adipogenesis in C3H10T1/2 cells depends on S-phase progression, but does not require mitotic clonal expansion*. 2004. p. 336-353.

92. Brown, N.F., et al., *Mouse white adipocytes and 3T3-L1 cells display an anomalous pattern of carnitine palmitoyltransferase (CPT) I isoform expression during differentiation. Inter-tissue and inter-species expression of CPT I and CPT II enzymes*. 1997. p. 225-231.

93. Deveaud, C., et al., *Regional differences in oxidative capacity of rat white adipose tissue are linked to the mitochondrial content of mature adipocytes.* Mol Cell Biochem, 2004. **267**(1-2): p. 157-66.

94. Shi, X., et al., *Paradoxical effect of mitochondrial respiratory chain impairment on insulin signaling and glucose transport in adipose cells.* J Biol Chem, 2008. **283**(45): p. 30658-67.

95. Wilson-Fritch, L., et al., *Mitochondrial biogenesis and remodeling during adipogenesis and in response to the insulin sensitizer rosiglitazone.* Mol Cell Biol, 2003. **23**(3): p. 1085-94.

96. Wilson-Fritch, L., et al., *Mitochondrial remodeling in adipose tissue associated with obesity and treatment with rosiglitazone.* J Clin Invest, 2004. **114**(9): p. 1281-9.

97. Gertow, K., et al., *Fatty acid handling protein expression in adipose tissue, fatty acid composition of adipose tissue and serum, and markers of insulin resistance.* Eur J Clin Nutr, 2006. **60**(12): p. 1406-1413.

98. Robidoux, J., T.L. Martin, and S. Collins, *Beta-adrenergic receptors and regulation of energy expenditure: A family affair.* Annu Rev Pharmacol Toxicol, 2004. **44**(1): p. 297-323.

99. Sell, H., Y. Deshaies, and D. Richard, *The brown adipocyte: update on its metabolic role.* The International Journal of Biochemistry & Cell Biology, 2004. **36**(11): p. 2098-2104.

100. Lowell, B.B. and B.M. Spiegelman, *Towards a molecular understanding of adaptive thermogenesis.* Nature, 2000. **404**(6778): p. 652-660.

101. Nedergaard, J., T. Bengtsson, and B. Cannon, *Unexpected evidence for active brown adipose tissue in adult humans*. 2007. p. E444-452.

102. Nicholls, D.G. and R.M. Locke, *Thermogenic mechanisms in brown fat*. 1984. p. 1-64.

103. Cannon, B., U. Sundin, and L. Romert, *Palmitoyl coenzyme A: A possible physiological regulator of nucleotide binding to brown adipose tissue mitochondria.* FEBS Letters, 1977. **74**(1): p. 43-46.

104. Strieleman, P.J. and E. Shrago, *Specific interaction of fatty acyl-CoA esters with brown adipose tissue mitochondria*. 1985. p. E699-705.

105. Strieleman, P.J., K.L. Schalinske, and E. Shrago, *Fatty acid activation of the reconstituted brown adipose tissue mitochondria uncoupling protein*. 1985. p. 13402-13405.

106. van Marken Lichtenbelt, W.D., et al., *Cold-Activated Brown Adipose Tissue in Healthy Men.* N Engl J Med, 2009. **360**(15): p. 1500-1508.

107. Virtanen, K.A., et al., *Functional brown adipose tissue in healthy adults.* N Engl J Med, 2009. **360**(15): p. 1518-1525.

108. Cypess, A.M., et al., *Identification and importance of brown adipose tissue in adult humans.* N Engl J Med, 2009. **360**(15): p. 1509-1517.

109. Pedersen, J.I., et al., *The intracellular localization of long-chain acyl-CoA synthetase in brown adipose tissue.* Biochimica et Biophysica Acta (BBA) - Lipids and Lipid Metabolism, 1975. **398**(1): p. 191-203.

110. Darnley, A.C., C.A. Carpenter, and E.D. Saggerson, *Changes in activities of some enzymes of glycerolipid synthesis in brown adipose tissue of cold-acclimated rats.* Biochem. J., 1988. **253**: p. 351-355.

111. Mitchell, J.R. and E.D. Saggerson, *Activities of enzymes of glycerolipid synthesis in brown adipose tissue after treatment of rats with the adrenergic agonists BRL 26830A and phenylephrine, after exposure to cold and in streptozotocin-diabetes.* Biochem. J., 1991. **277**: p. 665-669.

112. Yu, X.X., et al., *Cold elicits the simultaneous induction of fatty acid synthesis and beta-oxidation in murine brown adipose tissue: prediction from differential gene expression and confirmation in vivo.* FASEB J., 2002. **16**: p. 155-168.

113. Malhotra, K.T., et al., *Identification and molecular characterization of acyl-CoA synthetase in human erythrocytes and erythroid precursors.* Biochem. J., 1999. **344**: p. 135-143.

114. Hofmann, W.E., et al., *Effects of genetic background on thermoregulation and fatty acid-induced uncoupling of mitochondria in UCP1-deficient mice.* J Bio Chem, 2001. **276**(15): p. 12460-12465.

115. Xue, B., et al., *Transcriptional Synergy and the Regulation of Ucp1 during Brown Adipocyte Induction in White Fat Depots*. 2005. p. 8311-8322.

116. Bachman ES, D.H., Zhang CY, Cinti S, Bianco AC, Kobilka BK, Lowell BB., *beta AR signaling required for diet-induced thermogenesis and obesity resistance.* Science, 2002. **297**(5582): p. 843-845.

117. Golozoubova, V., et al., *Only UCP1 can mediate adaptive nonshivering thermogenesis in the cold*. 2001. p. 00-0536fje.

118. Enerback, S., et al., *Mice lacking mitochondrial uncoupling protein are cold-sensitive but not obese.* Nature, 1997. **387**(6628): p. 90-94.

119. Lowell, B.B., et al., *Development of obesity in transgenic mice after genetic ablation of brown adipose tissue.* Nature, 1993. **366**(6457): p. 740-742.

120. Schuler, A.M., et al., *Synergistic heterozygosity in mice with inherited enzyme deficiencies of mitochondrial fatty acid [beta]-oxidation.* Molecular Genetics and Metabolism, 2005. **85**(1): p. 7-11.

121. Tolwani, R.J., et al., *Medium-chain acyl-CoA dehydrogenase deficiency in gene-targeted mice.* PLoS Genetics, 2005. **1**(2): p. e23.

122. Guerra C, K.R., Walsh K, Kurtz DM, Wood PA, Kozak LP., *Abnormal nonshivering thermogenesis in mice with inherited defects of fatty acid oxidation.* J Clin Invest, 1998 **102**(9): p. 1724-31.

123. Haemmerle, G., et al., *Defective lipolysis and altered energy metabolism in mice lacking adipose triglyceride lipase.* Science, 2006. **312**(5774): p. 734-737.

124. Cohen, A.W., et al., *Caveolin-1 expression is essential for proper nonshivering thermogenesis in brown adipose tissue.* Diabetes, 2005. **54**(3): p. 679-686.

125. Coleman, R.A. and R.M. Bell, *Submicrosomal localization of phosphatidylcholine, phosphatidylethanolamine, and triacylglycerol biosynthetic enzymes.* J. Cell Biol., 1978. **76**: p. 245-253.

126. Stremmel, W., et al., *A new concept of cellular uptake and intracellular trafficking of long-chain fatty acids.* Lipids, 2001. **36**(9): p. 981-9.

127. Li, L.O., et al., *Liver-specific loss of long-chain acyl-CoA synthetase-1 decreases triacylglycerol synthesis and β-oxidation, and alters phospholipid fatty acid composition.* J. Biol. Chem., 2009. **under revision**.

128. Berger, J. and D.E. Moller, *The mechanisms of action of PPARs.* Annu. Rev. Med., 2002. **53**: p. 409-435.

129. Hostetler, H.A., et al., *Peroxisome proliferator-activated receptor alpha interacts with high affinity and is conformationally responsive to endogenous ligands.* J Biol Chem, 2005. **280**(19): p. 18667-82.

130. Lowell, B.B. and B.M. Spiegelman, *Towards a molecular understanding of adaptive thermogenesis.* Nature, 2000. **404**(6778): p. 652-60.

131. Cohen, A.W., et al., *Caveolin-1 expression is essential for proper nonshivering thermogenesis in brown adipose tissue.* Diabetes, 2005. **54**(3): p. 679-86.

132. Haman, F., *Shivering in the cold: from mechanisms of fuel selection to survival.* J Appl Physiol, 2006. **100**(5): p. 1702-8.

133. Yoshida, T., et al., *Anti-obesity effect of CL 316,243, a highly specific beta 3-adrenoceptor agonist, in mice with monosodium-L-glutamate-induced obesity.* Eur J Endocrinol, 1994. **131**(1): p. 97-102.

134. Bachman, E.S., et al., *betaAR signaling required for diet-induced thermogenesis and obesity resistance.* Science, 2002. **297**(5582): p. 843-5.

135. Vergnes, L., et al., *Agpat6 deficiency causes subdermal lipodystrophy and resistance to obesity.* J. Lipid Res., 2006. **47**: p. 745-754.

136. Makowski, L., et al., *Metabolic profiling of PPARalpha-/- mice reveals defects in carnitine and amino acid homeostasis that are partially reversed by oral carnitine supplementation.* Faseb J, 2009. **23**(2): p. 586-604.

137. Qi, C., Y. Zhu, and J.K. Reddy, *Peroxisome proliferator-activated receptors, coactivators, and downstream targets.* Cell Biochem Biophys, 2000. **32 Spring**: p. 187-204.

138. Ruderman, N.B., A.K. Saha, and E.W. Kraegen, *Minireview: malonyl CoA, AMP-activated protein kinase, and adiposity.* Endocrinology, 2003. **144**: p. 5166-5171.

139. Guerra, C., et al., *Abnormal nonshivering thermogenesis in mice with inherited defects of fatty acid oxidation.* J Clin Invest, 1998. **102**(9): p. 1724-31.

140. Schuler, A.M., et al., *Synergistic heterozygosity in mice with inherited enzyme deficiencies of mitochondrial fatty acid beta-oxidation.* Mol Genet Metab, 2005. **85**(1): p. 7-11.

141. Tolwani, R., et al., *Medium-chain acyl-CoA dehydrogenase deficiency in gene-targeted mice.* PLOS Genet., 2005. **1**(2): p. e23.

142. Strieleman, P.J., K.L. Schalinske, and E. Shrago, *Fatty acid activation of the reconstituted brown adipose tissue mitochondria uncoupling protein.* J Biol Chem, 1985. **260**(25): p. 13402-5.

143. Strieleman, P.J. and E. Shrago, *Specific interaction of fatty acyl-CoA esters with brown adipose tissue mitochondria.* Am J Physiol, 1985. **248**(6 Pt 1): p. E699-705.

144. Shabalina, I.G., et al., *Native UCP1 displays simple competitive kinetics between the regulators purine nucleotides and fatty acids.* J Biol Chem, 2004. **279**(37): p. 38236-48.

145. Lodhi, I.J. and C.F. Semenkovich, *Why we should put clothes on mice.* Cell Metab, 2009. **9**(2): p. 111-2.

146. Lobo, S., B.M. Wiczer, and D.A. Bernlohr, *Functional analysis of long-chain acyl-coa synthetase 1 in 3T3-L1 adipocytes.* J Biol Chem, 2009.

147. Polokoff, M.A. and R.M. Bell, *Limited palmitoyl-CoA penetration into microsomal vesicles as evidenced by a highly latent ethanol acyltransferase activity.* J. Biol. Chem., 1978. **253**: p. 7173-7178.

148. Nagle, C.A., et al., *Identification of a novel sn-glycerol-3-phosphate acyltransferase isoform, GPAT4 as the enzyme deficient in Agpat6-/- mice.* J. Lipid Res., 2008. **49**: p. 823-831.

149. Warne, J.P., et al., *Gene deletion reveals roles for annexin A1 in the regulation of lipolysis and IL-6 release in epididymal adipose tissue.* Am J Physiol Endocrinol Metab, 2006. **291**(6): p. E1264-73.

150. Varma, V., et al., *Thrombospondin-1 is an adipokine associated with obesity, adipose inflammation, and insulin resistance.* Diabetes, 2008. **57**(2): p. 432-9.

151. Cao, W., et al., *Beta -adrenergic activation of p38 MAP kinase in adipocytes. cAMP induction of the uncoupling protein 1 (UCP1) gene requires p38 MAP kinase. .* 2001. **276**(29): p. 27077-27082.

152. Bligh, E.G. and W.J. Dyer, *A rapid method of total lipid extraction and purification.* Can. J. Biochem. Physiol., 1959. **37**: p. 911-917.

153. Cannon, B. and J. Nedergaard, *Studies of thermogenesis and mitochondrial function in adipose tissues.* Methods Mol Biol, 2008. **456**: p. 109-21.

154. Noland, R.C., et al., *Peroxisomal-mitochondrial oxidation in a rodent model of obesity-associated insulin resistance.* Am. J. Physiol. Endocrinol. Metab., 2007. **293**: p. E986-E1001.

155. van der Lee, K.A.J.M., et al., *Long-chain fatty acid-induced changes in gene expression in neonatal cardiac myocytes*. 2000. p. 41-47.

156. Schoonjans, K., B. Staels, and J. Auwerx, *Role of the peroxisome proliferator-activated receptor (PPAR) in mediating the effects of fibrates and fatty acids on gene expression.* J. Lipid Res., 1996. **37**: p. 907-925.

157. Schoonjans, K., et al., *Acyl-CoA synthetase mRNA expression is controlled by fibric-acid derivatives, feeding and liver proliferation.* Eur. J. Biochem., 1993. **216**: p. 615-622.

158. Brinkmann, J.F.F., et al., *New insights into long-chain fatty acid uptake by heart muscle: a crucial role for fatty acid translocase/CD36*. 2002. p. 561-570.

159. Aoyama, T., et al., *Altered constitutive expression of fatty acid-metabolizing enzymes in mice lacking the peroxisome proliferator-activated receptor alpha (PPARalpha).* J. Biol. Chem., 1998. **273**: p. 5678-5684.

160. Huss, J.M., et al., *The nuclear receptor ERRalpha is required for the bioenergetic and functional adaptation to cardiac pressure overload.* Cell Metabolism, 2007. **6**(1): p. 25-37.

161. Dufour, C.R., et al., *Genome-wide orchestration of cardiac functions by the orphan nuclear receptors ERRalpha and gamma.* Cell Metabolism, 2007. **5**(5): p. 345-356.

162. Alaynick, W.A., et al., *ERRgamma directs and maintains the transition to oxidative metabolism in the postnatal heart.* Cell Metabolism, 2007. **6**(1): p. 13-24.

163. Saddik, M. and G.D. Lopaschuk, *Myocardial triglyceride turnover and contribution to energy substrate utilization in isolated working rat hearts.* J. Biol. Chem., 1991. **266**: p. 8162-8170.

164. Glatz JF, V.J., *Postnatal development of palmitate oxidation and mitochondrial enzyme activities in rat cardiac and skeletal muscle.* Biochim Biophys Acta. , 1982 **711**(2): p. 327-35.

165. Chiu, H.C., et al., *Transgenic expression of fatty acid transport protein 1 in the heart causes lipotoxic cardiomyopathy.* Circ. Res, 2005. **96**: p. 225-233.

166. Chiu, H.-C., et al., *Transgenic Expression of Fatty Acid Transport Protein 1 in the Heart Causes Lipotoxic Cardiomyopathy*. 2005. p. 225-233.

167. Gimeno, R.E., et al., *Characterization of a heart-specific fatty acid transport protein.* J. Biol. Chem., 2003. **278**: p. 16039-16044.

168. van der Vusse GJ, et al., *Fatty acid homeostasis in the normoxic and ischemic heart.* Physiol Rev., 1992. **72**(4): p. 881-940.

169. Stanley WC, Recchia FA, and L. GD., *Myocardial substrate metabolism in the normal and failing heart.* Physiol Rev., 2005. **85**(3): p. 1093-1129.

170. Levy, D., et al., *Echocardiographically detected left ventricular hypertrophy: revalence and risk factors. The Framingham Heart Study.* Ann Intern Med, 1988. **108**(1): p. 7-13.

171. Savage, D.D., et al., *Association of echocardiographic left ventricular mass with body size, blood pressure and physical activity (the Framingham study).* The American Journal of Cardiology, 1990. **65**(5): p. 371-376.

172. Lehman, J.J. and D.P. Kelly, *Gene regulatory mechanisms governing energy metabolism during cardiac hypertrophic growth.* Heart Failure Reviews, 2002. **7**(2): p. 175-185.

173. Rajabi, M., et al., *Return to the fetal gene program protects the stressed heart: a strong hypothesis.* Heart Failure Reviews, 2007. **12**(3): p. 331-343.

174. Koepsell, H., K. Lips, and C. Volk, *Polyspecific organic cation transporters: structure, function, physiological roles, and biopharmaceutical implications.* Pharma Res, 2007. **24**(7): p. 1227-1251.

175. Melegh, B., et al., *Phenotypic manifestations of the OCTN2 V295X mutation: Sudden infant death and carnitine-responsive cardiomyopathy in Roma families.* Am J Med Genet A, 2004. **131A**(2): p. 121-126.

176. Suenaga, M., et al., *Identification of the up- and down-regulated genes in the heart of juvenile visceral steatosis mice.* Biolo Pharma Bull, 2004. **27**(4): p. 496-503.

177. Kaido M, F.H., Ono A, Toyooka K, Yoshikawa H, Nishimura T, Ozaki K, Narama I, Kuwajima M., *Mitochondrial abnormalities in a murine model of primary carnitine deficiency. Systemic pathology and trial of replacement therapy.* Eur Neurol., 1997. **38**(4): p. 302-9.

178. Kuwajima, M., et al., *Characteristics of cardiac hypertrophy in the juvenile visceral steatosis mouse with systemic carnitine deficiency.* J Mole Cell Cardiol, 1998. **30**(4): p. 773-781.

179. Asai T, et al., *Combined therapy with PPAR{alpha} agonist and L-carnitine rescues lipotoxic cardiomyopathy due to systemic carnitine deficiency.* Cardiovasc Res., 2006. **70**(3): p. 566-577.

180. van der Leij FR, D.A., Kuipers JR., *Rationale for a conditional knockout mouse model to study carnitine palmitoyltransferase I deficiencies.* Adv Exp Med Biol., 1999. **466**: p. 377-85.

181. Nyman, L.R., et al., *Homozygous carnitine palmitoyltransferase 1a (liver isoform) deficiency is lethal in the mouse.* Molecular Genetics and Metabolism, 2005. **86**(1-2): p. 179-187.

182. Ji, S., et al., *Homozygous carnitine palmitoyltransferase 1b (muscle isoform) deficiency is lethal in the mouse.* Molecular Genetics and Metabolism, 2008. **93**(3): p. 314-322.

183. Lee RS, L.C., Lai CK, Yuen YP, Chan KY, Shek CC, Chan AY, Chow CB., *Carnitine-acylcarnitine translocase deficiency in three neonates presenting with rapid deterioration and cardiac arrest.* Hong Kong Med J, 2007. **2007**(13): p. 1.

184. Choong, K., et al., *Lethal cardiac tachyarrhythmia in a patient with neonatal carnitine–acylcarnitine translocase deficiency.* Pediatric and Developmental Pathology, 2001. **4**(6): p. 573-579.

185. Shuho Semba, H.Y.T.T.H.Y., *Autopsy case of the neonatal form of carnitine palmitoyltransferase-II deficiency triggered by a novel disease-causing mutation del1737C*. 2008. p. 436-441.

186. Marín-García, J. and M.J. Goldenthal, *Understanding the impact of mitochondrial defects in cardiovascular disease: A review.* Journal of Cardiac Failure, 2002. **8**(5): p. 347-361.

187. Vianey-Saban, C., et al., *Mitochondrial very-long-chain acyl-coenzyme A dehydrogenase deficiency: clinical characteristics and diagnostic considerations in 30 patients.* Clinica Chimica Acta, 1998. **269**(1): p. 43-62.

188. Exil, V.J., et al., *Very-long-chain acyl-coenzyme a dehydrogenase deficiency in mice.* Circ Res, 2003. **93**(5): p. 448-455.

189. Werdich AA, et al., *Polymorphic ventricular tachycardia and abnormal Ca2+ handling in very-long-chain acyl-CoA dehydrogenase null mice.* Am J Physiol Heart Circ Physiol., 2007. **292**(5): p. H2202-11.

190. Ibel H, et al., *Multiple respiratory chain abnormalities associated with hypertrophic cardiomyopathy and 3-methylglutaconic aciduria.* Eur J Pediatr., 1993. **152**(8): p. 665-70.

191. Romero NB, et al., *Infantile familial cardiomyopathy due to mitochondrial complex I and IV associated deficiency.* Neuromuscul Disord, 1993. **3**(1): p. 31-42.

192. Heddi A, et al., *Coordinate induction of energy gene expression in tissues of mitochondrial disease patients.* J Biol Chem, 1999. **274**(33): p. 22968-22976.

193. Fosslien, E., *Review: Mitochondrial medicine--cardiomyopathy caused by defective oxidative phosphorylation.* Ann Clin Lab Sci., 2003. **33**(4): p. 371-395.

194. Hansson A, et al., *A switch in metabolism precedes increased mitochondrial biogenesis in respiratory chain-deficient mouse hearts.* Proc Natl Acad Sci U S A., 2004. **101**(9): p. 3136-3141.

195. Duncan JG, et al., *Insulin-resistant heart exhibits a mitochondrial biogenic response driven by the peroxisome proliferator-activated receptor-alpha/PGC-1alpha gene regulatory pathway.* Circulation, 2007. **115**(7): p. 909-917.

196. Graham, B.H., et al., *A mouse model for mitochondrial myopathy and cardiomyopathy resulting from a deficiency in the heart/muscle isoform of the adenine nucleotide translocator.* Nat Genet, 1997. **16**(3): p. 226-234.

197. Augustus A, et al., *Cardiac-specific knock-out of lipoprotein lipase alters plasma lipoprotein triglyceride metabolism and cardiac gene expression.* J Biol Chem, 2004. **279**(24): p. 25050-25057.

198. Noh HL, et al., *Acute lipoprotein lipase deletion in adult mice leads to dyslipidemia and cardiac dysfunction.* Am J Physiol Endocrinol Metab. , 2006. **291**(4): p. E755-760.

199. King, K.L., et al., *Fatty acid oxidation in cardiac and skeletal muscle mitochondria is unaffected by deletion of CD36.* Archives of Biochemistry and Biophysics, 2007. **467**(2): p. 234-238.

200. Coburn, C.T., et al., *Defective uptake and utilization of long chain fatty acids in muscle and adipose tissues of CD36 knockout mice.* J Biol Chem, 2000. **275**(42): p. 32523-32529.

201. Binas, B., et al., *Requirement for the heart-type fatty acid binding protein in cardiac fatty acid utilization*. 1999. p. 805-812.

202. Lihong Cheng1, G.D., Qianhong Qin1, Yao Huang1, William Lewis2, Nu He3, Ronald M Evans4, Michael D Schneider5, Florence A Brako1, Yan Xiao1, Yuqing E Chen1 & Qinglin Yang1, *Cardiomyocyte-restricted peroxisome proliferator-activated receptor- deletion*

perturbs myocardial fatty acid oxidation and leads to cardiomyopathy. Nature Medicine, 2004 **10**: p. 1245-1250.

203. Neubauer S, et al., *Myocardial phosphocreatine-to-ATP ratio is a predictor of mortality in patients with dilated cardiomyopathy.* Circulation, 1997. **96**(7): p. 2190-2196.

204. Tian R, et al., *Increased adenosine monophosphate-activated protein kinase activity in rat hearts with pressure-overload hypertrophy.* Circulation, 2001. **104**(14): p. 1664-1669.

205. Ide T, et al., *Mitochondrial DNA damage and dysfunction associated with oxidative stress in failing hearts after myocardial infarction.* Circ Res, 2001. **88**(5): p. 529-535.

206. el Alaoui-Talibi, Z., et al., *Fatty acid oxidation and mechanical performance of volume-overloaded rat hearts.* Am J Physiol 1992. **262**(4): p. H1068-1074.

207. Sharma, S., et al., *Intramyocardial lipid accumulation in the failing human heart resembles the lipotoxic rat heart.* FASEB J, 2004. **18**(14): p. 1692-1700.

208. Jinghai Chen, Y.C.W.Z.Y.H.B.H.R.X.L.D.Y.C.X.C.Y.Y.S.H.X.C., *Specific LPA receptor subtype mediation of LPA-induced hypertrophy of cardiac myocytes and involvement of Akt and NFkappaB signal pathways*. 2008. p. 1718-1731.

209. Nishizuka, Y., *Intracellular signaling by hydrolysis of phospholipids and activation of protein kinase C* Science, 1992. **258**(5082): p. 607-614.

210. Takeishi, Y., et al., *Effect of angiotensin-converting enzyme inhibition on protein kinase C and SR proteins in heart failure.* Am J Physiol. , 1999. **276**(1): p. H53-62.

211. Takeishi Y, C.G., Kirkpatrick DM, Li Z, Wakasaki H, Kranias EG, King GL, Walsh RA., *In vivo phosphorylation of cardiac troponin I by protein kinase Cbeta2 decreases cardiomyocyte calcium responsiveness and contractility in transgenic mouse hearts.* J Clin Invest, 1998. **102**(1): p. 72-8.

212. Bowling, N., et al., *Increased protein kinase C activity and expression of Ca2+-sensitive isoforms in the failing human heart.* Circulation, 1999. **99**(3): p. 384-391.

213. Limatola C, S.D., Moolenaar WH, van Blitterswijk WJ., *Phosphatidic acid activation of protein kinase C-zeta overexpressed in COS cells: comparison with other protein kinase C isotypes and other acidic lipids.* Biochem J, 1994. **304**(3): p. 1001-8.

214. Jones, G.A. and G. Carpenter, *The regulation of phospholipase C-gamma 1 by phosphatidic acid. Assessment of kinetic parameters.* J. Biol Chem, 1993. **268**(28): p. 20845-20850.

215. Pierce, G.N. and K.D. Philipson, *Binding of glycolytic enzymes to cardiac sarcolemmal and sarcoplasmic reticular membranes.* J. Biol Chem, 1985. **260**(11): p. 6862-6870.

216. Glitsch HG, T.A., *The Na+/K+ pump of cardiac Purkinje cells is preferentially fuelled by glycolytic ATP production.* Pflugers Arch, 1993. **422**(4): p. 380-5.

217. Jeremy, R.W., et al., *Relation between glycolysis and calcium homeostasis in postischemic myocardium*. 1992. p. 1180-1190.

218. Kermode, H., et al., *Glycolytic pathway intermediates activate cardiac ryanodine receptors.* FEBS Letters, 1998. **431**(1): p. 59-62.

219. Zima, A.V., J. Kockskamper, and L.A. Blatter, *Cytosolic energy reserves determine the effect of glycolytic sugar phosphates on sarcoplasmic reticulum Ca2+ release in cat ventricular myocytes*. 2006. p. 281-293.

220. Sharma, S., et al., *Glucose phosphorylation is required for insulin-dependent mTOR signalling in the heart.* Cardiovascular Research, 2007. **76**(1): p. 71-80.

221. van der Vusse, G.J., et al., *Fatty acid homeostasis in the normoxic and ischemic heart.* Physiol Rev, 1992. **72**(4): p. 881-940.

222. Stanley, W.C., F.A. Recchia, and G.D. Lopaschuk, *Myocardial substrate metabolism in the normal and failing heart.* Physiol Rev, 2005. **85**(3): p. 1093-129.

223. Ingwall, J.S., *Energy metabolism in heart failure and remodelling.* Cardiovasc Res, 2009. **81**(3): p. 412-9.

224. McMullen, J.R. and G.L. Jennings, *Differences between pathological and physiological cardiac hypertrophy: novel therapeutic strategies to treat heart failure.* Clin Exp Pharmacol Physiol, 2007. **34**(4): p. 255-62.

225. Suenaga, M., et al., *Identification of the up- and down-regulated genes in the heart of juvenile visceral steatosis mice.* Biol Pharm Bull, 2004. **27**(4): p. 496-503.

226. Rupp, H. and R. Jacob, *Metabolically-modulated growth and phenotype of the rat heart.* Eur Heart J, 1992. **13 Suppl D**: p. 56-61.

227. Cox, K.B., et al., *Cardiac hypertrophy in mice with long-chain acyl-CoA dehydrogenase or very long-chain acyl-CoA dehydrogenase deficiency.* Lab Invest, 2009. **89**(12): p. 1348-54.

228. Exil, V.J., et al., *Very-long-chain acyl-coenzyme a dehydrogenase deficiency in mice.* Circ Res, 2003. **93**(5): p. 448-55.

229. Black, P.N. and C.C. DiRusso, *Transmembrane movement of exogenous long-chain fatty acids: proteins, enzymes, and vectorial esterification.* Microbiol. Mol. Biol. Rev., 2003. **67**: p. 454-472.

230. Glatz, J.F. and J.H. Veerkamp, *Postnatal development of palmitate oxidation and mitochondrial enzyme activities in rat cardiac and skeletal muscle.* Biochim Biophys Acta, 1982. **711**(2): p. 327-35.

231. Ghatpande, S., et al., *Signal transduction and transcriptional adaptation in embryonic heart development and during myocardial hypertrophy.* Mol Cell Biochem, 1999. **196**(1-2): p. 93-7.

232. Mirebeau-Prunier, D., et al., *Estrogen-related receptor alpha and PGC-1-related coactivator constitute a novel complex mediating the biogenesis of functional mitochondria.* Febs J. **277**(3): p. 713-25.

233. Cunningham, J.T., et al., *mTOR controls mitochondrial oxidative function through a YY1-PGC-1alpha transcriptional complex.* Nature, 2007. **450**(7170): p. 736-40.

234. Balasubramanian, S., et al., *mTOR in growth and protection of hypertrophying myocardium.* Cardiovasc Hematol Agents Med Chem, 2009. **7**(1): p. 52-63.

235. Diniz, G.P., M.S. Carneiro-Ramos, and M.L. Barreto-Chaves, *Angiotensin type 1 receptor mediates thyroid hormone-induced cardiomyocyte hypertrophy through the Akt/GSK-3beta/mTOR signaling pathway.* Basic Res Cardiol, 2009. **104**(6): p. 653-67.

236. Kuzman, J.A., T.D. O'Connell, and A.M. Gerdes, *Rapamycin prevents thyroid hormone-induced cardiac hypertrophy.* Endocrinology, 2007. **148**(7): p. 3477-84.

237. Avruch, J., et al., *Amino acid regulation of TOR complex 1.* Am J Physiol Endocrinol Metab, 2009. **296**(4): p. E592-602.

238. Sharma, S., et al., *Glucose phosphorylation is required for insulin-dependent mTOR signalling in the heart.* Cardiovasc Res, 2007. **76**(1): p. 71-80.

239. Huang, J. and B.D. Manning, *A complex interplay between Akt, TSC2 and the two mTOR complexes.* Biochem Soc Trans, 2009. **37**(Pt 1): p. 217-22.

240. Soesanto, W., et al., *Mammalian target of rapamycin is a critical regulator of cardiac hypertrophy in spontaneously hypertensive rats.* Hypertension, 2009. **54**(6): p. 1321-7.

241. Inoki, K., et al., *TSC2 integrates Wnt and energy signals via a coordinated phosphorylation by AMPK and GSK3 to regulate cell growth.* Cell, 2006. **126**(5): p. 955-68.

242. Cao, A., et al., *Long chain acyl-CoA synthetase-3 is a molecular target for peroxisome proliferator-activated receptor delta in HepG2 hepatoma cells.* J Biol Chem, 2010. **285**(22): p. 16664-74.

243. Sun, X., et al., *Nicotine stimulates PPARbeta/delta expression in human lung carcinoma cells through activation of PI3K/mTOR and suppression of AP-2alpha.* Cancer Res, 2009. **69**(16): p. 6445-53.

244. Melegh, B., et al., *Phenotypic manifestations of the OCTN2 V295X mutation: sudden infant death and carnitine-responsive cardiomyopathy in Roma families.* Am J Med Genet A, 2004. **131**(2): p. 121-6.

245. Chiu, H.C., et al., *A novel mouse model of lipotoxic cardiomyopathy.* J Clin Invest, 2001. **107**(7): p. 813-22.

246. Lee, C.H., K. Inoki, and K.L. Guan, *mTOR pathway as a target in tissue hypertrophy.* Annu Rev Pharmacol Toxicol, 2007. **47**: p. 443-67.

247. Kemi, O.J., et al., *Activation or inactivation of cardiac Akt/mTOR signaling diverges physiological from pathological hypertrophy.* J Cell Physiol, 2008. **214**(2): p. 316-21.

248. Essop, M.F., et al., *Reduced heart size and increased myocardial fuel substrate oxidation in ACC2 mutant mice.* Am J Physiol Heart Circ Physiol, 2008. **295**(1): p. H256-65.

249. Cunningham, J.T., et al., *mTOR controls mitochondrial oxidative function through a YY1-PGC-1alpha transcriptional complex.* Nature, 2007. **450**(7170): p. 736-740.

250. Lee, Y., et al., *Hyperleptinemia prevents lipotoxic cardiomyopathy in acyl CoA synthase transgenic mice.* Proc Natl Acad Sci U S A, 2004. **101**(37): p. 13624-9.

251. Ellis, J.M., et al., *Adipose acyl-CoA synthetase-1 (ACSL1) directs fatty acids towards β-oxidation and is required for cold thermogenesis.* Cell Metab., 2010. **in press**.

252. An, J., et al., *Hepatic expression of malonyl-CoA decarboxylase reverses muscle, liver and whole-animal insulin resistance.* Nat. Med., 2004. **10**: p. 268-274.

253. Watkins, S.M., et al., *Lipid metabolome-wide effects of the PPARgamma agonist rosiglitazone.* J Lipid Res, 2002. **43**(11): p. 1809-17.

254. Neschen, S., et al., *Prevention of hepatic steatosis and hepatic insulin resistance in mitochondrial acyl-CoA:glycerol-sn-3-phosphate acyltransferase 1 knock out mice.* Cell Metab., 2005. **2**: p. 55-65.

255. Manfredi, G., et al., *Measurements of ATP in mammalian cells.* Methods, 2002. **26**(4): p. 317-26.

256. Chen, Y., et al., *Development of an ion-pair HPLC method for investigation of energy charge changes in cerebral ischemia of mice and hypoxia of Neuro-2a cell line.* Biomed Chromatogr, 2007. **21**(6): p. 628-34.

257. Ventura-Clapier R, Garnier A, and V. V., *Energy metabolism in heart failure.* J Physiol, 2004. **555**(1): p. 1-13.

258. Szczepaniak, L.S., et al., *Forgotten but not gone: The rediscovery of fatty heart, the most common unrecognized disease in america.* Circ Res, 2007. **101**(8): p. 759-767.

259. Brindley, D.N., et al., *Shedding light on the enigma of myocardial lipotoxicity: the involvement of known and putative regulators of fatty acid storage and mobilization.* Am J Physiol Endocrinol Metab, 2010. **298**(5): p. E897-908.

260. Burwell, L.S., S.M. Nadtochiy, and P.S. Brookes, *Cardioprotection by metabolic shut-down and gradual wake-up.* Journal of Molecular and Cellular Cardiology, 2009. **46**(6): p. 804-810.

261. Di Paola, R. and S. Cuzzocrea, *Peroxisome proliferator-activated receptors ligands and ischemia-reperfusion injury.* Naunyn-Schmiedeberg's Archives of Pharmacology, 2007. **375**(3): p. 157-175.

262. Yue, T.-l., et al., *Activation of Peroxisome Proliferator-Activated Receptor-{alpha} Protects the Heart From Ischemia/Reperfusion Injury.* Circulation, 2003. **108**(19): p. 2393-2399.

263. Færgeman, N.J., et al., *The acyl-CoA synthetases encoded within FAA1 and FAA4 in Saccharomyces cerevisiae function as components of the fatty acid transport system linking import, activation, and intracellular utilization.* J. Biol. Chem., 2001. **276**: p. 37051-37059.

264. Ellis, J., et al., *Adipose acyl-CoA synthetase-1 (ACSL1) directs fatty acids towards β-oxidation and is required for cold thermogenesis.* Cell Metabolism, 2010. **12**(1): p. 53-64.

265. Noland, R.C., et al., *Peroxisomal-mitochondrial oxidation in a rodent model of obesity-associated insulin resistance.* Am J Physiol Endocrinol Metab, 2007. **293**(4): p. E986-1001.

266. Gauthier, M.-S., et al., *AMP-activated Protein Kinase Is Activated as a Consequence of Lipolysis in the Adipocyte.* Journal of Biological Chemistry, 2008. **283**(24): p. 16514-16524.